Blackwell Publishing

Cladistics 22 (2006) 297–368

Cladistics

www.blackwell-synergy.com

Higher-level phylogeny of the Ithomiinae (Lepidoptera: Nymphalidae): classification, patterns of larval hostplant colonization and diversification

Keith R. Willmott[1]* and André V. L. Freitas[2]

[1]*McGuire Center for Lepidoptera and Biodiversity, Florida Museum of Natural History, University of Florida, SW 34th Street and Hull Road, PO Box 112710, Gainesville, FL 32611-2710, USA,* [2]*Departamento de Zoologia and Museu de História Natural, Instituto de Biologia, Universidade Estadual de Campinas, CP 6109, CEP 13083-970, Campinas, São Paulo, Brazil*

Accepted 22 February 2006

Abstract

We present a higher-level phylogenetic hypothesis for the diverse neotropical butterfly subfamily Ithomiinae, inferred from one of the largest non-molecular Lepidoptera data sets to date, including 106 species (105 ingroup) and 353 characters (306 informative) from adult and immature stage morphology and ecology. Initial analyses resulted in 1716 most parsimonious trees, which were reduced to a single tree after successive approximations character weighting. The inferred phylogeny was broadly consistent with other past and current work. Although some deeper relationships are uncertain, tribal-level clades were generally strongly supported, with two changes required to existing classification. The tribe Melinaeini is polyphyletic and *Athesis* + *Patricia* require a new tribe. *Methona* should be removed from Mechanitini into the restored tribe Methonini. Dircennini was paraphyletic in analyses of all data but monophyletic based on adult morphology alone, and its status remains to be confirmed. *Hypothyris*, *Episcada*, *Godyris*, *Hypoleria* and *Greta* are paraphyletic. A simulation analysis showed that relatively basal branches tended to have higher partitioned Bremer support for immature stage characters. Larval hostplant records were optimized on to a reduced, generic-level phylogeny and indicate that ithomiines moved from Apocynaceae to Solanaceae twice, or that Tithoreini re-colonized Apocynaceae after a basal shift to Solanaceae. Ithomiine clades have specialized on particular plant clades suggesting repeated colonization of novel hostplant niches consistent with adaptive radiation. The shift to *Solanum*, comprising 70% of neotropical Solanaceae, occurs at the base of a clade containing 89% of all ithomiines, and is interpreted as the major event in the evolution of ithomiine larval hostplant relationships.

The nymphalid butterfly subfamily Ithomiinae (ithomiines) is one of the best studied groups of Lepidoptera, and has served as a model in research on biogeography, chemical ecology and evolution. The subfamily is exclusively neotropical, containing approximately 370 species (Lamas, 2004; Willmott and Lamas, unpub. data) occurring in humid forests from sea level to 3000 m, from Mexico to southern Brazil, Paraguay, and across three Caribbean islands.

Adults of all Ithomiinae are unpalatable and warningly colored (Fig. 1), and many are models for palatable species of other lepidopteran taxa. Observing these butterflies stimulated Bates (1862) to formulate his theory of mimicry, which is now one of the best studied examples of natural selection. Ithomiines are also extensively involved in Müllerian mimicry rings, which they numerically dominate, along with butterflies of the nymphalid subfamily Heliconiinae (Müller, 1879; Beccaloni, 1997a). Ithomiine unpalatability results from dehydropyrrolizidine alkaloids, which are obtained in the majority of species by adult males feeding on Asteraceae flowers and dried or withered Boraginaceae

*Corresponding author:*E-mail address:* kwillmott@flmnh.ufl.edu

Fig. 1. Adult male representatives of outgroup *Tellervo* and Ithomiinae tribes. (A) *Tellervo zoilus*, Australia; (B) *Tithorea tarricina*, Ecuador; (C) *Methona themisto*, Brazil; (D) *Melinaea menophilus*, Ecuador; (E) *Athesis clearista*, Venezuela; (F) *Mechanitis lysimnia*, Ecuador; (G) *Placidina euryanassa*, Brazil; (H) *Ithomia terra*, Ecuador; (I) *Napeogenes apulia*, Ecuador; (J) *Hyposcada anchiala*, Peru; (K) *Oleria santineza*, Ecuador; (L) *Callithomia lenea*, Ecuador; (M) *Dircenna jemina*, Ecuador; (N) *Pteronymia lonera* Costa Rica; (O) *Godyris zavaleta*, Belize; (P) *Veladyris pardalis*, Ecuador.

plants (Brown, 1984, 1985; Trigo and Brown, 1990). The same alkaloids are also the precursors for volatile pheromones, which males disseminate through hair-like, alar androconial organs (Edgar et al. 1976; Schulz et al., 1988, 2004).

Many Ithomiinae are abundant, conspicuous and easily sampled, which has led to a relatively thorough knowledge of distribution in some groups. Ithomiine distribution data have therefore been used in identifying areas of endemism in the neotropical lowlands and testing the refuge hypothesis (Brown, 1977b, 1982), as well as examining geographic modes of speciation (Whinnett et al., 2005b; Jiggins et al. 2006).

Perhaps most notably, ithomiines are remarkable in their larvae feeding almost exclusively on plants of the family Solanaceae, on which they are one of the relatively few herbivores (Drummond and Brown, 1987; Brown and Freitas, 1994; Willmott and Mallet, 2004). Although several other insect groups also feed on Solanaceae, notably Chrysomelidae (Hsiao, 1986), few are as specialized or abundant in the habitats where ithomiines occur. This close association between herbivore and host led to the group being used in seminal studies of insect–plant coevolution (Drummond, 1986; Brown and Henriques, 1991). These studies found no evidence for traditional coevolution, or matching cladogenesis of herbivore and host, but nevertheless the ecology of ithomiine–host interaction is likely to have been significant in the subfamily's diversification (Drummond, 1986; Willmott and Mallet, 2004).

Though the Ithomiinae have already proved a model study group in many fields, a robust phylogenetic hypothesis, which would permit the use of phylogenetic comparative methods, is still needed. The Ithomiinae are defined by a clear morphological synapomorphy, the presence in males of an elongate patch of erectile, hair-like androconial scales at the anterior edge of the dorsal hindwing, apparently first remarked upon by Doubleday (1847). The subfamily forms a clade with the Tellervinae, containing the single Australasian genus *Tellervo*, together with the largely Old World Danainae, of which the Ithomiinae have been regarded as a tribe (Godman et al., 1879–80; Haensch, 1909–10; Ackery et al., 1999; Brower et al., 2006). The close relationship between these three taxa has been recognized since at least the time of Doubleday (1847) and confirmed in subsequent papers (Brower, 2000; Freitas and Brown, 2004), and we follow Lamas (2004) in according each subfamilial status.

One of the earliest attempts to portray the relationships among Ithomiinae genera was that of Doubleday (1847), who used characters of the venation and male foreleg to successfully unite several ithomiine genera and order them from basal to derived (Fig. 2). His overall arrangement was refined, but little improved upon, by subsequent authors (Godman and Salvin, 1879–80; Haensch, 1909–10), until D'Almeida (1941) and Fox (1940, 1956) established the currently recognized tribes and formed the foundation for future work (Fig. 2).

Brown and Henriques (1991) provided the first explicit phylogeny of ithomiine genera, based on analysis of 90 morphological and ecological characters from adult and immature stages for representatives of most genera. This was followed by Brown and Freitas (1994), in which the immature stage character matrix was provided in addition to three cladograms based, respectively, on adult, immature and all characters combined (Fig. 2). These cladograms permitted the first assessment of monophyly of the tribes that had been recognized for the preceding half century.

The Tithoreini of Fox (1940, 1956), founded largely on the possession of a less reduced male foreleg (apparently a symplesiomorphy), proved to be broadly paraphyletic, splitting into at least four branches. The genus *Aeria*, placed in Oleriini by Fox (1956), moved to a more basal position near *Tithorea*. The highly autapomorphic genera *Placidina* and *Methona*, placed in two separate tribes by Fox (1956), moved far from their putative relatives to form a sister clade to the Mechanitini. Finally, although the remaining five tribes formed a monophyletic group, the tribe Dircennini disintegrated into a broad paraphyletic assemblage scattered across this clade. In particular, three small, highly autapomorphic genera, *Callithomia*, *Talamancana* (described by Brown and Freitas, 1994, for a single Costa Rican species) and *Velamysta*, assumed a basal position for the clade, which contains the majority of ithomiine species.

The cladograms of Brown and Freitas (1994) showed that a stable tribal classification for the Ithomiinae has yet to be reached, with four of the generally recognized eight tribes proving not to be monophyletic. Their study also demonstrated that immature stages could provide important information in resolving major, more basal nodes. For example, larval morphology clearly showed *Aeria* to be a basal ithomiine, and the larval hostplant family, Apocynaceae, is otherwise used in the Ithomiinae only by the basal genera *Tithorea* and *Elzunia*. Brown and Freitas (1994) therefore suggested that future studies concentrate on including more taxa and trying to obtain life history information for certain key genera.

Our primary goal therefore is to incorporate new data and taxa from all species clades within the Ithomiinae to attempt to resolve these currently problematic areas of ithomiine phylogeny. In particular, we focus on the monophyly, relationships and classification of the basal clades (former Tithoreini, Melinaeini and Mechanitini), the phylogenetic position of certain highly autapomorphic and enigmatic genera (including, among others, *Methona*, *Placidina*, *Callithomia*, *Velamysta* and *Talamancana*), and the monophyly of the Dircennini.

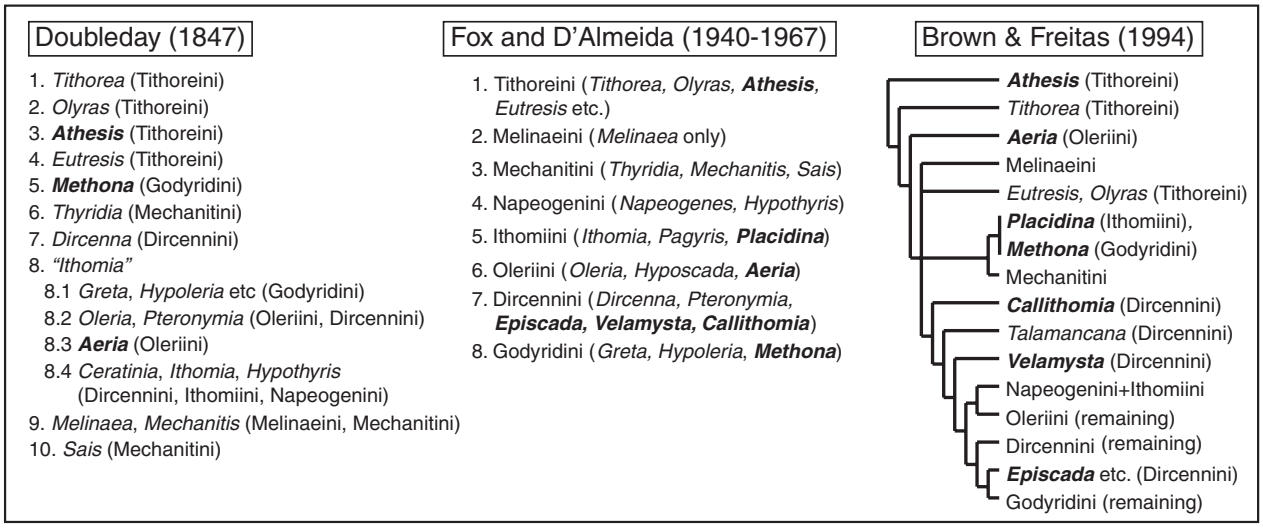

Fig. 2. History of classification and inferred relationships among ithomiine tribes. Bold genera show frequent changes in classification.

Because the data set presented here will be combined with a DNA sequence data set of collaborators (Brower et al., 2006) for a total evidence analysis in the near future, we refrain from making taxonomic changes here.

Our second goal is to attempt to confirm for the first time, using cladistic methods, the monophyly of all recognized genera, or highlight areas in need of future study. As a basis for discussions of classification in this paper we use the recent tribal and generic classification of Lamas (2004), which is based largely on that author's own morphological knowledge, Brown and Freitas (1994) and discussions with the authors of this paper.

Finally, in the last decade much new hostplant data have been obtained, so we take this opportunity to re-examine patterns of host evolution using the phylogenetic hypotheses presented here. While the shift to Solanaceae has been seen as a key event in ithomiine evolution, the cladograms of Brown and Freitas (1994) imply that the plant family was either colonized twice, or that one or more reversals to feeding on Apocynaceae occurred.

Methods

Study taxa and outgroup choice

In choosing study taxa within the Ithomiinae we attempted to include representatives from all species clades, those with immature stage information and preserved specimens for molecular analysis by collaborators, and type species for genera, where possible. Species clades are clusters of species with similar or identical male genitalia and androconia, character sets that are most reliable in defining monophyletic species groups (Willmott and Lamas, unpub. data). In genera lacking clear synapomorphies for species groups we selected species to represent most of the morphological variation within the genus. We used published revisions and our own study to choose representative species from 20 genera containing 111 ithomiine species (see Table 1). For the remaining 25 genera, containing 256 species, we examined wing venation, androconia and genitalic dissections for males of 229 species to define species clades. Omitted species were either clear members of monophyletic groups already represented by exemplar species (20 spp., based on wing venation and androconia), or unavailable for dissection due to rarity (seven spp.). Other information (female morphology, wing venation from photographs) suggests that these latter species are likely to be closely related to examined species and that their omission does not compromise this study (see also discussion in Table 1). From each species clade one or more representative species were selected to maximize available character information and to include, usually, the type species. In *Elzunia*, *Velamysta* and *Haenschia* the type species was not used because it lacked life history and/or molecular data and is morphologically very similar to the chosen exemplar species. In total we selected 105 ithomiine species from all genera for analysis (Appendix 2).

The relationships between the Ithomiinae, Danainae and the monotypic Tellervinae remain unclear, so initially we included a single species from each of five genera representing major lineages of the Danainae (*Lycorea*, *Anetia*, *Danaus*, *Euploea* and *Ideopsis*, see Ackery and Vane-Wright, 1984) and *Tellervo zoilus*, the type species for *Tellervo* (Table 1). Morphologically, the Danainae proved to be extremely divergent from the Ithomiinae, and many character states could not be coded or were autapomorphic. As *Tellervo* is much more morphologically similar to Ithomiinae, and a single

Table 1
Summary of species examined and included in phylogenetic analysis

Taxon	Genera	Species	Dissected species (male)	Included species	References
Ithomiinae					
Tithoreini	2	5	4	3	Fox (1956), Brown (1977b)
Aeria	1	3	2	2	Lamas (2004)
Methona	1	7	2	2	Lamas (1973)
Melinaeini	5	18	9	7	Fox (1960), Lamas (1973, 1979), Brown (1977a)
Athesis + Patricia	2	6	4	2	Fox (1956)
Mechanitini	4	16	10	8	Fox (1967), Lamas (1973), Brown (1977a)
Napeogenini	5	56	36	13	Fox and Real (1971), Brown (1980)
Subtotal (revised tribes)	**20**	**111**	**67**	**37**	
Ithomiini	3	28	19	6	Lamas (1986)
Oleriini	4	63	63	12	
Dircennini[1]	7	92	83	28	Brown and D'Almeida (1970), Brown et al. (1970)
Godyridini[1]	11	73	64	22	Lamas (1980)
Subtotal (non-revised tribes)	**25**	**256**	**229**	**68**	
Total all tribes	**45**	**367**	**296**	**105**	
Danainae	**11**	**162**	**4**	–	Ackery and Vane-Wright (1984)
Tellervinae	**1**	**6**	**1**	**1**	Ackery (1987)

[1]The recently described genus *Meizocellis* Brabant, 2004 (type species *Meizocellis infuscans* Brabant, 2004) is regarded as a synonym of *Pteronymia*. The taxon described as the type of *Meizocellis* is regarded as a subspecies of the northern Andean *Pteronymia serrata* Hewitson, which is morphologically almost identical to *Pteronymia alida*, included here in the ingroup. The genus *Oxapampa* Brabant, 2004 (type species *Oxapampa electrea* Brabant, 2004) is somewhat intermediate in male wing venation between *Velamysta* and *Veladyris*, and we suspect that it will prove to form a clade with one or both of these genera. An additional undescribed and apparently closely related species is also known from Peru. Unfortunately, we have been unable to dissect any specimens of *O. electrea* or the undescribed Peruvian species due to their rarity, and no illustrations or discussion of the genitalia of *O. electrea* were given in the original description (Brabant, 2004). Thus, although *Veladyris* and *Velamysta* have a number of unique morphological apomorphies that could readily resolve the relationships of *Oxapampa*, its taxonomic status is still uncertain.

character (see Discussion) suggests it is the sister clade, we used *Tellervo* alone as the outgroup for character state polarization.

Ithomiinae species names and generic combinations mostly follow Lamas (2004), except as follows (latter name is that used in Lamas, 2004): *Pteronymia carlia* = *Pteronymia sylvo*; *Episcada canaria* = *Episcada doto canaria*; *Pteronymia inania* = *Pteronymia dispaena inania*; and *Heterosais nephele* = *Heterosais giulia nephele*. The type illustration of *Hymenitis sylvo* Geyer, 1832, appears to show an *Episcada* taxon, probably *Episcada carcinia* Schaus, 1902, while additional distribution data and/or morphological differences argue for the remaining three changes in name status. No formal name changes are made, however, as these will be discussed in greater detail in forthcoming generic revisions.

Character sources

This study includes all potential character sources known to us except molecular data (Brower et al., 2006), chromosome number, which varies at the intraspecific level (Brown et al., 2004), and microscopic characters of the eggs and first instar, which have been studied by Motta (2003). The latter were excluded because of high levels of homoplasy in that data set and our inability to examine many of our exemplar species due to lack of material. Both informative and uninformative characters were included, as the latter may prove to be synapomorphies for genera or species clades represented here by single species.

Most Ithomiinae larvae feed on Solanaceae (Drummond and Brown, 1987), so immature stages of many species were located by searching Solanaceae plants. Where possible, ovipositing females were also followed, or eggs expressed from gravid females and reared on a range of potential hostplants. The majority of the immature stage information has been obtained by K. Brown (pers. comm.) in many countries, and by K. Brown and AVLF in Brazil, over many years, at both field sites and on cultivated hostplants at the Universidade Estadual de Campinas, Campinas (Freitas, 1993, 1996; Brown and Freitas, 1994; Freitas and Brown, 2002, 2005; Appendix 2). Additional information for Andean species was collected by KRW during a 3-month period in two Ecuadorian cloud-forest localities (Willmott and Mallet, 2004; Appendix 2). Eggs and larvae were usually reared in plastic bags with fresh hostplant leaves provided every 2–3 days. Where possible, eggs and larvae, especially first and last instars, were preserved in locally available industrial alcohol (ethanol). All observations of oviposition behavior, larval behavior, development and appearance were recorded and photographs taken of dorsal and lateral

views of larvae, and dorsal, lateral and ventral views of pupae (http://www.flmnh.ufl.edu/butterflies/neotropica/ith_imm.html). At least some immature stage information was available for all but 20 of the 106 species included in the study (Appendix 3).

Adult body morphology was studied using a Wild M4 stereomicroscope with 6–50× magnification and camera lucida. The antennal morphology, color pattern and scale morphology of the frons, head, labial palpi, thorax and abdomen were examined for males of all species (no dimorphism was noted). The morphology of the legs, abdomen and genitalia of both sexes were examined by soaking these body parts in 10% KOH for 10 min before dissection and storage in glycerol (Appendix 3). Drawings of the male genitalia in dorsal, lateral, ventral and posterior views, aedeagus in dorsal and lateral view, the terminal 3 segments of the female abdomen in dorsal, lateral, ventral and posterior views and the abdomen interior in dorsal view were prepared for all species. Attempts to evert the vesica (internal, tubular membrane) from the aedeagus were successful for all except a few Godyridini in which the aedeagus is extremely narrow. Where possible, a standard 1 mL insulin syringe was inserted into the ductus ejaculatorius and water injected to evert the vesica, but for smaller species the aedeagus was cut in two (after drawing the lateral and dorsal view) just anterior of the zone and then inserted into the syringe needle itself, held in place with forceps. Wing venation was studied in both cleared (with bleach, mounted in Euparal) and uncleared specimens of both sexes. The distribution and morphology of male hindwing androconial scales was studied and drawn for all species by removal of the right forewing to reveal these structures. These scales were examined further with a Hitachi S2500 scanning electron microscope at 15 kV, with magnification 30–5000×, for 86 of the 105 ithomiine species, representing all genera. Included species were all those that showed morphological differences under the stereomicroscope and those whose phylogenetic position was uncertain. Excluded species are marked with an asterisk in the data matrix (Appendix 2). Sections of wing for SEM study, containing both normal wing scales and androconial scales, were mounted on stubs with PVA glue and coated with a 20 nm layer of gold/palladium (95% gold) using a Cressington Sputter Coater. Terminology for genitalic structures follows a combination of Klots (1970), Eliot (1973) and common usage, and is indicated on Fig. 21(D) (male) and Fig. 28(J) (female). The pedunculi of Klots (1970), projections from the anterio-ventral portion of the tegumen, articulate with the vinculum, but as the point of connection is often not discernible we use "vinculum" to include both structures. We use the Comstock and Needham (1918) system for naming wing veins (see Fig. 14A,D,J), referring to cells by the veins bounding them. Terminology for wing scales follows Downey and Allyn (1975).

Character coding

All characters were initially equally weighted and multistate characters unordered. The majority of characters are discrete but in some cases we used continuous characters, where characters that were discrete in one part of the tree showed more continuous variation elsewhere. These characters are conceptually little different from discrete characters except in being objectively quantifiable. Here, continuous characters represent either angles or ratios between two variables. The numerical limits of states were chosen to reflect in coding the initially observed variation and to minimize homoplasy, based on cladistic relationships inferred from other characters. We thus effectively use the same criterion of parsimony in setting character states (that number of steps should be minimal), which we use in searching for optimal tree topologies.

Analyses

We used PAUP* 4.0b10 (Swofford, 1998) to analyze our data, with maximum parsimony as our optimality criterion. To reduce the problem of tree islands and maximize the number of most parsimonious topologies we employed a two-stage search. We first conducted 2000 replicate searches with TBR branch swapping, obtaining starting trees by stepwise addition using a random-addition sequence, retaining no more than five trees per search. Resulting trees were used as starting trees for a single subsequent heuristic search. Successive approximations character weighting (SACW) (Farris, 1969) was used to attempt to reduce the number of most parsimonious trees (MPTs) and improve consensus tree resolution. Characters were reweighted based on the maximum value of their consistency index, and subsequent two-stage searches were conducted using 1000 replicates retaining no more than two trees per search.

We examined the effect of adult and immature stage characters on tree topology by conducting separate analyses of matrices of each data type. All species were included in analyses of the adult data matrix, but 26 species were excluded from the analysis of the immature stage matrix due to lack of information (indicated in Appendix 2). Our goal in these partitioned analyses was to identify clades supported by both data sets and therefore likely to prove robust and to evaluate whether the time required to obtain immature stage data is justified in such studies. The incongruence length difference (ILD) test (Farris et al., 1995) is widely used to examine for supposed inconsistencies in phylogenetic signal between data partitions (e.g., Freitas and Brown,

2004). However, as we believe that the best phylogenetic hypothesis results from a combined analysis of all data (e.g., Nixon and Carpenter, 1996; Baker and DeSalle, 1997; Wahlberg et al., 2005), and given possible inconsistencies in the ILD test as a measure of incongruence (Dolphin et al., 2000; Barker and Lutzoni, 2002; Darlu and Lecointre, 2002), we do not use it here.

Strict consensus trees are used to summarize shortest tree topologies. We estimated the strength of support for branches based on our data by bootstrapping, as well as by partitioned Bremer support values (Bremer, 1988, 1994), to evaluate the relative contribution of two major data partitions (adult versus immature stage characters) to the tree topology in the total evidence analysis. Two hundred bootstrap replicates were run for each analysis. Searches for each bootstrap replicate used starting trees obtained by stepwise addition with 20 random-addition sequences, retaining no more than two trees from each search. Bremer support was calculated using constraint searches generated by TreeRot v.2 (Sorenson, 1999) and run in PAUP. Each constrained search included 100 replicate TBR searches with no more than five trees retained per search. Decay indices for trees obtained after SACW were derived using the same character weights used in the final round of searches.

Brown and Freitas (1994) suggested that immature stage characters might provide particularly important support to more basal nodes, a common viewpoint in Lepidoptera phylogenetic studies that we wished to test (e.g., Kitching, 1984, 1985; Harvey, 1991; Tyler et al., 1994; Parsons, 1996). Our null expectation is that for a given node the ratios of PBS values between data partitions will be the same as the ratio of characters between data partitions. We therefore identify those nodes that have an immature stage PBS value exceeding this expected value as "strongly supported" by immature stage characters. We assigned each node a score based on the nodal distance to the base of the tree, with the basal node scored 0, and calculated the average base-node distance of nodes strongly supported by immature stage characters (for $n = N_{imm}$ nodes). To determine whether this average distance was lower than expected by chance (i.e., nodes tend to be more basal) we obtained a null distribution of averages by generating 500 random samples of N_{imm} nodes from the empirical base-node distance values. The proportion of null averages that are lower than the observed average provides an estimate of the probability that nodes supported by immature stage characters are nearer the base of the tree than expected by chance alone. Random samples of base-node distances were generated in Microsoft Excel 2003 by pairing the column of empirical base-node values with a column of random numbers ("= RAND()"), then reordering both columns by the random number column. The first N_{imm} base-node distances were then used to calculate a null average base-node distance for N_{imm} nodes. This process was repeated 500 times by recording the initial series of actions (reordering the empirical values and calculating the average of the first N_{imm} base-node distances) in a macro and replicating the macro text 500 times.

Character changes were examined using ACCTRAN optimization and are given for major clades in Table 2.

Evolution of hostplant choice

We examined the evolution of hostplant choice in the Ithomiinae by optimization of hostplant character states on to a generic-level cladogram (reduced from our preferred species-level cladogram). Within genera there is little evidence, to date, of major differences in hostplant clades between species groups, so examining broad patterns at the generic level is sensible. Hostplant was coded as a single multistate character with states representing major plant clades based on phylogenies presented by Olmstead et al. (1999). Plant clades were arbitrarily defined to represent the smallest clades utilized by any single ithomiine genus, and are members of distinct tribes (or higher taxa) in all cases except *Lycianthes* and *Capsicum*. Although *Lycianthes* and *Capsicum* form a clade, because *Napeogenes* feed only on *Lycianthes* the two genera were kept distinct. Hostplant records for Ithomiinae were compiled from Drummond and Brown (1987), Brown and Freitas (1994), Beccaloni (1997b), Haber (2001), Willmott and Mallet (2004), Janzen and Hallwachs (2005) and AVLF (unpub. data), and are summarized in Table 3.

Ithomiines were coded for hostplant usage in two ways, first with each genus (or species, if genus polyphyletic) being coded as polymorphic including all known records of plant clades (Char H1, end of Appendix 1), and secondly as monomorphic for only the dominant plant clade (Char H2, end of Appendix 1). *Velamysta* has only two host records, one on *Lycianthes* and one on *Cuatresia* (*Withania* + *Physalis* + *Iochroma* clade), and so was coded polymorphic in both cases. Character coding for each genus/terminal taxon is given in Table 3. Character states were optimized with maximum parsimony using ACCTRAN in MacClade 3.05 (Maddison and Maddison, 1995) on to a generic-level cladogram reduced from the consensus tree resulting from successive approximations weighting of the entire matrix.

Results

Characters

A total of 353 characters (306 informative, 45 uninformative, two constant) were coded (Appendix

Table 2
Clades, synapomorphies and autapomorphies. Note: Synapomorphies are given for genera with more than one species analyzed. Current generic synonyms and revised tribes in parentheses

Clade no.	Clade name	Unambiguous synapomorphies[1]	Ambiguous synapomorphies[1]
1	Ithomiinae	23:0, 67:0, 70:1, 84:0, 86:0, 90:0, 93:0, 94:0, 95:0, 96:0, 97:0, 107:1, 114:1, 135:0, 143:0, 146:0, 148:0, **156:1**, 205:0, 266:0, 270:0, 282:0, 292:0, 298:0, 319:0, 323:0, 329:1, 338:0	11:1, 34:0, 60:0, 88:0, 115:0, 250:0, 284:0
2	*Methona*; Methonini	49:1, 261:1 9:1, 22:1, 54:0, **55:1**, 56:0, 59:1, 90:1, 91:1, 93:3, **95:6**, 96:5, **97:7**, 99:1, **105:1**, 114:2, 121:1, 140:1, 147:1, 154:1, 169:1, 227:1, **230:1**, 240:2, **242:1**, **246:1**, 278:5, 295:5, **297:1**, 298:1, **299:1**, 326:1, **341:3**	39:1, 58:1, 100:2, 179:2, 286:1 88:1, 101:0, 115:2, 164:0, 284:2, 304:1, 317:1, 319:1
3	Tithoreini	65:4, 68:2, 73:1, 161:1, **167:1(n)**, 170:1, 180:0, 307:2	11:0, 62:1, 79:1, **153:2**, 159:2, 254:1
	Aeria	**34:2**, 50:1, 75:0, 76:1, 90:3, 144:1, **184:2**, **193:1**, 249:1, **278:3**, 285:1, 308:1, 311:2, 331:1	58:0, 115:3, 179:1
4	*Tithorea* + *Elzunia*	103:0, 107:0, 109:1, 264:1, **276:1**	17:1, **81:1**, 86:1, 95:1, 100:0, **153:4**, 172:2, 183:2
5		4:1, 61:1, 76:1, 78:1, 331:1	34:3, 40:1, 62:1, 63:3, 79:1, 119:1, 122:1, 177:1, 183:3, 250:1, 254:1, 284:5, 317:1
6	Melinaeini	17:1, 124:1, **153:3(s)**, 154:1, **167:3**	25:2, 39:1, 58:1, 118:1, **146:1**, 158:1, 172:2, 191:1, 194:1, 326:1
7		97:2, 159:2, 284:1, **350:1**, 352:1	6:1, 51:1, 88:1, 172:3, 250:2
8	*Paititia* + *Olyras*	4:0, **96:6**, 121:1, 135:1, 143:1, **171:1**, 227:1, 241:2, **251:3**, 253:1, 312:1, 315:2, **319:2**, 351:1, **353:1**	158:0, 191:0, 194:0, 254:0
9	*Athyrtis* + *Melinaea*	**87:1**, 91:2, 120:0, 208:1	9:1, **25:3**, 40:0, 49:1, 54:2, 56:0, 57:2, 59:1, 62:0, 63:0, 75:0, 118:2, 122:0, 179:2, **278:4**
	Melinaea	94:5, 100:1, **108:1**, 124:2, 135:1, 142:1, 143:1, 161:1, 164:3, 170:1, 249:1, 261:1, 296:1, 311:2, **319:4**, 334:1	122:2, 179:1
10		**15:1(m)**, 65:3, 72:1, 73:6, 121:0, 175:0	**14:1**, 60:1, 173:1, 178:0, 243:1, 351:1
11	*Athesis* + *Patricia*	**44:1**, **45:2**, 66:1, 74:1, 83:1, 147:1, 170:1, 183:4, 184:0, **229:1**, 240:2, 241:2, 244:1, 278:5, 341:1	110:1, 119:0, 172:0, 177:0, 243:3, 250:0, 254:0
12		22:1, 46:1, 51:1, 100:2, 169:1	20:1, 54:0, 68:2, 80:1, 162:0, 164:1, 222:1
13	Mechanitini	**27:1**, 56:0, 73:1, 102:1, 106:1, 135:1, 143:1, 284:0, 285:1, 349:1	58:1, 60:0, 63:0, 65:4, 93:2, **96:2**, 124:1, 208:1, 334:1, 351:0
14		61:0, 85:1, 109:1, 113:1, 120:0, 140:3, 180:0, **198:1**, **199:1**, **200:1**, **201:1**, 249:1, 298:2, **324:1**	2:1, 3:1, 4:0, 77:1, 94:5, 124:2, 142:1, **146:2**
15	*Sais* + *Scada*	64:1, 66:1, 70:0, 99:1, 284:1, **341:4**	54:1, 58:0, 63:3, 208:0, 243:0
	Scada	18:1, 19:1, 29:1, 59:1, 74:1, 84:1, 115:3, 122:0, 222:0, 240:2, 250:2, 251:2, 257:3, 262:1, 270:2, 273:1, 283:1, 317:0, 335:1, 349:0	2:0, 77:0, 94:0, 243:3, 334:0
16	*Forbestra* + *Mechanitis*	6:1, **45:3(m)**, **95:B**, 118:1, **150:1**, 155:1, 179:2, **181:1**, 207:1, **290:1**, 334:2	**3:2(m)**, 10:1, 110:1, 286:1, 296:1
	Forbestra	144:1	142:0, 164:2
	Mechanitis	**28:1**, **31:1**, 50:1, 52:1, 84:1, **278:2**	80:0, 121:1
17		13:1, 19:1, 33:1, **146:3(n)**, 338:9	32:1, 50:1, 54:2, 90:1, 114:2, 118:1, 140:1, 308:1, 317:0
18		59:1, 61:0, 73:4, 179:0, 187:1, 188:1, 190:1, 315:2	68:1, 94:3, 120:0, 173:2, **175:2**, 178:1, 243:0
19	Ithomiini	92:1, 117:0, 122:0, 244:2	6:1, 18:1, 50:0, 52:1, 54:1, 89:2, 121:2, 162:1, 164:0, **189:1**, 195:2, 208:1, 312:1, 317:1, 347:3
20	*Placidina* + *Pagyris*	33:0, 51:0, 62:0, 64:1, **69:2(m)**, 71:1, **82:1**, **271:1**, 337:1, **338:7**	207:1
	Pagyris	88:2, 169:0, **257:1**, 303:1	3:3, 12:1, 66:1
	Ithomia	75:0, 94:1, **116:1**, **138:1**, 241:2, 250:2, 278:1, 280:1	120:1, 308:0
21	Napeogenini	91:2, 119:2, 125:1, **160:1**	3:3, 47:1, 90:0, 114:1, 118:2, 140:0, 251:2
22	*Aremfoxia* + *Epityches*	86:1, 115:2, 144:1, **155:2**, 250:2, 284:2, **313:1**	9:1, 56:0, 63:2, 65:1, 68:0, 70:0, 73:5, 74:1
23		64:1, 66:1, 124:2, **139:1**, 243:2	121:1, 122:2, 222:0, 254:0, **316:1**, 322:1
	Napeogenes	180:0, 187:0, **195:4**, **228:1**, 241:0, 248:1, **309:2**, 337:1	17:3, 19:0, 20:0, 54:1, 61:1, 251:1
24		89:2, 102:1, 143:1, **217:3**, **247:2(ns)**, 252:3, 278:1, 280:1, 300:1, 315:0, 319:7	3:0, 47:0, 57:1, 65:0, **69:1(m)**

Table 2
Continued

Clade no.	Clade name	Unambiguous synapomorphies[1]	Ambiguous synapomorphies[1]
25		90:2, 124:1, 239:1, 246:2, 323:1	
	Hyalyris	86:1, 88:2, 240:2	66:2, 143:0
26		75:0, 88:1, 183:1, 227:1, 253:1, 283:1	65:2, 66:2, 70:0, 74:1, 109:1, 164:2, 184:1, 222:0, 254:0, 284:1
27	Oleriini	3:1, **63:1(ms)**, 83:1, 92:1, 247:1, **282:1**	67:1, 79:0, 80:0, 121:1, 169:0, 294:1
28	*Megoleria* + *Hyposcada*	**11:2(m)**, 250:0	64:1, 73:2, 114:1, 118:0, 119:0, 243:2, 279:1, **320:2**
	Hyposcada	251:2, 278:5	18:1, 226:1, 294:0, 308:0
29	*Oleria*	4:0, 61:0, 91:2, 244:1, 262:1, **281:1**, 293:1, 329:0, 338:0	54:1, 65:0, 66:1, 68:0, 90:0
30	(*Ollantaya*)	300:1	19:0, 20:0, 79:1, 120:0, 173:2, 334:1
31		18:1, **287:1**	59:1, 67:0, 177:0, 241:2
32		17:5, 41:1, 46:0, 117:0, 125:1, **153:5**, **154:2**, 248:2, 251:2, 278:5, 288:7, 300:2, 326:1, 327:1	32:0, 35:0, 60:0, 177:0, 180:0, 268:1, 284:3, 308:0
	Callithomia	88:3, 93:5, 118:2, 119:2, 140:2, **216:2**, **223:5**, **231:1**, 240:0, 241:3, **257:4**, 270:1, **305:2**, 341:1, 344:1	20:0, 30:1, 35:1, 42:1, 43:1, 58:1, 64:1, 65:4, 66:0, 70:1, 74:0, 78:0, 90:2, 109:0, 143:1, 164:1, 187:1
33		12:1, 16:1, 18:1, 33:0, 51:2, 63:2, 338:8	3:3, 59:1, 68:0, 122:0, 243:2, 345:1
34	Dircennini (excl. *Callithomia*)	115:1, 183:0	92:1, 204:1, 225:4, 266:1, 267:1
35	*Hyalenna* + *Dircenna*	5:1, 8:1, 21:1, **45:1(m)**, **53:1(m)**, 57:1, 58:1, 93:1, 102:1, 141:1, 164:0, 185:1	90:0, 110:1, 172:2, 227:0, 345:0
	Dircenna ss	125:0, 169:0, **236:1**, 244:1, 270:1, 307:2, **338:4**, 352:1	90:1, 92:0, 110:0, 122:1, 266:0, 267:0, 268:0
36		36:0, 37:0, 61:0, 66:1, 176:1, 219:2, 223:2, 244:1, 333:1	38:2, 64:1, 122:1, 125:0, 126:1, 169:0, 184:3, 187:1, 307:2, 338:3
37		226:1, 270:2, **340:1**	92:0, 115:3, 122:2, 266:0, 267:0, 268:0, 339:1
38	*Episcada*, in part	112:1, **163:1**, 183:1	180:1, 224:2
39	*Episcada*, in part + *Ceratinia* (*Ceratiscada*)	88:3, 121:1 91:2	56:0, 84:1, 109:0, 184:0
	Ceratinia	16:0, 35:1, 114:1, 140:2, 141:1	5:1, 39:1, 41:0, 56:1, 122:1
40	*Haenschia* + *Pteronymia*	**269:2(s)**	16:0, 35:1, 42:1, **48:1(m)**, 68:2, 204:0
	Pteronymia	128:1, 179:0, 212:1, 288:1	
41	Godyridini	119:0, 144:1, 161:1, **167:2(n)**, 179:0, 288:9	17:4, 65:1, 73:5, 79:0, 118:0, 140:3, 170:1, 180:1, 240:2, 241:2, 268:0, 304:1, 352:2
42		**217:2**, 223:2, 225:5, 323:2	307:2
43		37:0, 186:1, 187:2, 284:4, 289:1, 291:1, 305:1	42:1, 57:1, 131:1, 140:1, 345:0, 352:0
	Heterosais	94:1, 115:3, 128:1, **134:1**, 144:2, 164:1, **165:1**, 180:0, 195:1, **206:1**, 219:2, 226:1, 227:3, 294:1, 334:2	304:2
44		41:0, 66:0, **133:1**, 179:1	38:1, 57:2, 140:2, 170:0, 307:0, 338:0
	Godyris (excl. *G. mantura*)	**1:1(m)**, 79:1, 119:1, 130:1, 161:0, **237:1**, 244:1	67:1, 70:1, 93:1, 102:1, 114:1, 141:1, 210:1, 224:3, 345:1
45		**216:1**, **220:1**, 225:0, 227:2, 247:1, 284:3, **343:1**, 344:1	38:5, 57:1, 304:2
46		122:1, **172:3**, 174:1, 187:0, 210:1	66:1, 131:0, 161:0
47	*Mcclungia* + *Brevioleria*	177:1, 243:1, 248:0	170:1
	Brevioleria	164:0, 168:2, 173:2, 294:2, 334:1	3:0, 12:0, 16:0, 37:1
48		12:0, 16:0, 37:1, 41:1, 66:2, 94:4, 115:3, 144:0, 244:1, 272:1	57:0, 90:0, 131:0, 145:1, 177:2, 183:4, 226:1, 252:2, 275:1, 277:1
	Greta diaphanus + *morgane*	161:0, 169:1, 187:0, 225:0, 284:5, 294:1, 327:0	126:1, 170:0, 304:0, 326:0, 341:2
49		92:1, 132:1, 137:1, 140:1, 180:0, 223:2, 227:2, **258:1**, 338:8	59:0, 298:1, 307:0
50		67:1, 71:1, 126:1, 162:1, 173:0, 187:0, 227:3, 334:0, **336:1**, 338:9	60:1, 298:0
	Pseudoscada	94:0	17:4, 38:1, 42:2, 59:1, 66:0, 85:1, 145:0

[1]Bold type indicates a unique synapomorphy for members of a clade, where for some species within clade: (m) = missing character information; (n) = nonapplicable character; (s) = some species with different derived character state.

Table 3
Ithomiine larval hostplant records. Recorded number of species–species interactions between ithomiine genera and major hostplant families and Solanaceae clades with resultant hostplant character coding (H1, H2). Note: More basal plant clades (within Solanaceae) are at left of table, more basal butterfly clades at top. Dominant hostplant clades are in bold type.

		Plant clade and character state											Character	
Subfamily Tribe	Genus	Apocynaceae (state 0)	Gesneriaceae (state 1)	*Brunfelsia* (state 2)	*Cestrum* clade (state 3)	*Nicandra* clade (state 4)	*Datura* clade (state 5)	*Solanum* clade (state 6)	*Solandra* clade (state 7)	*Capsicum* (state 8)	*Lycianthes* (state 9)	*Withania* + *Iochroma* + *Physalis* clades (state A)	H1	H2
Tellervinae	*Tellervo*	records (total not recorded)											0	0
Tithoreini	*Tithorea*	**14**											0	0
Tithoreini	*Elzunia*	**3**											0	0
Tithoreini	*Aeria*	**6**											0	0
Methonini	*Methona*			**15**									2	2
Melinaeini	*Eutresis*								**3**				7	7
Melinaeini	*Paititia*												?	?
Melinaeini	*Olyras*								**1**				7	7
Melinaeini	*Athyrtis*												?	?
Melinaeini	*Melinaea*								**14**				7	7
New tribe	*Athesis*									**1**			8	8
New tribe	*Patricia*									**1**			8	8
Mechanitini	*Thyridia*							**9**					6	6
Mechanitini	*Scada*							**6**					6	6
Mechanitini	*Sais*												?	?
Mechanitini	*Forbestra*							**1**					6	6
Mechanitini	*Mechanitis*					1	1	**105**				1	456A	6
Ithomiini	*Placidina*						**6**						5	5
Ithomiini	*Pagyris*						1					**3**	5A	A
Ithomiini	*Ithomia*							1		2	3	**33**	689A	A
Napeogenini	*Aremfoxia*												?	?
Napeogenini	*Epityches*									2		**4**	8A	A
Napeogenini	*Napeogenes*							1			**8**		69	9
Napeogenini	*Hyalyris*							**10**					6	6
Napeogenini	*Hypothyris*							**48**			1		69	6
Oleriini	*Megoleria*		**1**										1	1
Oleriini	*Hyposcada*		**6**										1	1
Oleriini	*Oleria*							**19**			5		69	6
Dircennini	*Callithomia*							**5**			1		69	6
Dircennini	*Hyalenna*							**6**				1	6A	6
Dircennini	*Dircenna*							**50**					6	6
Dircennini	*Ceratinia*							**7**					6	6
Dircennini	*Episcada*				5			**16**					36	6
Dircennini	*Haenschia*												?	?
Dircennini	*Pteronymia*				1		1	**50**	1		4	1	3569A	6
Godyridini	*Veladyris*												?	?
Godyridini	*Velamysta*										1	1	9A	9A
Godyridini	*Heterosais*				**3**								3	3
Godyridini	*Godyris*				**9**			3					36	3
Godyridini	*"Hypoleria" adasa*				**3**								3	3
Godyridini	*"Godyris" mantura*												?	?
Godyridini	*Mcclungia*				**4**								3	3

Table 3
Continued

Subfamily	Tribe	Genus	Plant clade and character state											Character	
			Apocynaceae (state 0)	Gesneriaceae (state 1)	*Brunfelsia* (state 2)	*Cestrum* clade (state 3)	*Nicandra* clade (state 4)	*Datura* clade (state 5)	*Solanum* clade (state 6)	*Solandra* clade (state 7)	*Capsicum* (state 8)	*Lycianthes* (state 9)	*Withania* + *Iochroma* + *Physalis* clades (state A)	H1	H2
Godyridini		*Brevioleria*				**2**								3	3
Godyridini		*Hypoleria*				**5**			1					36	3
Godyridini		*Greta*				**6**			1			1		369	3
Godyridini		*Pseudoscada*				**41**			6					36	3

1), including 75 from the immature stages (ecology: eight; egg: five; first instar: four; last instar: 36; pupa: 22) and 278 from adult stages (ecology and chemistry: six; body: 27; venation: 37; wing scales and androconia: 56; male abdomen and genitalia: 105; female abdomen and genitalia: 45; wing pattern: 2). Fourteen characters were continuous.

Total evidence analysis with equal weighting

In the equally weighted search including all characters and taxa, the initial search found 707 trees of length 1828 steps, while the subsequent search increased the number of MPTs to 1716, also of 1828 steps (CI = 0.32, RI = 0.73) The strict consensus of these trees is shown in Fig. 3. The majority of nodes had bootstrap support > 50%, with Bremer support as high as 13 (*Callithomia*), 18 (*Scada*) and 22 (*Methona*). Partitioned Bremer support indicated substantial conflict between the two data partitions (immature and adult stage), with only 16 of the 69 resolved nodes (23%) having positive support for both partitions.

Five of the eight currently recognized tribes (Lamas, 2004) were recovered as monophyletic, with the status of Mechanitini and Melinaeini unresolved and Dircennini paraphyletic, at least. The basal node is a polytomy of eight clades, resulting from five distinct topologies summarized with a representative genus from each clade in Fig. 4(A). In all trees a single clade is sister to remaining clades, either *Tithorea* (*Tithorea* + *Elzunia* + *Aeria*) one tree or *Methona* (four trees). Trees 3–5 are identical except in the placement of *Athesis* (*Athesis* + *Patricia*). In all cases neither Mechanitini or Melinaeini was monophyletic, and in four of the five trees their representative clades are far removed from one another.

The tribe Dircennini was paraphyletic, with *Callithomia* sister to a clade containing Godyridini and remaining Dircennini. The basal node of the latter clade was a polytomy of nine branches, resulting from 11 distinct topologies. In five of these topologies, members of the Dircennini form a clade sister to Godyridini. The remaining six consist of three basic topologies, summarized in Fig. 4(B), with the three unfigured topologies being similar to 1 with alternative topologies in the *Dircenna* + *Hyalenna* + *Haenschia* clade.

Total evidence analysis with successive approximations character weighting

A single round of SACW reduced the number of MPTs to a single tree, and tree length stabilized at 600 steps after a further round of weighting (CI = 0.51, RI = 0.81) (Fig. 5). Branches were relatively well supported, with 81 branches having a bootstrap value > 50% (average 81%), and Bremer support as high as

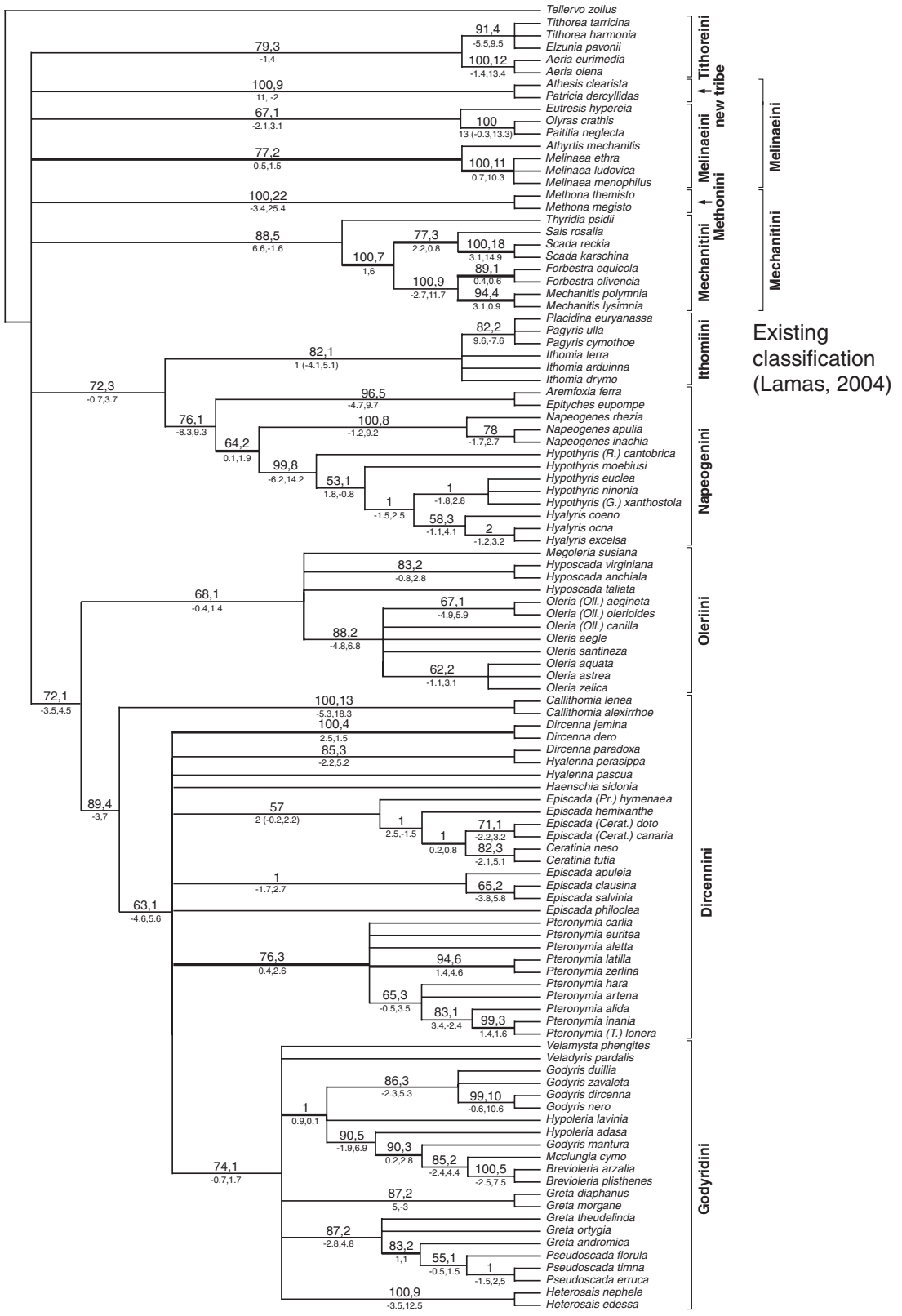

Fig. 3. Strict consensus of 1716 most parsimonious trees (length 1828, CI 0.32) for complete data matrix with 353 equally weighted characters. Bootstrap and Bremer support values above branches, partitioned Bremer support below (immature stages, chars 1–75, ecology and adult, chars 76–353). Branches in bold have positive Bremer support for both data partitions.

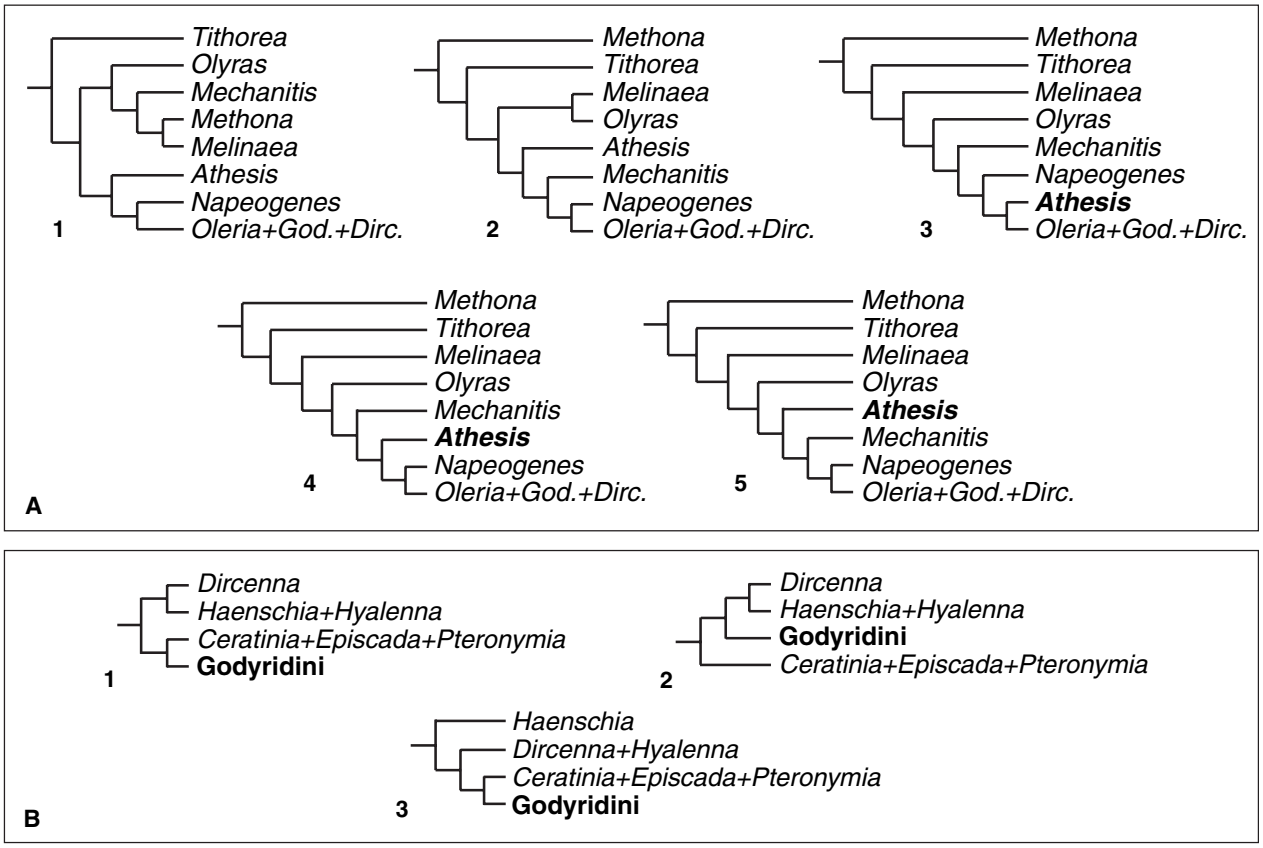

Fig. 4. Alternative tree topologies collapsed in consensus trees. (A) Alternative reduced MPTs from equally weighted analysis of all characters (Fig. 3), tribal level. (B) Alternative reduced MPTs from equally weighted analysis of all characters (Fig. 3), within Dircennini + Godyridini only, excluding *Callithomia*.

12.6 (*Methona*). Conflict between the immature stage and adult stage data sets was reduced substantially by SACW, with 61 of the 103 nodes (69%) having no conflict in partitioned Bremer support values (both partitions were positive, or one of the partitions was zero). Notably, poorly supported parts of the tree include the relationships between clade 17 and remaining tribal-level clades, between species in *Episcada* and *Ceratinia*, and between most of the Godyridini genera.

Much of the topology is similar to that of the equally weighted analysis, with the same five tribes monophyletic and Mechanitini, Melinaeini and Dircennini not monophyletic. However, *Methona* was placed as sister to *Aeria* + *Tithorea*, a topology not found in the equally weighted analysis, and this combined clade (clade 2) was sister to all other ithomiines (clade 5). Within clade 5, *Melinaea*, *Athyrtis*, *Paititia*, *Eutresis* and *Olyras* formed a clade sister to the remaining ithomiines (clade 10), as in some equally weighted trees. Within clade 10, *Athesis* + *Patricia* formed a clade sister to the remaining species (clade 12). Clade 12 consisted of Mechanitini (excluding *Methona*) sister to remaining tribes (clade 17). Clade 17 was similar topologically to the unweighted analysis, but Dircennini excluding *Callithomia* formed a clade sister to Godyridini, as in some equally weighted trees.

Partitioned analyses

The analysis of adult characters only (236 informative) found 2610 MPTs of length 1409 (CI = 0.33, RI = 0.74). One round of SACW reduced the number of MPTs to 3, which stabilized at length 483 after an additional round of weighting (CI = 0.52, RI = 0.81). The strict consensus of these three MPTs (Fig. 6A) differs from that from the equally weighted analysis (not shown) mainly in resolving the basal node, which was a polytomy of six clades including *Aeria*, *Tithorea* + *Elzunia*, *Methona*, *Athesis* + *Patricia*, Oleriini + Dircennini + Godyridini and Melinaeini + Mechanitini + Napeogenini.

With only immature stage characters included (70 informative), multiple MPTs of 349 steps (CI = 0.33, RI = 0.78) were found, with the search stopped at 10 000 trees. After SACW the number of MPTs remained above 10 000 (length 118.1 steps, CI = 0.52,

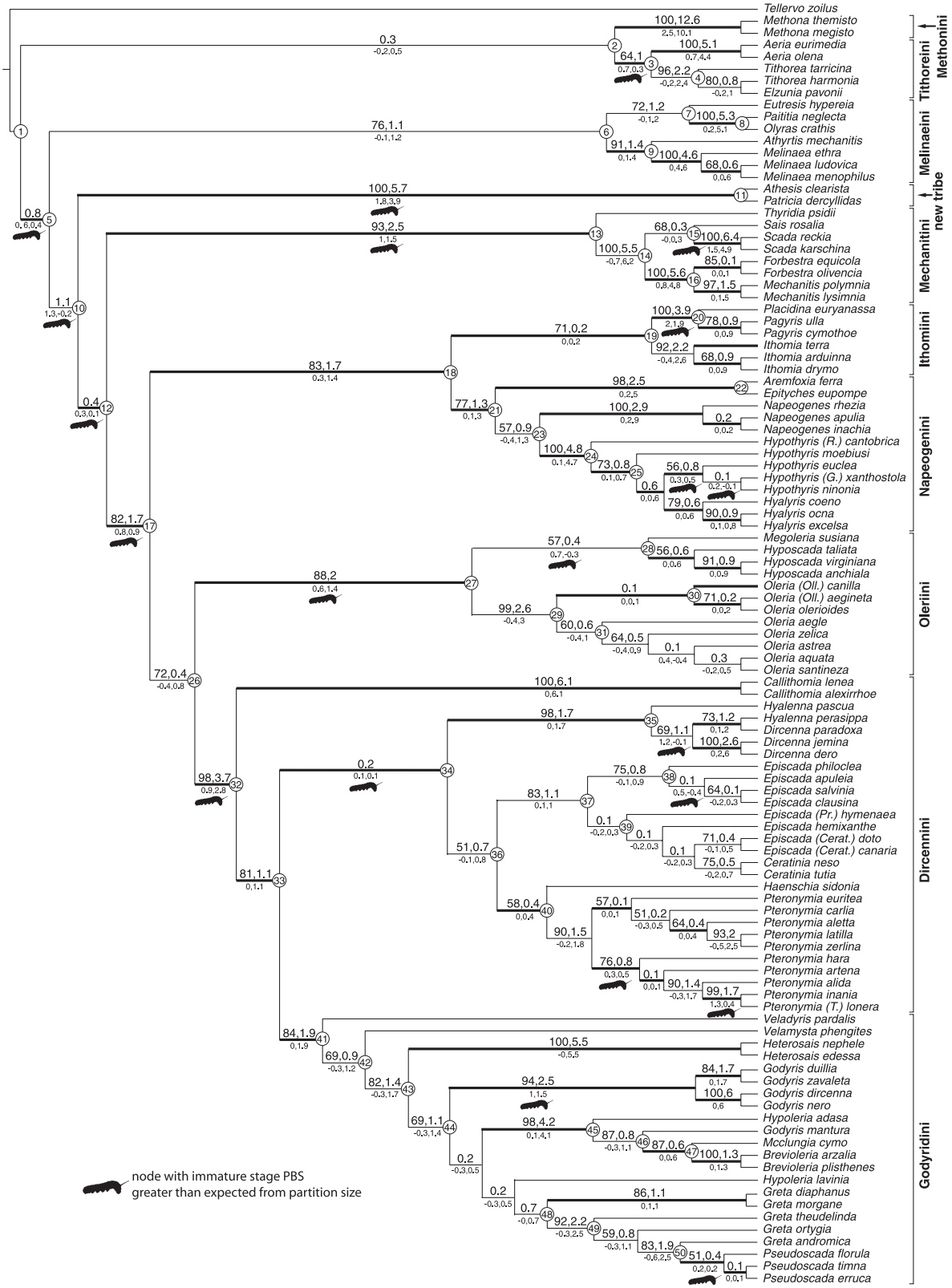

Fig. 5. Single most parsimonious tree (length 600, CI 0.51) for complete data matrix with 353 characters, after successive approximations weighting. Bootstrap and Bremer support values above branches, partitioned Bremer support below (immature stages, chars 1–75, adult, chars 76–353). Branches in bold have non-conflicting partioned Bremer support values. Nodes discussed in text and Table 2 are numbered.

Fig. 6. Strict consensus trees for partitioned character analyses. (A) Strict consensus of three MPTs (length 1857, CI = 0.31) from analysis of 236 informative adult and ecological characters after successive approximations character weighting. (B) Strict consensus of 10 000 MPTs (length 349, CI = 0.33) from analysis of 70 informative characters from immature stages. Taxa without immature stage data excluded.

RI = 0.83) with a slight increase in resolution of the strict consensus tree (Fig. 6B), although the basal node remained a polytomy of 11 clades.

The adult SACW consensus tree recovered the same tribal level clades as the total evidence SACW consensus tree, with the exception of *Aeria* + *Tithorea* and in placing *Callithomia* with remaining Dircennini, implying Dircennini as currently conceived (Lamas, 2004) is monophyletic. In contrast, the immature stage SACW consensus tree recovered only four of the 10 tribal level clades found in the total evidence SACW consensus tree. However, the deeper topology of the adult SACW tree differs significantly from the total evidence SACW tree in placing Melinaeini, Mechanitini, Ithomiini and Napeogenini as a single clade. Although relationships between members of these clades are poorly resolved in the immature stage SACW tree, this tree nevertheless has the major clade 17 as in the total evidence SACW analysis. Adding immature stage data to adult data therefore had the most significant effect on topology among the more basal nodes.

Homoplasy and distribution of support from partitioned data sets

Immature stage characters were more homoplasious than adult stage characters. The average consistency index for informative immature stage characters (1–75) in the total evidence SACW analysis was 0.42, while that for adult characters (76–353) was 0.52. In partitioned analyses, consistency and retention index values for MPTs were similar in the immature and adult data sets, even though the larger adult data matrix would be expected to have lower indices (Sanderson and Donoghue, 1989). In addition, 7% of immature stage character states could not be coded because of missing data; had these characters been known they would almost certainly have introduced additional homoplasy.

In the total evidence SACW analysis, 21 nodes had immature stage PBS values higher than expected from the ratio of immature to adult characters in the data matrix, and simple inspection of Fig. 5 suggests that these nodes tend to be more basal. The average number of nodes between the base of the tree and a given node was 9.17 ($n = 103$), the average for nodes supported by higher immature stage PBS values than expected was 7.76 ($n = 21$), and the average for nodes supported by higher adult stage PBS values than expected was 9.52 ($n = 82$). In the simulation analysis, of the 500 random samples of 21 nodes, 13 had average nodal distances of less than 7.76, indicating that immature stage characters tend to support branches nearer the base of the tree than expected by chance alone ($P = 0.026$). However, the distribution of support across the tree from adult characters did not differ from null expectations ($P = 0.302$).

Generic monophyly

The majority of currently recognized genera (Lamas, 2004) were found to be monophyletic in the total evidence SACW analysis. *Tithorea* was paraphyletic with respect to *Elzunia*, although there was only low, conflicting Bremer support for this hypothesis. *Hypothyris* contained *Hyalyris*, although, again, there was weak bootstrap and Bremer support for nodes within the inclusive clade (clade 24). Neither *Hyalenna* nor *Dircenna* proved to be monophyletic, though both form a strongly supported clade, with *Hyalenna pascua* sister to all other *Hyalenna* and *Dircenna* and *Hyalenna perasippa* sister to *Dircenna paradoxa*. *Episcada* was paraphyletic with respect to *Ceratinia*, which clustered with *E. canaria*, *E. doto* and *E. hemixanthe*. Within the Godyridini, *Godyris* proved to be polyphyletic, with *G. mantura* forming a very strongly supported clade with *Brevioleria*, *Mcclungia* and *Hypoleria adasa*. *Greta* was paraphyletic with the inclusion of the monophyletic *Pseudoscada*, with strong bootstrap and Bremer support values.

Evolution of hostplant choice

Hostplant records were obtained for 164 ithomiine species and *c*. 270 plant species, representing 572 butterfly–plant species interactions (Table 3). Genera with no confirmed records include *Paititia* (one sp.), *Athyrtis* (one sp.), *Sais* (one sp.), *Aremfoxia* (one sp.), *Haenschia* (four spp.) and *Veladyris* (one sp.). Although most ithomiine tribes and genera are polyphagous to some extent, almost all show a distinct preference for a particular plant clade (Table 3). Generic polyphagy typically reflects specific polyphagy (e.g., *Pteronymia artena* has been recorded on both *Solanum* and *Lycianthes*) rather than any finer scale specialization among species groups. The evolution of hostplant choice is shown in Fig. 7A, representing monomorphic coding of dominant hostplant clades only (Char H2, Table 3). Polymorphic coding of all recorded plant clades (Char H1, Table 3) produced similar results (not shown), except that the inferred ancestral character state for Napeogenini + Ithomiini was *Solanum*.

Discussion

Characters

A large amount of new character information was uncovered during this study. The immature stage data set of Brown and Freitas (1994) was significantly

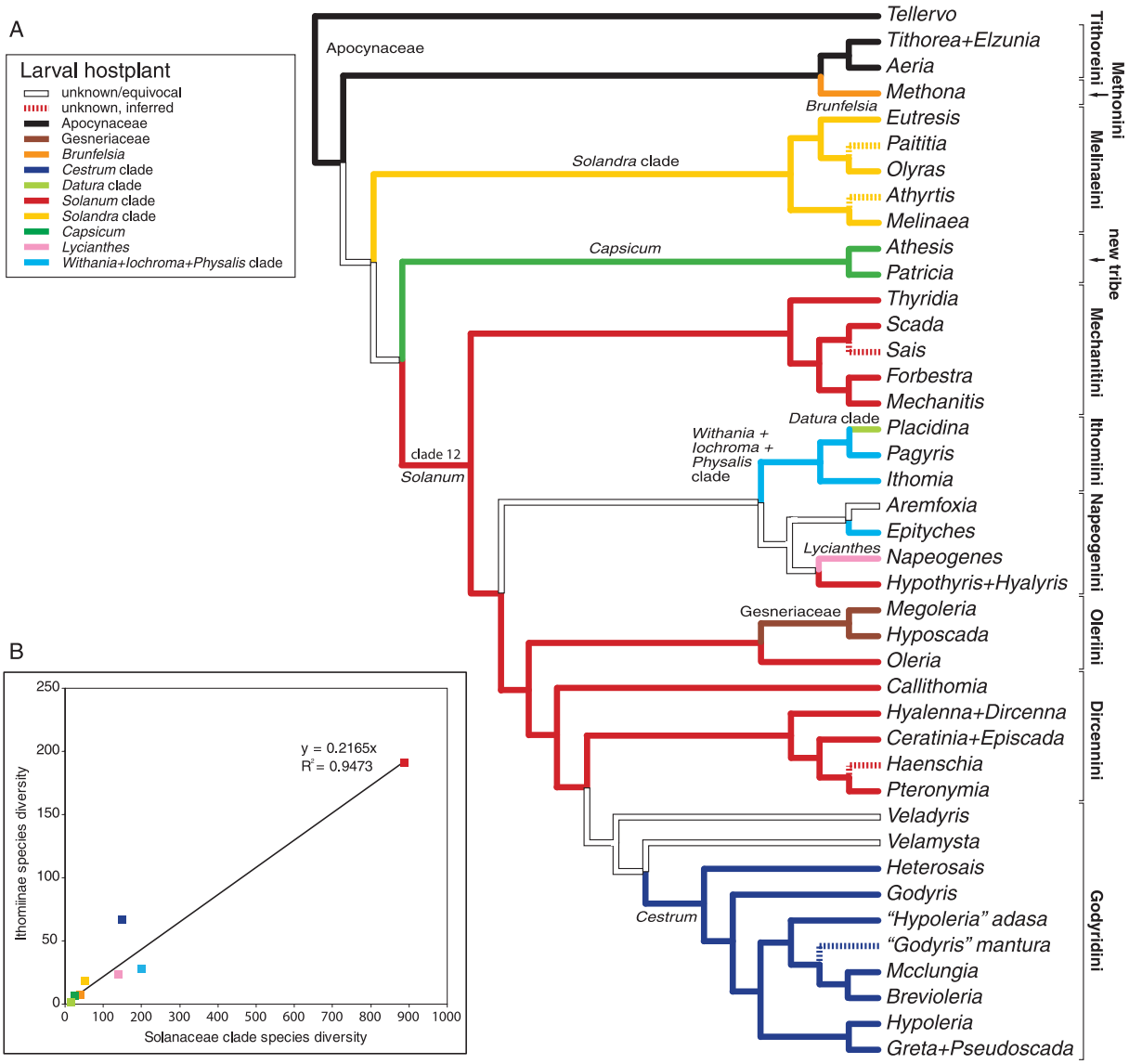

Fig. 7. (A) Optimization of preferred larval hostplant clades on to Ithomiinae generic level tree reduced from the SACW tree. (B) Relationship between Solanaceae clade diversity and associated ithomiine herbivore diversity.

expanded and revaluated with addition of new life history information, both for species that had been partially studied and for those for which we previously had no knowledge. As in the sister subfamily Danainae (Ackery and Vane-Wright, 1984), adult morphology also provided a wealth of characters. Both subfamilies have a rich diversity of androconial structures (e.g., Danainae, Boppré and Vane-Wright, 1989), and while these structures are much less elaborate in the Ithomiinae, they still provided 78 characters, almost all of which have not been coded previously, with 21 coded through scanning electron microscopy. Other novel character sources included body color and scale pattern (11 characters), the vesica and cornuti (13 characters), and in particular the female abdomen and genitalia (45 characters), about which Fox (1956, p. 17) once remarked: 'There is very little variation in the chitinous female genitalia, and I have made no attempt to analyze them systematically.' It is clear, then, that morphology can continue to provide important new character information even in groups that have been relatively well studied.

Despite the comparatively few characters coded from immature stages, there are two lines of evidence that suggest that these characters are especially important for resolving more basal nodes. First, while analyses of adult data alone or combined adult and immature stage data showed little difference in the more terminal clades,

there were marked differences among more basal nodes (Figs 5 and 6). Considering the higher homoplasy of immature stage characters this result must be due to relatively strong support for more basal nodes in the immature stage data compared with the adult data, demonstrating that the data sets are complementary. Secondly, partitioned Bremer support suggested that basal nodes tended to be more strongly supported by immature stage data than expected, and the simulation analysis confirms this hypothesis. In the context of a combined evidence analysis therefore immature stages provide particularly strong support for more basal nodes. The time and expense in obtaining life history information is therefore likely to be repaid in phylogenetic studies alone, as concluded in previous papers using this source of information (Kitching, 1984, 1985; Brown and Freitas, 1994; Freitas and Brown, 2004).

Deep tree topology

The inferred phylogeny from the total evidence analysis after SACW represents our preferred hypothesis for ithomiine relationships and forms the basis for the following discussion. The SACW tree was broadly similar to other phylogenetic studies (Brown and Freitas, 1994; Brower et al., 2006), and would have been recognizable even to Doubleday as he prepared his classification of the subfamily over 150 years ago (Doubleday, 1847). The subfamily is divisible into two sections: genera placed by Fox in the Tithoreini, Melinaeini and Mechanitini, and the remaining genera, in the Napeogenini, Ithomiini, Oleriini, Dircennini and Godyridini, which form a clade (clade 17). The latter five tribes were also found to form a clade by Brown and Freitas (1994; with the exception of *Placidina*) and by Brower et al. (2006), and are convincingly united by the pale first instar thoracic legs (Char 13:1) and pitchfork-shaped ground scales in transparent wing areas (Char 146:3), among other synapomorphies. Within clade 17 Dircennini and Godyridini form a strongly supported clade, although their sister group is uncertain, with the Oleriini identified in our analysis but Napeogenini by Brower et al. (2006). Brown and Freitas (1994) found a third topology, with Oleriini + Napeogenini + Ithomiini forming a clade. No unique synapomorphies support Oleriini as sister to Dircennini + Godyridini (clade 26), and only a single character is relatively convincing, the fusion of the expanded base of the uncus with the appendices angulares (Char 283:1).

Within the first section the relationships between major clades remains uncertain. Clade 5 is not upheld by any very convincing characters (except possibly a larval shift to Solanaceae—see below) and has weak support, although clade 10 is supported by the loss of body rings in the first instar larva (Char 15:1) and absence of a dorsal black stripe on the 8–9th abdominal segment suture in the last instar larva (Char 72:1). Clade 12 excludes *Methona* and all ithomiines placed by Fox in Tithoreini (Fox, 1956), and is also found in analyses of molecular data (Brower et al., 2006). Despite low bootstrap and Bremer support it has several significant apomorphies, including: loss of larval subdorsal filaments (Char 22:1, also inferred to be independently lost in *Methona*), gain of a lateral larval stripe (Char 46:1, later lost in clade 32, Dircennini + Godyridini), white to yellow ventral larval color (Char 51:1, changing to 51:2 in clade 33) and fused male foreleg tibia and tarsus (Char 100:2, independently fused in *Aeria* and some *Melinaea* and *Methona*).

Tribal classification

Aeria, *Tithorea* and *Elzunia*, the only ithomiine genera known to feed on Apocynaceae, form a clade (Fig. 5, clade 3), with moderate support from both immature and adult stages, and were treated as the Tithoreini by Lamas (2004). As Apocynaceae are also the larval hostplants of the outgroup *Tellervo*, this association is either a symplesiomorphy or synapomorphy, depending on optimization. Only one character (Char 167:1), the extent of male dorsal hindwing androconial scales, is a unique autapomorphy for Tithoreini, and cannot be assessed in the genus *Elzunia* due to partial loss of these scales. Nevertheless, the monophyly of Tithoreini seems likely and has been corroborated in other studies (Motta, 2003; Brower et al., 2006).

The affinities of the small genus *Methona* remain almost as unclear as they have ever been. This genus appears in different positions in most analyses, and the final hypothesis of a sister relationship with Tithoreini is novel but was also suggested by Brower et al. (2006). However, bootstrap, Bremer and character support for this relationship are weak, with only two unambiguous synapomorphies, both also occurring in other relatively close genera. Whatever the relationships of the genus, it is so highly autapomorphic we believe it should be treated in its own tribe, for which the name Methonini Mielke and Brown, 1979, is already available.

The tribe Melinaeini as currently conceived (Lamas, 2004) is paraphyletic, with *Athesis* + *Patricia* forming a separate, strongly supported clade in all analyses (Harvey, 1991; Brown and Freitas, 1994; Brower et al., 2006) that is diagnosed by numerous synapomorphies. With the removal of the latter two genera, which require a new tribe, Melinaeini (clade 6) is monophyletic and relatively strongly supported.

Mechanitini are monophyletic and strongly supported, with the inclusion of *Thyridia*, which was, however, suggested by Brower et al. (2006) to be sister to *Methona*. Particularly convincing synapomorphies for the genera in Mechanitini include lateral tubercles just

above the prolegs (Char 27:1), the four-segmented female foretarsus (Char 102:1), anteriorly projecting gnathos (Char 285:1), and attenuated corpus bursae (Char 349:1).

Oleriini, Ithomiini and Napeogenini are each monophyletic and well supported, with *Placidina* strongly supported as a member of Ithomiini, sister to *Pagyris*, in both partitioned analyses and the total evidence analysis. The monotypic south-east Brazilian *Epityches*, suggested by Brown and Freitas (1994) to possibly merit its own tribe, was well supported as sister to the monotypic Andean *Aremfoxia*, with both forming a clade sister to remaining Napeogenini. The sister relationship between Ithomiini and Napeogenini was also robust, and the topology of the clade containing these two tribes (clade 18) is the same as that found by Brower et al. (2006).

The analyses of Brown and Freitas (1994) found *Callithomia*, *Velamysta* and *Pteronymia lonera* (as *Talamancana lonera*) to be sister to remaining Dircennini + Godyridini. The total evidence SACW tree also placed *Callithomia* in a similar position, but *Velamysta* is within the well supported Godyridini and *P. lonera* is sister to *P. inania* within *Pteronymia*. Adult characters alone recovered a monophyletic Dircennini, as did Brower et al. (2006), so a combined morphological and molecular analysis should establish the true systematic position of *Callithomia*.

Generic classification

This study represents the first attempt to test the monophyly of ithomiine genera using cladistic methods, and a number of problems were uncovered in the four most diverse tribes. In Napeogenini, the only one of these tribes that has been subjected to recent systematic revision, *Hypothyris* proved paraphyletic with respect to *Hyalyris*. In their revision of both of these genera, Fox and Real (1971, p. 100) stated: "[*Hyalyris*] is distinguished from *Hypothyris* not so much by any single, well emphasized, consistent structural difference, as by the fact that in nearly every morphologic detail, there is some variation, often slight … sufficient to justify generic separation." Fox and Real (1971) also placed *Hypothyris cantobrica* and *H. xanthostola* in the monotypic *Rhodussa* and *Garsauritis*, respectively. While *H. cantobrica* is basal to remaining species, *H. xanthostola* appeared here as sister to *H. ninonia*, the type of the *Hypothyris*, justifying the recent synonymy of *Garsauritis* (Lamas, 2004). Even though *Hyalyris* was monophyletic, there are no clear synapomorphies, especially when other members of the genus are considered, and a species-level study is necessary to resolve the classification of this assemblage.

Ten years ago Brown and Freitas (1994) described the genus *Ollantaya* to include *Ithomia canilla* Hewitson, *Ithomia aegineta* Hewitson and *Leucothyris baizana* Haensch. However, *Ollantaya* was recently synonymized with *Oleria* by Lamas (2004). The first two of these species form a clade sister to remaining *Oleria*, with the inclusion of *Hyposcada olerioides* D'Almeida, a result confirmed by molecular data (A. Whinnett, pers. comm.). An undescribed species from the Peruvian Andes is also an apparent member of this clade (Lamas and Willmott, unpub. data), but morphological and molecular data place *Leucothyris baizana* near to *Oleria santineza* (Willmott, unpub. data, A. Whinnett, unpub. data.). *Ollantaya* might therefore be resurrected for *canilla*, *aegineta*, *olerioides* and the new species, but the systematic position of *Oleria aegle* is uncertain, as it lacks the synapomorphies of either *Ollantaya* or remaining *Oleria*. Hopefully, molecular data currently under study will provide a solution.

The systematics of *Hyalenna* and *Dircenna* have been addressed by Willmott and Lamas (2006), who concluded that *Ithomia paradoxa* should be transferred to *Hyalenna*. Elsewhere in the Dircennini, there are clear problems with the classification of *Episcada*, *Ceratinia* and relatives. *Ceratinia* forms a clade with several species often placed in different genera, including *Episcada canaria*, *E. doto* (formerly both placed in *Ceratiscada*), *E. hemixanthe* (formerly placed in *Pteronymia*) and *E. hymenaea* (formerly placed in *Prittwitzia*). Despite weak branch support for relationships in this clade, there is no evidence that *Episcada* as currently conceived is monophyletic, and a species-level analysis including molecular data is necessary.

In the Godyridini, there is strong evidence showing *Godyris mantura* to be distantly related to other *Godyris*. This species shares a number of synapomorphies with *Ithomia cleomella* Hewitson and two undescribed Andean species and should be placed in a new genus (Willmott and Lamas, unpub. data). *Hypoleria adasa* clustered with *G. mantura*, *Mcclungia* and *Brevioleria*, with strong branch support, so *Hypoleria* will need to be subdivided. Finally, the small genus *Pseudoscada* appeared within *Greta*, one of the largest ithomiine genera, a position with strong branch and character support. The type species of *Greta*, *G. diaphanus*, formed a relatively isolated clade with *G. morgane*, so *Greta* should probably be restricted to include only these two species. While it seems likely that certain other *Greta* species form a monophyletic group, especially the high Andean *G. theudelinda*, *G. ortygia* and most remaining species, there are no synapomorphies yet known that support this hypothesis and a species-level analysis is called for.

Larval hostplant choice and ithomiine diversification

The tight association between the diverse, exclusively neotropical Ithomiinae and their speciose, largely

neotropical larval hostplant family Solanaceae has been studied in admirable depth and detail by Keith Brown and co-workers since the early 1980s (e.g., Brown, 1984, 1985, 1987; Drummond, 1986; Brown et al., 1991; Trigo et al., 1996). Early studies of the Ithomiinae–Solanaceae interface tested Ehrlich and Raven's (1965) hypothesis of plant–herbivore coevolution, but found little positive evidence for simultaneous diversification (Brown, 1985). Our results support earlier conclusions that there is no evidence for phylogenetic tracking between Solanaceae hosts and ithomiine herbivores (Drummond, 1986; Brown, 1987). For example, the relatively basal Melinaeini use the relatively derived *Solandra* clade, while Godyridini specialize on the relatively primitive *Cestrum* (Olmstead et al., 1999) (Table 3; Fig. 7A).

The origin of Ithomiinae larval feeding on Solanaceae has been seen as a key event in the diversification of the butterfly group (Brown, 1987; Brown and Henriques, 1991). *Tellervo*, the likely sister to the Ithomiinae, feeds on Apocynaceae (Ackery, 1987), as do many Danainae (Ackery and Vane-Wright, 1984), and this seems a plausible ancestral hostplant for the subfamily. Nevertheless, our phylogenetic hypothesis (and that of Brower et al., 2006) suggests either that two independent shifts occurred on to Solanaceae (*Methona* and clade 5), or that the shift on to Solanaceae by the ancestor of the subfamily was followed by reversal to Apocynaceae by Tithoreini (clade 3). Exclusion of larval hostplant as a character in the matrix does not affect this scenario. Discrimination between these two hypotheses may not be possible using phylogenetic methods, but resolution of the position of *Methona*, which feeds exclusively on the Solanaceae genus *Brunfelsia*, might settle the question. Brown (1987, p. 380) reported that *Aeria* larvae did not accept any Solanaceae in captivity and Freitas (1999) found that *Methona* can accept *Prestonia* (Apocynaceae) in experiments of host shift, so two origins of Solanaceae feeding is perhaps the more plausible hypothesis given our phylogeny. Regardless of how Solanaceae was colonized, however, we suggest that it was not a shift to Solanaceae *per se* that facilitated Ithomiinae diversification, but further specialization on distinct Solanaceae clades, which are usually exclusive to a single ithomiine clade (Fig. 7A).

In addition to *Methona*, the two basal tribes Melinaeini and new tribe (*Athesis* + *Patricia*) are also specialists on different plant clades, also used very infrequently by other ithomiine tribes. All Melinaeini are entirely restricted to the *Solandra* clade, on which only two other ithomiines have been recorded feeding (*Pteronymia carlia*, Dircennini; unidentified species, probably *Hypothyris*). Oleriini and Mechanitini can also readily accept *Juanulloa* (*Solandra* clade) as an alternative hostplant in captivity (Brown and Freitas, 1994; Freitas, 1999). Many members of the *Solandra* clade are hemi-epiphytes, and female Melinaeini are usually scarce in the forest understorey, presumably because they spend much time searching for hostplants in the canopy (Beccaloni, 1997b). *Athesis* and *Patricia* have almost identical immature stages, both feeding on *Capsicum*, which is used occasionally in nature by *Epityches* and *Ithomia* in the sister tribes Napeogenini and Ithomiini.

The vast genus *Solanum* is used by members of six tribes, the Mechanitini, Ithomiini, Napeogenini, Oleriini, Dircennini and Godyridini (Table 3). Brown (1987) proposed that existing adaptations among Ithomiinae to classes of secondary chemicals in ancestral hostplants permitted colonization of new, chemically similar and already diversified hosts. He suggested that at least four radiations of Ithomiinae showed similar patterns of host colonization, with shifts on to *Capsicum* and the *Solandra* clade leading to feeding on *Solanum*, and a cladogram indicating hypothesized patterns was presented by Brown and Henriques (1991, fig. 4.6). Our phylogeny and optimization of hostplant states suggests, however, that only a single shift on to *Solanum* occurred, at the base of clade 12 (Fig. 7A). Although we found no evidence for the ancestral hostplant before this shift, both the *Solandra* clade and *Capsicum* are occasionally used by members of clade 12 and thus possible candidates.

Clade 12 includes all species with non-"danaoid" larvae, which lack complete body color rings and flexible thoracic tubercles. Among the basal tribes of Ithomiinae outside clade 12, data suggesting chemical protection of the immature stages are known only for the tribe Tithoreini, whose larvae have been shown to sequester pyrrolizidine alkaloids from their apocynaceous hostplants (Trigo and Brown, 1990). There are no data of this kind available for *Methona*, Melinaeini or *Athesis* + *Patricia*, but the aposematic larval color pattern and behavior in these clades are similar to those of Tithoreini (Fig. 9H,R) and of most danaines (Brown and Freitas, 1994). Larvae within these tribes may also therefore have some chemical protection and larvae of *Methona* are reportedly rejected by young birds (Massuda and Trigo, pers. comm.). In contrast, the largely cryptic larvae of species in clade 12 appear to be palatable to predators (with two possible exceptions, Freitas et al., 1996; Massuda and Trigo, pers. comm.), although a novel defense mechanism has recently been discovered involving chemical camouflage from predatory ants through similarity of larval and plant cuticular lipids (Portugal and Trigo, 2005). Additional information on behavior and chemical protection within Ithomiinae will therefore surely lead to a better understanding of the ecological shifts associated with the origin of clade 12.

Although all tribes in clade 12 feed on *Solanum*, there are at least four main shifts in preferred hostplant. The

Ithomiini are concentrated on a clade of small, chemically similar genera (Brown, 1987) and *Napeogenes* feed almost exclusively on *Lycianthes*, with both sharing these resources with a few other ithomiines. The shift by *Megoleria* and *Hyposcada* on to Gesneriaceae, which is used only by these two sister genera, remains to be investigated. Finally, another important host shift occurs near the base of the Godyridini, the second largest ithomiine tribe, on to *Cestrum*, the second largest Solanaceae genus. Brown (1987) suggested that this shift might have been facilitated by the presence of a similar, pungent oil in *Cestrum* and *Solanum* section *Geminata* (the predominant group used by the Dircennini), and our phylogeny is consistent with this hypothesis, with *Cestrum*-feeders evolving from a *Solanum*-feeding ancestor.

The overall picture then, of specialization by ithomiine tribes and generic clades on particular plant clades, with relatively little overlap, suggests the possibility of multiple instances of adaptive radiation driven by new ecological opportunities (Simpson, 1953). Schluter (2000) outlined four criteria for diagnosing adaptive radiation, including common ancestry, a correspondence between divergent traits and different niches, evidence that particular traits enhance fitness within particular niches, and correlation between key adaptations and increased speciation rate. The first and last of these criteria can be considered in the light of our results, while the second and third are now briefly reviewed.

Within clades of sympatric ithomiines, larvae frequently specialize on different, but often related, hostplant species (Willmott and Mallet, 2004). Whether such specialization might represent resource partitioning to reduce competition from other herbivores (as proposed for *Heliconius* butterflies; Benson, 1978), limit attacks by parasitoids and predators, or is a by-product of other niche shifts, such as a change in adult microhabitat, remains largely unexplored. Two other divergent traits likely correlated with larval hostplant are adult wing pattern and microhabitat preference. Adults of all Ithomiinae have warningly colored wing patterns that advertise their unpalatability, and are mimetic, facilitating learning in predators (Bates, 1862; Müller, 1879). Ithomiine communities may contain up to eight or more distinct types of warning color pattern, or mimicry rings (Beccaloni, 1997a), with evidence for comimetic species flying within the same area of forest (DeVries et al., 1999) and at the same height above ground (Beccaloni, 1997b). Species that share larval hostplant are often mimetic (Willmott and Mallet, 2004), suggesting that plant microhabitat and adult flight microhabitat are linked (Beccaloni, 1997b). However, despite the accumulating evidence for correlations between traits and hostplants, little research to date has tested whether such traits directly enhance fitness.

Considering the remaining two criteria for adaptive radiation, our results indicate that most ithomiines which specialize on the same hostplant clade do form monophyletic groups (Fig. 7A), with the occasional exclusion of one to a few other clades. Exploitation of a new clade of plants can be seen as a key innovation providing access to a formerly underutilized or vacant resource, and may be accompanied by a suite of adaptations. Thus colonization of the largely hemiepiphytic *Solandra* clade might require ovipositing Melinaeini females to identify new hostplants, novel mimicry patterns in adults to provide protection from predators in the subcanopy, and larval ability to overcome plant physical and chemical defenses and avoid predation and parasitism. The two largest tribes, Dircennini and Godyridini, which dominate understorey ithomiine communities and feed on the diverse *Solanum* and *Cestrum* growing there, have the most highly transparent wing patterns, a trait hypothesized to enhance protection from predators in low light conditions (Brown, 1988).

Access to new hostplants is likely to provide opportunities for adaptive speciation, so we might expect plant diversity to be correlated with herbivore diversity and important host shifts to be associated with an increase in speciation rate. Using the phylogeny and optimized hostplant character states we inferred the number of ithomiine species that feed on each plant clade, and there is indeed a strong positive correlation between plant and associated herbivore clade diversity, at least within the Solanaceae (Table 4; Fig. 7B; $P < 0.01$). This is not simply an artifact of more diverse ithomiine clades having a broader host range, as there is no correlation between plant generic diversity and ithomiine diversity (Table 4). Larger ithomiine clades might also have broader geographic ranges and access to more plant species, but there is no strong correlation between clade and range size, with many small ithomiine genera (e.g., *Mechanitis*, *Tithorea*, *Dircenna*, *Ceratinia*) being very widespread (Willmott, unpub. data).

Solanum comprises about 70% of neotropical Solanaceae (Hunziker, 1979), and clade 12 (*Solanum* feeders) comprises 89% of the Ithomiinae, so the shift on to *Solanum* is perhaps the most significant event in ithomiine hostplant evolution. Although host shifts away from *Solanum* occur in several clades within clade 12, we suggest such shifts are likely to have been facilitated by the evolution of morphological, biochemical and/or behavioral traits, which accompanied the original shift to *Solanum*. Using the test of clade imbalance proposed by Slowinski and Guyer (1989), clade 12 (328 spp.) is significantly more diverse than its sister clade 11 (*Athesis* + *Patricia*, six spp.; $P = 0.04$), but given uncertainties regarding topology in this part of the tree, the test provides no strong support for increased speciation. Nevertheless, the correlation

Table 4
Taxon diversity in clades of Solanaceae plants and inferred Ithomiinae herbivores

Solanaceae clade	Plant species diversity	Plant generic diversity	Ithomiineae species diversity	Clade diversity	Notes
Datura	16	2	1	Nee (2001a)	
Capsicum	25	1	6	Nee (2001a)	
Brunfelsia	40	1	7	Nee (2001a)	
Solandra	52	9	18	Nee (2001a)	
Lycianthes	140	1	23	Nee (2001b, p. 109) slightly smaller than Cestrum	Plant species number an estimate, Hunziker (1979) estimates 250 species
Withania, etc. clade	202	15	28	Nee (2001a)	Half plant species diversity in single genus *Physalis*, with center of diversity in Mexico at limit of Ithomiinae range
Cestrum	150	1	66	Nee (2001b)	Plant species number an estimate, Hunziker (1979) estimates 250 species
Solanum	888	1	191	Nee (2001a)	Plant species number an estimate

between other host shifts and higher taxonomic categories is notable. Although the rank and inclusiveness of higher taxa are arbitrary, the features that led initially to their recognition, namely relatively greater character distance between them in comparison with character distances between their members, are consistent with an increase in speciation rate.

To conclude, ecological study to date suggests that shifts in hostplant species are likely to be associated with a number of trait shifts in ithomiines, of which microhabitat and wing pattern (Jiggins et al., 2001) in particular are likely to lead to reproductive isolation. Hostplant interactions are thus likely to have played a key role in Ithomiinae speciation. Phylogenetic patterns are consistent with this hypothesis, and it seems likely that the diversity of new niches presented by *Solanum* and other plant clades was important in increasing ithomiine diversification through ecological speciation.

Conclusions and future work

The phylogeny presented here is the most detailed hypothesis to date of ithomiine relationships, and in combination with molecular data (Brower et al., 2006) will provide a solid foundation for tribal classification. While some tribal relationships are firmly supported (Napeogenini + Ithomiini, Dircennini + Godyridini, and monophyly of these four tribes plus Oleriini), others (especially between Tithoreini, *Methona*, Melinaeini and *Athesis* + *Patricia*) are weakly resolved and tend to differ depending on what characters are included, in both morphological and molecular data sets. It therefore seems unlikely that combination of existing data sets alone will convincingly resolve these relationships, and we suggest that additional character sources such as those from the egg and first instar larva (e.g., Motta, 2003) and additional gene regions (e.g., *tektin*, Whinnett et al., 2005a) should be examined.

There exist clear problems with generic classification in each of the four most diverse tribes (Napeogenini, Oleriini, Dircennini and Godyridini), with at least five genera paraphyletic or polyphyletic. Morphological characters identified here will permit a revision of several of these genera (e.g., *Godyris mantura* and relatives), but more intensive morphological and molecular sampling will be required in other cases (e.g., *Episcada*, *Ceratinia* and relatives). The position of the recently described genus *Haenschia* remains poorly resolved and any information on the immature stages could prove significant in establishing its true position.

Knowledge of ithomiine hostplants may be the most detailed available for any diverse (> 200 spp.) neotropical butterfly group and there are clear macroevolutionary patterns emerging. Nevertheless, there remains much work to be done in the field of ithomiine hostplant ecology. We have little knowledge of whether hostplant differences are maintained by adult microhabitat specialization or female recognition of specific chemical cues (Brown, 1987), and which of these adaptations occurs first. Furthermore, much detailed ecological study is required to determine whether host shifts are driven by improved larval growth rates, reduced predation and parasitism, adult microhabitat shifts, or other factors. Finally, more detailed molecular phylogenies will permit identification of periods of increased speciation rate (Nee et al., 1996) and therefore provide a better understanding of the role of adaptive radiation in the evolution of the Ithomiinae.

Acknowledgments

We thank the museum curators who permitted us to examine and borrow specimens for morphological study, including Phil Ackery (Natural History Museum, London), Lee and Jackie Miller (Allyn Museum, Sarasota, now at Florida Museum of

Natural History, Gainesville), Wolfram Mey (Museum für Naturkunde, Berlin), Matthias Nuss (Staatliches Museum für Tierkunde, Dresden), Heinz Schröder (Senckenberg Museum, Frankfurt am Main), Axel Hausmann (Zoologische Sammlung des Bayerischen Staates, Munich), Miguel Monné (Museu Nacional do Rio de Janeiro, Rio de Janeiro), Olaf Mielke (Universidade Federal do Paraná, Curitiba), Marcelo Duarte (Museu de Zoologia da Universidade de São Paulo, São Paulo), Bob Robbins (National Museum of Natural History, Washington, DC) and Eric Quinter (American Museum of Natural History, New York). We are very grateful to Gerardo Lamas for his assistance with numerous taxonomic matters and insightful discussions into Ithomiinae systematics and morphology, and Keith Brown for his exceptional work on ithomiines, enthusiasm and encouragement which have proved so inspirational in our own research. We thank Dick Vane-Wright and two anonymous reviewers for thoughtful comments on the manuscript and Andrei Sourakov and George Beccaloni for providing immature stage specimens and photographs of *Greta diaphanus* and *Hyposcada anchiala*, respectively. KRW thanks Julia Robinson-Willmott, Ismael and Raul Aldas for field assistance, Sandy Knapp for identifying Solanaceae hostplants, and S. Knapp and Michael Nee for comments on Solanaceae diversity. Permits for fieldwork in Ecuador were provided by the Ministerio del Ambiente and Museo Ecuatoriano de Ciencias Naturales, Quito. Museum and field work of KRW was funded by Leverhulme Trust Standard Research Project grant F/00696/C, and field work by the National Geographic Society (Research and Exploration grant no. 5751-96) and National Science Foundation (Biodiversity Surveys & Inventories grant no. 0103746). AVLF was funded by Fapesp, Faepex and the National Science Foundation (Fapesp grants 00/01484-1 and 04/05269-9 to AVLF; BIOTA-FAPESP program—98/05101-8; NSF DEB-0316505). AVLF thanks Ronaldo Bastos Francini (Unisantos, Santos), Paulo Cesar Motta (UnB, Brasília), Keith S. Brown Jr., José Roberto Trigo, João Vasconcellos-Neto (Unicamp, Campinas), Marco Aurélio Pizo (Unisinos, São Leopoldo) and Sandra Inês Uribe (Unalmed, Medellín) for assistance in fieldwork and for providing material for many species of Ithomiinae.

References

Ackery, P.R., 1987. The danaid genus *Tellervo* (Lepidoptera, Nymphalidae)—a cladistic approach. Zool. J. Linn. Soc. 89, 203–274.

Ackery, P.R., Vane-Wright, R.I., 1984. Milkweed Butterflies. Their Cladistics and Biology. British Museum (Natural History), London.

Ackery, P.R., De Jong, R., Vane-Wright, R.I., 1999. The butterflies: Hedyloidea, Hesperioidea and Papilionoidea. In: Kristensen, N.P. (Ed.) Lepidoptera: Moths and Butterflies. 1. Evolution, Systematics and Biogeography. Handbook of Zoology, 4(35), Lepidoptera. De Gruyter, Berlin, pp. 263–300.

Arms, K., Feeny, P., Lederhouse, R.C., 1974. Sodium: stimulus for puddling behavior by tiger swallowtail butterflies, *Papilio glaucus*. Science 185, 372–374.

Baker, R.H., DeSalle, R., 1997. Multiple sources of character information and the phylogeny of Hawaiian drosophilids. Syst. Biol. 46, 654–673.

Barker, F.K., Lutzoni, F.M., 2002. The utility of the Incongruence Length Difference Test. Syst. Biol. 51, 625–637.

Bates, H.W., 1862. Contributions to an insect fauna of the Amazon Valley. Lepidoptera: Heliconidae. Trans. Linn. Soc. Lond. 23, 495–566.

Beccaloni, G.W., 1997a. Ecology, natural history and behaviour of ithomiine butterflies and their mimics in Ecuador (Lepidoptera: Nymphalidae: Ithomiinae). Trop. Lepid. 8, 103–124.

Beccaloni, G.W., 1997b. Vertical stratification of ithomiine butterfly (Nymphalidae: Ithomiinae) mimicry complexes: the relationship between adult flight height and larval host-plant height. Biol. J. Linn. Soc. 62, 313–341.

Benson, W.W., 1978. Resource partitioning in passion vine butterflies. Evolution, 32, 493–518.

Boppré, M., Vane-Wright, R.I., 1989. Androconial systems in Danainae (Lepidoptera): functional morphology of *Amauris*, *Danaus*, *Tirumala* and *Euploea*. Zool. J. Linn. Soc. 97, 101–133.

Brabant, R., 2004. Un nouvel Ithomiide, originaire du centre du Perou. Lambillionea, 104, 423–428.

Bremer, K., 1988. The limits of amino acid sequence data in angiosperm phylogenetic reconstruction. Evolution, 42, 795–803.

Bremer, K., 1994. Branch support and tree stability. Cladistics, 1, 295–304.

Brévignon, C., 2003. Inventaire des Ithomiinae de Guyane Francaise (Lepidoptera, Nymphalidae). Lambillionea, 103, 41–58.

Brower, A.V.Z., 2000. Phylogenetic relationships among the Nymphalidae (Lepidoptera) inferred from partial sequences of the *wingless* gene. Proc. R. Soc. Lond. B, 267, 1201–1211.

Brower, A.V.Z., Freitas, A.V.L., Lee, M.-M., Silva Brandão, K.L., Whinnett, A., Willmott, K.R., 2006. Phylogenetic relationships among the Ithomiini (Lepidoptera: Nymphalidae) inferred from one mitochondrial and two nuclear gene regions. Syst. Entomol., 31, 288–301.

Brown, K.S., 1967. Chemotaxonomy and chemomimicry: the case of 3-hydroxy-kynurenine. Syst. Zool. 16, 213–216.

Brown, K.S., 1977a. Geographical patterns of evolution in neotropical Lepidoptera: differentiation of the species of *Melinaea* and *Mechanitis* (Nymphalidae: Ithomiinae). Syst. Entomol. 2, 161–197.

Brown, K.S., 1977b. Centros de evolução, refúgios quaternários e conservação de patrimônios genéticos na região neotropical: padrões de diferenciação em Ithomiinae (Lepidoptera: Nymphalidae). Acta Amaz. 7, 75–137.

Brown, K.S., 1980. A review of the genus *Hypothyris* Hübner (Nymphalidae), with descriptions of three new subspecies and the early stages of *H. daphnis*. J. Lep. Soc. 34, 152–172.

Brown, K.S., 1982. Historical and ecological factors in the biogeography of aposematic neotropical butterflies. Am. Zool. 22, 453–471.

Brown, K.S., 1984. Adult-obtained pyrrolizidine alkaloids defend ithomiine butterflies against a spider predator. Nature 309, 707–709.

Brown, K.S., 1985. Chemical ecology of dehydropyrrolizidine alkaloids in adult Ithomiinae (Lepidoptera: Nymphalidae). Rev. Bras. Biol. 44, 453–460.

Brown, K.S., 1987. Chemistry at the Solanaceae/Ithomiinae interface. Ann. Missouri Bot. Gdn. 74, 359–397.
Brown, K.S., 1988. Mimicry, aposematism and crypsis in neotropical Lepidoptera: the importance of dual signals. Bull. Soc. Zool. Fr. 113, 83–119.
Brown, K.S., D'Almeida, R.F., 1970. The Ithomiinae of Brazil (Lepidoptera: Nymphalidae). II. A new genus and species of Ithomiinae with comments on the tribe Dircennini d'Almeida. Trans. Am. Entomol. Soc. 96, 1–18.
Brown, K.S., Freitas, A.V.L., 1994. Juvenile stages of Ithomiinae : overview and systematics (Lepidoptera: Nymphalidae). Trop. Lepid. 5, 9–20.
Brown, K.S., Henriques, S.A., 1991. Chemistry, co-evolution, and colonisation of Solanaceae leaves by ithomiine butterflies. In: Hawkes, J.G., Lester, R.N., Nee, M., Estrada, N. (Eds.), Solanaceae III: Taxonomy, Chemistry, Evolution. Linnean Society of London, London, pp. 51–68.
Brown, K.S., Mielke, O.H.H., Ebert, H., 1970. Os Ithomiinae do Brasil. I: *Prittwitzia* g. n. para *Ithomyia hymenaea* Prittwitz e suas subespécies (Lepidoptera, Nymphalidae). Rev. Bras. Biol. 30, 269–273.
Brown, K.S., Trigo, J.R., Francini, R.B., Morais, A.B.B., Motta, P.C., 1991. Aposematic insects on toxic host plants: coevolution, colonization and chemical emancipation. In: Price, P.W., Lewinsohn, T.M., Fernandes, G.W., Benson, W.W. (Eds.), Plant–Animal Interactions: Evolutionary Ecology in Tropical and Temperate Regions. J. Wiley, New York, pp. 357–402.
Brown, K.S., Schoultz, B.V., Suomalainem, E., 2004. Chromosome evolution in Neotropical Danainae and Ithomiinae (Lepidoptera). Hereditas 141, 216–236.
Comstock, J.H., Needham, J.G., 1918. The wings of insects. Am. Nat. 32, 231–257.
D'Almeida, R.F., 1941. Contribução ao estudo dos Mechanitidae (Lep. Rhopalocera) (4a. nota). Pap. Avuls. Dept. Zool. Sec. Agric. 1, 79–85.
Darlu, P., Leconitre, G., 2002. When does the incongruence length difference test fail? Mol. Biol. Evol. 19, 432–437.
DeVries, P.J., Lande, R., Murray, D., 1999. Associations of co-mimetic ithomiine butterflies on small spatial and temporal scales in a neotropical rainforest. Biol. J. Linn. Soc. 67, 73–85.
Dolphin, K., Belshaw, R., Orme, C.D.L., Quicke, D.L.J., 2000. Noise and incongruence: interpreting results of the incongruence length difference test. Mol. Phylogenet. Evol. 17, 401–406.
Doubleday, E., 1847. The Genera of Diurnal Lepidoptera: Comprising their Generic Characters, a Notice of their Habits and Transformations, and a Catalogue of the Species of Each Genus 1, 87–106, pl. 16–19. Longman, Brown, Green & Longmans, London.
Downey, J.C., Allyn, A.C., 1975. Wing-scale morphology and nomenclature. Bull. Allyn Mus. 31, 1–32.
Drummond, B.A., 1986. Coevolution of ithomiine butterflies and solanaceous plants. In: D'Arcy, W.G. (Ed.), Solanaceae: Biology and Systematics. Columbia University Press, New York, pp. 307–327.
Drummond, B.A., Brown, K.S., 1987. Ithomiinae (Lepidoptera: Nymphalidae): summary of known larval food plants. Ann. Missouri Bot. Gdn. 74, 341–358.
Edgar, J.A., Culvenor, C.C.J., Pliske, T.E., 1976. Isolation of lactone, structurally related to the esterifying acids of pyrrolizidine alkaloids, from the costal fringes of male Ithomiinae. J. Chem. Ecol. 2, 263–270.
Ehrlich, P.R., Raven, P.H., 1965. Butterflies and plants: a study in coevolution. Evolution, 18, 586–608.
Eliot, J.N., 1973. The higher classification of the Lycaenidae (Lepidoptera): a tentative arrangement. Bull. Br. Mus. Nat. Hist. (Entomol.), 28, 373–506.
Farris, J.S., 1969. A successive approximations approach to character weighting. Syst. Zool. 18, 374–385.
Farris, J.S., Källersjö, M., Kluge, A.G., Bult, C., 1995. Constructing a significance test for incongruence. Syst. Biol. 44, 570–572.
Fox, R.M., 1940. A generic review of the Ithomiinae (Lepidoptera, Nymphalidae). Trans. Am. Entomol. Soc. 66, 161–207.
Fox, R.M., 1956. A monograph of the Ithomiidae (Lepidoptera). Part I. Bull. Am. Mus. Nat. Hist. 111, 1–76.
Fox, R.M., 1960. A monograph of the Ithomiidae (Lepidoptera). Part II. The tribe Melinaeini Clark. Trans. Am. Entomol. Soc. 86, 109–171.
Fox, R.M., 1967. A monograph of the Ithomiidae (Lepidoptera). Part III. The tribe Mechanitini Fox. Mem. Am. Entomol. Soc. 22, 1–190.
Fox, R.M., Real, H.G., 1971. A monograph of the Ithomiidae (Lepidoptera). Part IV. The tribe Napeogenini Fox. Mem. Am. Entomol. Inst. 15, 1–368.
Freitas, A.V.L., 1993. Biology and population dynamics of *Placidula euryanassa*, a relict ithomiine butterfly (Nymphalidae: Ithomiinae). J. Lepid. Soc. 47, 87–105.
Freitas, A.V.L., 1996. Population biology of *Heterosais edessa* (Nymphalidae) and its associated Atlantic Forest Ithomiinae community. J. Lepid. Soc. 50, 273–289.
Freitas, A.V.L., 1999. Nymphalidae (Lepidoptera), filogenia com base em caracteres de imaturos, com experimentos de troca de plantas hospedeiras. PhD Thesis. Universidade Estadual de Campinas, Campinas.
Freitas, A.V.L., Brown, K.S., 2002. Immature stages of *Sais rosalia* (Nymphalidae, Ithomiinae). J. Lepid. Soc. 56, 104–106.
Freitas, A.V.L., Brown, K.S., 2004. Phylogeny of the Nymphalidae (Lepidoptera). Syst. Biol. 53, 363–383.
Freitas, A.V.L., Brown, K.S., 2005. Immature stages of *Napeogenes sulphurina* Bates, 1862 (Lepidoptera, Nymphalidae, Ithomiinae) from Northeastern Brazil. J. Lepid. Soc. 59, 35–37.
Freitas, A.V.L., Trigo, J.R., Brown, K.S., Witte, L., Hartmann, T., Barata, L.E.S., 1996. Tropane and pyrrolizidine alkaloids in the ithomiines *Placidula euryanassa* and *Miraleria cymothoe* (Lepidoptera: Nymphalidae). Chemoecology, 7, 61–67.
Galluser, S., Guadagnuolo, R., Rahier, R., 2004. Genetic (RAPD) diversity between *Oleria onega agarista and Oleria onega* ssp. (Ithomiinae, Nymphalidae, Lepidoptera) in north-eastern Peru. Genetica 121, 65–74.
Godman, F.D., Salvin, O., 1879-1880. Biologia Centrali-Americana. Insecta. Lepidoptera-Rhopalocera. Dulau & Co., Bernard Quaritch, London, 1, 6–56, pls. 1–4 (1879), 57–62, pl. 5 (1880).
Haber, W.A., 1978. Evolutionary Ecology of Tropical Mimetic Butterflies (Lepidoptera: Ithomiinae). PhD Thesis. University of Minnesota, Minnesota.
Haber, W.A., 2001. Guide to Costa Rican Ithomiinae. http://www.cs.umb.edu/~whaber/Monte/Ithomid/Intro.html.
Haensch, R., 1909–10. 3. Familie: Danaidae. In: Seitz, A. (Ed.), Die Gross-Schmetterlinge der Erde, 5. Alfred Kernen, Stuttgart, pp. 113–171. pl. 31–41.
Hall, J.P.W., Willmott, K.R., 2000. Patterns of feeding behaviour in adult male riodinid butterflies and their relationship to morphology and ecology. Biol. J. Linn. Soc. 69, 1–23.
Hall, S.K., 1996. Behaviour and natural history of *Greta oto* in captivity (Lepidoptera: Nymphalidae: Ithomiinae). Trop. Lepid. 7, 161–165.
Harvey, D.J., 1991. Higher classification of the Nymphalidae. In: Nijhout, H.F. (Eds.), The Development and Evolution of Butterfly Wing Patterns. Smithsonian Institution, Washington, pp. 255–273.
Hsiao, T.H., 1986. Specificity of certain chrysomelid beetles for Solanaceae. In: D'Arcy, W.G. (Ed.), Solanaceae: Biology and Systematics. Columbia University Press, New York, pp. 345–363.
Hunziker, A.T., 1979. South American Solanaceae: a synoptic survey. In: Hawkes, J.G., Lester, R.N., Skelding, A.D. (Eds.), The Biology and Taxonomy of the Solanaceae. Academic Press, London, pp. 49–85.

Janzen, D.H., Hallwachs, W., 2005. Philosophy, navigation and use of a dynamic database (ACG Caterpillars SRNP) for an inventory of the macrocaterpillar fauna, and its food plants and parasitoids, of the Area de Conservacion Guanacaste (ACG), northwestern Costa Rica. http://janzen.sas.upenn.edu.

Jiggins, C.D., Naisbit, R.E., Coe, R.L., Mallet, J., 2001. Reproductive isolation caused by colour pattern mimicry. Nature, 411, 302–305.

Jiggins, C.D., Mallarino, R., Willmott, K.R., Bermingham, E., 2006. The phylogenetic pattern of speciation and wing pattern change in neotropical *Ithomia* butterflies (Lepidoptera; Nymphalidae). Evolution, in press.

Kitching, I.J., 1984. The use of larval chaetotaxy in butterfly systematics, with special reference to the Danaini (Lepidoptera: Nymphalidae). Syst. Entomol. 9, 49–61.

Kitching, I.J., 1985. Early stages and classification of the milkweed butterflies (Lepidoptera: Danainae). Zool. J. Linn. Soc. 85, 1–97.

Klots, A.B., 1970. 20. Lepidoptera. In: Tuxen, S.L. (Ed.), Taxonomist's Glossary of Genitalia in Insects, 2nd edn. Munksgaard, Copenhagen, pp. 115–130.

Lamas, G., 1973. Taxonomia e evolução dos gêneros *Ituna* Doubleday (Danainae) e. *Paititia* gen. n., *Thyridia* Hübner e *Methona* Doubleday (Ithomiinae) (Lepidoptera, Nymphalidae). PhD Thesis. Universidade de São Paulo, São Paulo.

Lamas, G., 1979. *Paititia neglecta*, gen. n., sp. n. from Peru (Nymphalidae: Ithomiinae). J. Lepid. Soc. 33, 1–5.

Lamas, G., 1980. A revision of the genera *Hypomenitis* Fox and *Veladyris* Fox (Lepidoptera: Nymphalidae, Ithomiinae). Rev. Ciencias, 72, 36–46.

Lamas, G., 1986. Revisión del género *Pagyris* Boisduval (Lepidoptera, Nymphalidae: Ithomiinae). An. Inst. Biol. U. Nac. Aut. Mex. (Zool.) 56, 259–276.

Lamas, G., 2004. Ithomiinae. In: Heppner, J.B. (Ed.), Checklist: Part 4A. Hesperioidea—Papilionoidea. Atlas of Neotropical Lepidoptera, Vol. 5A. Association for Tropical Lepidoptera/Scientific Publishers, Gainesville, pp. 172–191.

Maddison, W.P., Maddison, D.R., 1995. MacClade: Analysis of Phylogeny and Character Evolution, Version 3.05. Sinauer Associates, Sunderland, MA.

Motta, P.C., 2003. Phylogenetic relationships of Ithomiinae based on first-instar larvae. In: Boggs, C., Ehrlich, P., Watt, W.B. (Eds.), Butterflies as Model Systems. Chicago University Press, Chicago, pp. 409–429.

Müller, F., 1879. *Ituna* and *Thyridia*: a remarkable case of mimicry in butterflies. Proc. Entomol. Soc. Lond. 2, xx–xxix.

Nee, M., 2001a. Solanaceae systematics for the 21st century. In: Van Den Berg, R.G., Barendse, G.W.M, Van der Weerden, G.M., Mariani, C. (Eds.), Solanaceae V: Advances in Taxonomy and Utilization. Nijmengen University Press, Nijmengen, pp. 3–22.

Nee, M., 2001b. An overview of *Cestrum*. In: Van Den Berg, R.G., Barendse, G.W.M, Van der Weerden, G.M., Mariani, C. (Eds.), Solanaceae V: Advances in Taxonomy and Utilization. Nijmengen University Press, Nijmengen, pp. 109–136.

Nee, S., Barraclough, T.G., Harvey, P., 1996. Temporal changes in biodiversity: detecting patterns and identifying causes. In: Gaston, K.J. (Ed.), Biodiversity: a Biology of Numbers and Difference. Blackwell Scientific, Oxford, pp. 230–252.

Nixon, K.C., Carpenter, J.M., 1996. On simultaneous analysis. Cladistics 12, 221–241.

Olmstead, R.G., Sweere, J.A., Spangler, R.E., Bohs, L., Palmer, J.D., 1999. Phylogeny and provisional classification of the Solanaceae based on chloroplast DNA. In: Nee, M., Symon, D.E., Lester, R.N., Jessop, J.P. (Eds.), Solanaceae IV. Royal Botanic Gardens, Kew, Richmond, pp. 111–137.

Parsons, M.J., 1996. Gondwanan evolution of the troidine swallowtails (Lepidoptera: Papilionidae): cladistic reappraisals using mainly immature stage characters, with focus on the Birdwings *Ornithoptera* Boisduval. Bull. Kitakyushu Mus. Nat. Hist. 15, 43–118.

Portugal, A.H.A., Trigo, J., 2005. Similarity of cuticular lipids between caterpillar and its host plants: a way to make prey undetectable for predatory ants? J. Chem. Ecol. 31, 2551–2561.

Sanderson, M.J., Donoghue, M.J., 1989. Patterns of variation in levels of homoplasy. Evolution 43, 1781–1795.

Schluter, D., 2000. The Ecology of Adaptive Radiation. Oxford University Press, Oxford.

Schulz, S., Francke, W., Edgar, J., Schneider, D., 1988. Volatile compounds from androconial organs of danaine and ithomiine butterflies. Zeit. Naturforsch. 43c, 99–104.

Schulz, S., Beccaloni, G., Brown, K.S., Boppré, M., Freitas, A.V.L., Ockenfels, P., Trigo, J.R., 2004. Semiochemicals derived from pyrrolizidine alkaloids in male ithomiine butterflies (Lepidoptera. Nymphalidae: Ithomiinae. Biochem. Syst. Ecol. 32, 699–713.

Simpson, G.G., 1953. The Major Features of Evolution. Columbia University Press, New York.

Slowinski, J.B., Guyer, C., 1989. Testing the stochasticity of patterns of organismal diversity: an improved null model. Am. Nat. 134, 907–921.

Sorenson, M.D., 1999. Treerot, Version 2. Boston University, Boston.

Sourakov, A., Emmel, T.C., 1995. Life history of *Greta diaphana* from the Dominican Republic. Trop. Lepid. 6, 155–157.

Swofford, D.L., 1998. PAUP*. Phylogenetic Analysis Using Parsimony (*and Other Methods), Version 4. Sinauer Associates, Sunderland, MA.

Trigo, J.R., Brown, K.S., 1990. Variation of pyrrolizidine alkaloids in Ithomiinae: a comparative study between species feeding on Apocynaceae and Solanaceae. Chemoecology 1, 22–29.

Trigo, J.R., Brown, K.S., Witte, L., Hartmann, T., Ernst, L., Euclides, L., Barata, S., 1996. Pyrrolizidine alkaloids: different acquisition and use patterns in Apocynaceae and Solanaceae feeding ithomiine butterflies (Lepidoptera: Nymphalidae). Biol. J. Linn. Soc. 58, 99–123.

Tyler, H.A., Brown, K.S., Wilson, K.H., 1994. Swallowtail butterflies of the Americas. A Study in Biological Dynamics, Ecological Diversity, Biosystematics and Conservation. Scientific Publishers, Gainesville, FL.

Wahlberg, N., Braby, M.J., Brower, A.V.Z., de Jong, R., Lee, M.-M., Nylin, S., Pierce, N.E., Sperling, F.A.H., Vila, R., Warren, A.D., Zakharov, E., 2005. Synergistic effects of combining morphological and molecular data in resolving the phylogeny of butterflies and skippers. Proc. R. Soc. Lond. B, 272, 1577–1586.

Whinnett, A., Brower, A.V.Z., Lee, M.-M., Willmott, K.R., Mallet, J., 2005a. The phylogenetic utility of *tektin*, a novel region for inferring systematic relationships amongst Lepidoptera. Ann. Entomol. Soc. Am. 98, 873–886.

Whinnett, A., Zimmermann, M., Willmott, K.R., Herrera, N., Mallarino, R., Simpson, F., Joron, M., Lamas, G., Mallet, J., 2005b. Strikingly variable divergence times inferred across an Amazonian butterfly 'sulture zone'. Proc. R. Soc. Lond. B, 272, 2525–2533.

Willmott, K.R., Lamas, G., 2006. A phylogenetic reassessment of *Hyalenna* Forbes and *Dircenna* Doubleday, with a revision of *Hyalenna* (Lepidoptera: Nymphalidae: Ithomiinae). Syst. Entomol., in press.

Willmott, K.R., Mallet, J., 2004. Correlations between adult mimicry and larval hostplants in ithomiine butterflies. Proc. R. Soc. Lond. B (Biol. Lett.) Suppl. 271, S266–S269.

Young, A.M., 1974. A natural historical account of *Oleria zelica pagasa* (Lepidoptera: Nymphalidae: Ithomiinae) in a Costa Rican mountain rainforest. Studies Neotr. Fauna, 9, 123–139.

Young, A.M., 1978. Notes on the biology of the butterfly *Hypoleria cassotis* (Bates) (Nymphalidae: Ithomiinae) in Northeastern Costa Rica. Brenesia 14/15, 97–108.

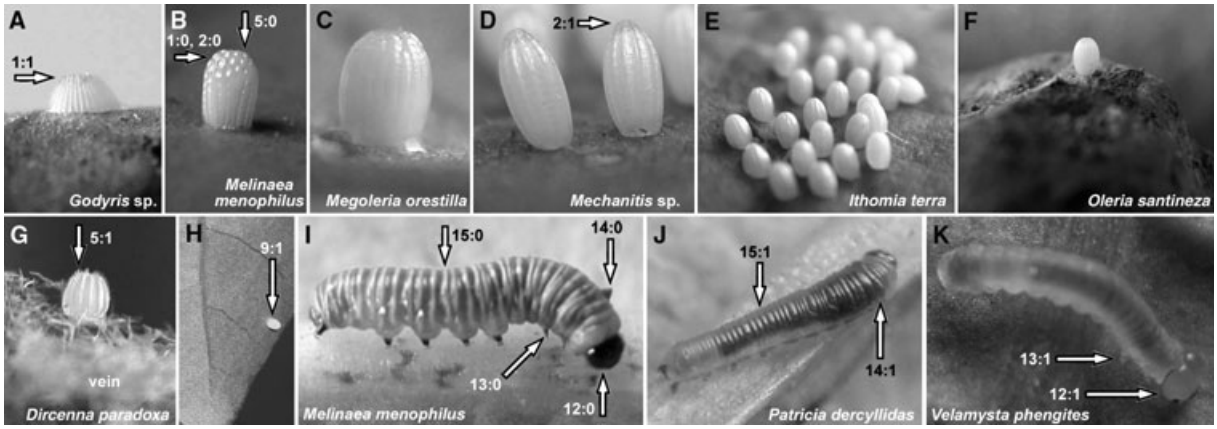

Fig. 8. Ovum, lateral view: (A) *Godyris* sp. (probably *G. panthyale panthyale*) (KRW-210), Ecuador; (B) *Melinaea menophilus zaneka* (KRW-187), Ecuador; (C) *Megoleria o. orestilla* (KRW-285), Ecuador; (D) *Mechanitis* sp., Costa Rica; (E) *Ithomia t. terra* (KRW-267), Ecuador; (F) *Oleria santineza* ssp. n. (KRW-161), egg deposited on stone, Ecuador; (G) *Dircenna paradoxa praestigiosa* (KRW-263), Ecuador; (H) *Methona themisto*, Brazil. First instar larva, dorsolateral view: (I) *Melinaea menophilus zaneka* (KRW-187), Ecuador; (J) *Patricia dercyllidas hazelea* (KRW-273), Ecuador; (K) *Velamysta p. phengites* (KRW-184), Ecuador.

Appendix 1. Character list

Immature stages

Egg and hostplant

1. *Egg with lateral aspect*: (0) ellipsoidal (Fig. 8B); (1) truncate (Fig. 8A). There is much variation in the overall shape of the egg, coded in Char. 3, but the egg of known *Godyris* is unique in resembling a truncated cone, distinct from other rounded or ellipsoidal eggs.

2. *Egg with apex*: (0) rounded (Fig. 8B); (1) pointed (Fig. 8D). Because Char. 1 also concerns shape of the apex, this character was coded as equivocal for species with state 1:1.

3. *Egg with ratio between vertical and horizontal axes,* r: (0) $1.2 < r < 1.5$ (Fig. 8A); (1) $1.5 < r < 1.7$ (Fig. 8B); (2) $r > 1.7$ (Fig. 8C); (3) $r < 1.2$ (Fig. 8D).

4. *Egg relative size*: (0) > 2.4 (e.g., Fig. 8D); (1) < 2.4 (e.g., Fig. 8B). Relative size is the cube root of egg volume (mm^3) (estimated by width × height × breadth) divided by forewing length (cm).

5. *Egg with longitudinal ridges with elevated carinae near micropyle*: (0) absent (Fig. 8B); (1) present (Fig. 8G).

6. *Eggs placed*: (0) in isolation (Fig. 8A–C); (1) in clusters (Fig. 8D,E). Most Ithomiinae lay isolated eggs, moving between each oviposition. Placing eggs in clusters from a single position has arisen rarely but occurs throughout the subfamily.

7. *Oviposition*: (0) on the larval hostplant (Fig. 8A–E); (1) on other substrates adjacent to the larval hostplant (Fig. 8F). While most Ithomiinae place eggs on the larval hostplant, several (but not all) *Oleria* have been observed to lay eggs on other substrates. One female of *Oleria santineza* was observed inspecting a fallen leaf of the larval hostplant *Solanum abitaguense* before laying five eggs on dead and dried leaves (of other plant species) and stones (Fig. 8F) around the leaf. One female of *Oleria fasciata* inspected several *Solanum anceps*, the larval hostplant, before eventually laying a single egg on a seedling of an unrelated plant species *c*. 0.2 m from the nearest *S. anceps*. *Oleria onega* has also been recorded to lay eggs off the hostplant (Galluser et al., 2004), and the trait may also occur in other highland *Oleria* (H. Greeney, pers. comm.).

8. *If oviposition occurs on the larval hostplant (Char. 7:0), then preferential placement of the egg near a leaf vein or a hole is*: (0) not marked (Fig. 8H); (1) marked (Fig. 8G). In species coded state 1, eggs are laid next to a leaf vein or area of feeding damage about half the time.

9. *If oviposition occurs on the larval hostplant (Char. 7:0), then eggs are placed*: (0) at random with respect to leaf border (Fig. 8D); (1) near the leaf border (Fig. 8H).

10. *If oviposition occurs on the larval hostplant (Char. 7:0), then chosen leaf surface is*: (0) underside (Fig. 8H); (1) upperside (Fig. 8D,E). Most species place eggs exclusively on the leaf underside, but in *Mechanitis* and *Ithomia terra*, all of which also lay eggs in clusters, eggs are always placed on the upperside.

11. *Larval hostplant family*: (0) Apocynaceae (Fig. 9T); (1) Solanaceae (e.g., Fig. 8A,B); (2) Gesneriaceae (Fig. 8C). Apocynaceae is the hostplant family of *Tellervo*, the most likely sister taxon to the Ithomiinae, and is common throughout the closely related Danainae

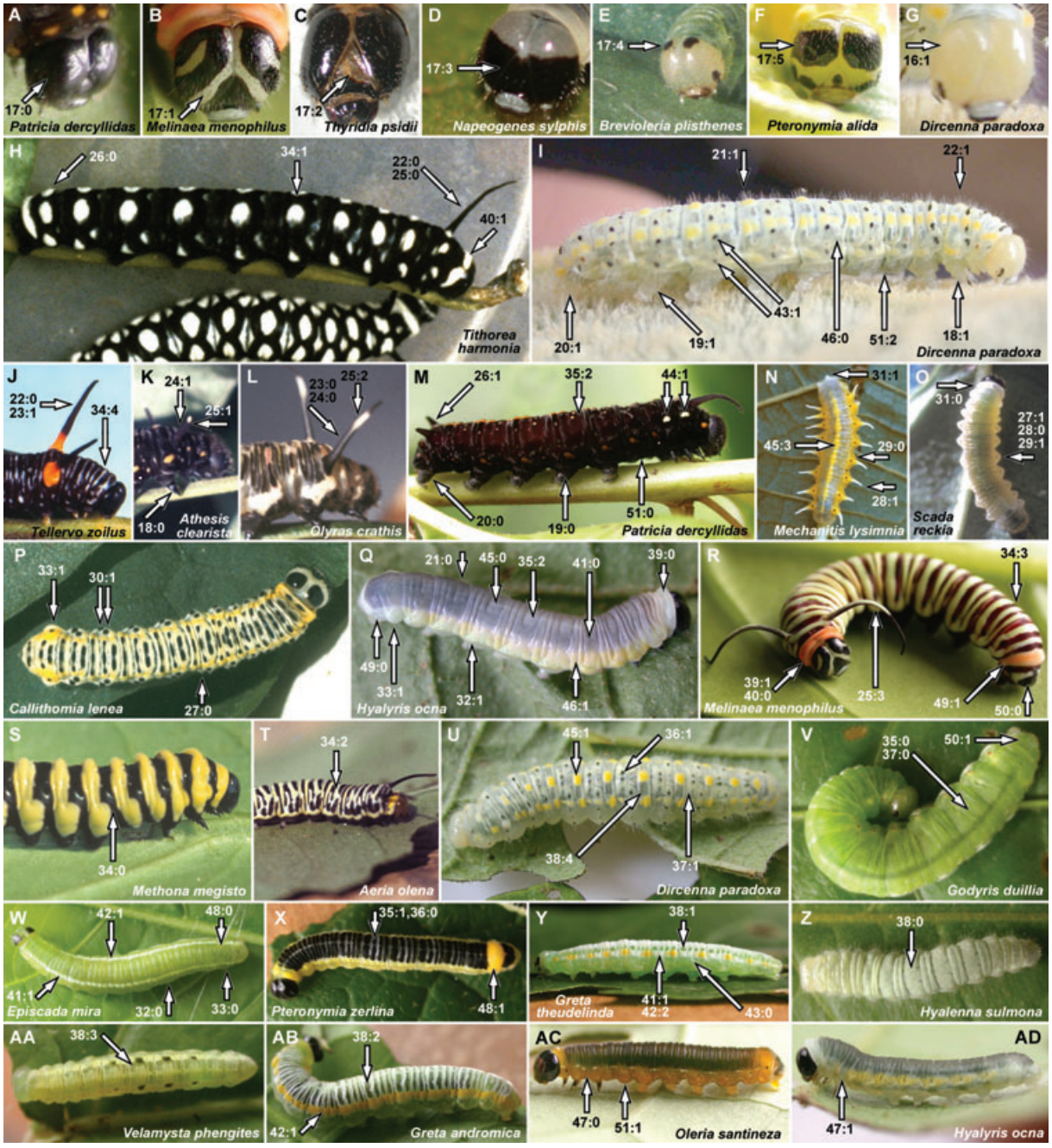

Fig. 9. Last instar larvae. Cephalic capsule, frontal view: (A) *Patricia dercyllidas hazelea* (KRW-275), Ecuador; (B) *Melinaea menophilus zaneka* (KRW-186), Ecuador; (C) *Thyridia psidii*, Brazil; (D) *Napeogenes sylphis corena*, Ecuador; (E) *Brevioleria plisthenes*, Brazil; (F) *Pteronymia alida* ssp. n. (KRW-081-2), Ecuador; (G) *Dircenna paradoxa praestigiosa* (KRW-020), Ecuador. Lateral view: (H) *Tithorea harmonia*, Brazil; (I) *Dircenna paradoxa praestigiosa* (KRW-020), Ecuador. Thoracic tubercules: (J) *Tellervo zoilus*, Australia; (K) *Athesis c. clearista*, Venezuela; (L) *Olyras c. crathis*, Venezuela. (M) *Patricia dercyllidas hazelea* (KRW-273), lateral view, Ecuador. Dorsal/dorsolateral view: (N) *Mechanitis l. lysimnia*, Brazil; (O) *Scada reckia theaphia*, Brazil; (P) *Callithomia lenea xantho*, Brazil; (Q) *Hyalyris ocna* ssp. n. (KRW-043), Ecuador; (R) *Melinaea menophilus zaneka* (KRW-186), Ecuador; (S) *Methona megisto*, Brazil; (T) *Aeria olena*, Brazil; (U) *Dircenna paradoxa praestigiosa* (KRW-110), Ecuador; (V) *Godyris duillia* (KRW-198), Ecuador; (W) *Episcada apuleia* (KRW-265), Ecuador; (X) *Pteronymia zerlina machay* (KRW-250), Ecuador; (Y) *Greta t. theudelinda* (KRW-224), Ecuador; (Z) *Hyalenna sulmona* ssp. n. (KRW-174), Ecuador; (AA) *Velamysta p. phengites* (KRW-238), Ecuador; (AB) *Greta andromica andania* (KRW-230), Ecuador; (AC) *Oleria santineza* ssp. n. (KRW-161), Ecuador; (AD) *Hyalyris ocna* ssp. n. (KRW-043), Ecuador.

(Ackery and Vane-Wright, 1984; Ackery, 1987). Among the Ithomiinae it occurs in only three primitive genera (Drummond and Brown, 1987). Remaining ithomiines all feed on Solanaceae with the exception of the two sister genera, *Megoleria* and *Hyposcada*, which feed on Gesneriaceae (Drummond and Brown, 1987; Willmott, pers. obs.; G. Beccaloni, pers. comm.; H. Greeney, pers. comm.).

Larva

First instar

12. First instar with color of cephalic capsule: (0) dark (Fig. 8I); (1) pale to transparent (Fig. 8K). Most known species have the cephalic capsule uniformly colored in the first instar; species with state 0 vary from black to brown, whereas those with state 1 lack any dark pigmentation.

13. *First instar with color of thoracic legs*: (0) dark (Fig. 8I); (1) pale to transparent (Fig. 8I).

14. *First instar with subdorsal thoracic filaments*: (0) conspicuous stubs (Fig. 8I); (1) a slight swelling (Fig. 8J). In *Patricia* and *Athesis* the future position of the later instar thoracic filaments are marked only by a slight subdorsal swelling, whereas in remaining species that have these filaments in later instars short protuberances are clearly visible. Species that lack thoracic filaments are coded as not applicable.

15. *First instar with entire transverse dark and light body "rings" extending to base of prolegs*: (0) present (Fig. 8I); (1) absent (Fig. 8J). Superficially similar rings are present in *Pteronymia inania* and *P. lonera*, but these extend only across the dorsum of the larvae, and are interpreted as non-homologous. These two species were therefore coded state 1.

Last instar

16. *Last instar with dark pigmentation in cephalic capsule*: (0) present (e.g., Fig. 9F); (1) absent (Fig. 9G). Although most species that have a dark cephalic capsule in the first instar (Char. 12:0) retain some dark pigmentation in the fifth instar (but not all; e.g., *Dircenna paradoxa*), there is considerable variation as to whether dark pigmentation develops in later instars of species that have pale first instars.

17. *If last instar cephalic capsule has dark pigmentation (Char. 16:0), then capsule*: (0) uniformly colored (Fig. 9A); (1) with a pale area at the edge of the vertex shaped like an inverted "v" (Fig. 9B); (2) with a pale area shaped like an inverted "v" inside the vertex, or vertex entirely pale (Fig. 9C); (3) with a frontal transverse black band (Fig. 9D); (4) with a dorsal black stripe or markings (Fig. 9E); (5) with two frontal transverse black bands, usually with much variation (Fig. 9F).

18. *Last instar thoracic legs*: (0) black (Fig. 9K); (1) light, lacking dark pigmentation (Fig. 9I).

19. *Last instar with an outer black plate on abdominal prolegs*: (0) present (Fig. 9M); (1) absent (Fig. 9I).

20. *Last instar with black plate on anal prolegs*: (0) large (Fig. 9M); (1) reduced or absent (Fig. 9I).

21. *Last instar with hairs on cuticle*: (0) short and sparse (Fig. 9Q); (1) long and dense (Fig. 9I). *Dircenna*, known *Hyalenna* and *Ceratinia neso* are distinctive in having the hairs on the cuticle notably denser and longer than in all other species.

22. *Last instar with subdorsal filaments*: (0) present (Fig. 9H,J); (1) absent (Fig. 9I). Subdorsal, motile filaments occur throughout the Danainae and in primitive Ithomiinae.

23. *If last instar has subdorsal filaments (Char. 22:0), then thoracic filaments are*: (0) on the mesothorax (Fig. 9L); (1) on the metathorax (Fig. 9J). Danainae show substantial variation in the position of filaments, which may occur on any thoracic or abdominal body segment (Ackery and Vane-Wright, 1984). The thoracic filaments in *Tellervo* are on the metathorax, and in all Ithomiinae on the mesothorax.

24. *If last instar has subdorsal filaments (Char. 22:0), then thoracic filaments are*: (0) longer than segment diameter (Fig. 9L); (1) shorter than segment diameter (Fig. 9K). State 1 occurs only in *Athesis clearista*.

25. *If last instar has subdorsal filaments (Char. 22:0), then thoracic filaments are*: (0) entirely dark (Fig. 9H); (1) dark with a white tip (Fig. 9K); (2) dark with a white transverse band (Fig. 9L); (3) dark with a white dorsal area (Fig. 9R).

26. *If last instar has subdorsal filaments (Char. 22:0), then these are*: (0) confined to thorax (Fig. 9H); (1) also present on eighth abdominal segment (Fig. 9M).

27. *Last instar with lateral tubercles just above prolegs*: (0) absent (Fig. 9P); (1) present (Fig. 9O).

28. *If last instar has lateral tubercles above prolegs (Char. 27:1), then they are*: (0) short (Fig. 9O); (1) long (Fig. 9N).

29. *If last instar has lateral tubercles above prolegs (Char. 27:1), then they are*: (0) yellow (Fig. 9N); (1) same color as body (Fig. 9O).

30. *Last instar with a pair of lateral swellings on each side of each segment*: (0) absent; (1) present (Fig. 9P). The upper swelling is positioned slightly dorsal to the lateral tubercles coded in Char. 27, while the ventral swelling is slightly dorsal to the sublateral swellings coded in Char. 32.

31. *Last instar prothoracic segment with two dorsolateral protuberances*: (0) absent (Fig. 9O); (1) present (Fig. 9N).

32. *Last instar with flattened, sublateral swellings, semicircular in dorsal view*: (0) absent (Fig. 9W); (1) present (Fig. 9Q). These slight swellings are positioned just below the spiracles and most easily observed in live larvae.

33. *Last instar with projecting lateral swellings on eighth abdominal segment*: (0) absent (Fig. 9W); (1) present (Fig. 9P,Q). This character is correlated almost entirely with Char. 32 with the exception of *Callithomia lenea* and *Pagyris cymothoe*; the former is coded 0,1 and the latter 1,0. This swelling forms a blunt, cone-like protuberance on which the spiracle sits, and merges with the sublateral swelling (Char. 32:1) ventrally.

34. *If last instar has transverse body rings (see Char. 15), then*: (0) rings occur singly in each segment (Fig. 9S); (1) dark rings merge with one another (Fig. 9H); (2) pale rings are irregular, disrupting black rings (Fig. 9T); (3) each ring is finely divided (Fig. 9R); (4) dark rings are merged to produce a uniform entire purplish brown coloration (Fig. 9J).

35. *If last instar lacks transverse body rings (see Char. 15), then dark dorsal pigmentation*: (0) absent (Fig. 9V); (1) present, forming a pattern above a pale background (Fig. 9X); (2) entirely covering dorsum (Fig. 9M,Q). There is a continuum between dorsal colors of gray, dark green to olive green, darker brown and black, so all these colors are considered to represent dark pigmentation. All Napeogenini, Ithomiini and Oleriini have almost uniform, dark dorsal coloration of this kind (state 2), while all Godyridini and Dircennini have pale green, largely translucent bodies on which there may or may not be isolated darker markings (states 0,1).

36. *If last instar has patterned dark dorsal pigmentation (Char. 35:1), it is expressed as*: (0) lines (Fig. 9X); (1) spots and dashes (Fig. 9U).

37. *If last instar has at least some area of dorsum lacking dark pigmentation (Char. 35:0,1) then pale green-white opaque markings are*: (0) absent (Fig. 9V); (1) present (Fig. 9U). Larvae may be entirely translucent green or also bear patches of opaque white, yellowish or green coloration.

38. *If last instar has pale green-white opaque markings (Char. 37:1), then translucent unmarked areas*: (0) are absent (i.e., entire dorsum is opaque) (Fig. 9Z); (1) form a series of small spots, four to each segment, in a line immediately dorsal of pale subdorsal line (Fig. 9Y); (2) form transverse lines, four to each segment, crossing the dorsum (these appear to represent expanded, joined spots of state 2) (Fig. 9AB); (3) form a "U"-shaped pattern in each segment, with the base of the "U" at the dorsal edge of the pale subdorsal line (Fig. 9AA); (4) are distributed in uneven patches (Fig. 9U); (5) are extensive, leaving thin opaque lines in each segment (Fig. 10D).

39. *Last instar with contrasting colored "collar" on prothorax*: (0) absent (Fig. 9Q); (1) present (Fig. 9R).

40. *If last instar has a contrastingly colored prothoracic "collar" (Char. 39:1), it is*: (0) yellow/orange (Fig. 9R); (1) white (Fig. 9H).

41. *Last instar with a pair of subdorsal stripes*: (0) absent (Fig. 9Q); (1) present (Fig. 9W,Y). State 1 is an apparent synapomorphy for the Godyridini and Dircennini. It is present in most known species and where it is absent it has apparently been lost due to overall reduction in body markings.

42. *If last instar has a subdorsal stripe (Char. 41:1), then it is*: (0) uniform pale blue/green (Fig. 9W); (1) uniform yellow (Fig. 9AB); (2) yellow in posterior end (usually half) of each segment, and pale in the anterior half (Fig. 9Y).

43. *Last instar with a pair of lateral black dots (one above, one below spiracle) in each segment*: (0) absent (Fig. 9Y); (1) present (Fig. 9I).

44. *Last instar with two conspicuous pale yellow lateral spots in segments 2A and 3A*: (0) absent; (1) present (Fig. 9M).

45. *Last instar with pale mid-dorsal markings*: (0) absent (Fig. 9Q); (1) a single pale yellow spot at posterior edge of each segment (Fig. 9U); (2) three orange spots on posterior 3 sections of each segment (Fig. 10A); (3) a complete yellowish line on abdominal segments only (Fig. 9N); (4) a complete, yellowish line broken in the middle of each segment (Fig. 10C); (5) a complete, pale greenish line (Fig. 10B). *Hypothyris euclea* apparently bears a mid-dorsal line, but this is the black ground color visible between two subdorsal bands of pale markings, not homologous with the pale mid-dorsal lines coded here, which are green to yellow.

46. *Last instar with a colored lateral stripe (centred on spiracles)*: (0) absent (Fig. 9I); (1) present (Fig. 9Q). This stripe occurs in virtually all Mechanitini, Napeogenini, Ithomiini and Oleriini, but is absent elsewhere.

47. *If last instar has a lateral stripe (Char. 46:1), then it is*: (0) complete (Fig. 9AC); (1) present on the abdomen only (Fig. 9AD).

48. *Last instar with subdorsal stripe expanded on eighth abdominal segment to form a more or less complete dorsal band*: (0) absent (Fig. 9W); (1) present (Fig. 9X). State 1 is an apparent synapomorphy for *Pteronymia*, occurring in all known species. The yellow to yellow-green subdorsal stripe is always broader in the eighth segment than adjacent segments through dorsal expansion, and varies from being slightly expanded (Fig. 10B) to connecting across the segment and forming an entire colored band (Fig. 9X).

49. *Last instar with a conspicuous colored "ring" on the ninth abdominal segment*: (0) absent (Fig. 9Q); (1) present (Fig. 9R).

50. *Last instar with color of anal plate*: (0) mostly dark (Fig. 9R); (1) other (with dark pigmentation very reduced or absent) (Fig. 9V).

51. *Last instar ventral color*: (0) dark (Fig. 9M); (1) white to yellow (Fig. 9AC); (2) green (Fig. 9I).

Fig. 10. Final instar larva, dorsal view: (A) *Patricia dercyllidas* (KRW-273), Ecuador; (B) *Pteronymia alida* ssp. n. (KRW-81-2), Ecuador; (C) *Pteronymia euritea*, Brazil; (D) *Brevioleria plisthenes*, Brazil. Pupa, lateral view: (E) *Scada reckia theaphia*, Brazil; (F) *Oleria santineza* ssp. n. (KRW-161), Ecuador; (G) *Placidina euryanassa*, Brazil; (H) *Methona themisto*, Brazil; (I) *Greta andromica* (KRW060-2), Ecuador; (J) *Hyposcada anchiala* ssp. n., Ecuador (G.W. Beccaloni); (K) *Hyalyris ocna* ssp. n. (KRW-043), Ecuador; (L) *Episcada a. apuleia* (KRW-179), Ecuador; (M) *Tithorea harmonia gilberti*, Peru (K.S. Brown). Pupa, dorsal view: (N) *Episcada a. apuleia* (KRW-215), Ecuador; (O) *Dircenna paradoxa praestigiosa* (KRW-129), Ecuador; (P) *Melinaea menophilus zaneka* (KRW-186), Ecuador; (Q) *Greta andromica andania* (KRW-060-2), Ecuador; (R) *Melinaea menophilus zaneka* (KRW-187), Ecuador; (S) *Ithomia t. terra* (KRW-269), Ecuador; (T) *Dircenna paradoxa praestigiosa*, as J; (U) *Hylayris ocna* ssp. n. (KRW-058-1), Ecuador. Pupa, ventral view of abdomen tip and cremaster: (V) *Dircenna dero celtina*, Brazil; (W) *Melinaea menophilus zaneka* (KRW-187), Ecuador; (X) *Methona themisto*, Brazil; Eclosed pupa, lateral view: (Y) *Greta andromica andania* (KRW-60-2), Ecuador; (Z) *Episcada apuleia apuleia* (KRW-193), Ecuador. Final instar leaf shelter: (AA) *Dircenna adina lorica* (KRW-048), on *Solanum asperum*, Ecuador; (AB) *Dircenna adina lorica* (KRW-260), on *Solanum* sp. (sect. *torva*), Ecuador. Pharmacophagy: (AC) *Oleria tremona tremona*, male, feeding on Asteraceae flowers, Ecuador; (AD) various Ithomiinae and Danainae feeding at dried Boraginaceae bait, Brazil, Acre (1: *Melinaea menophilus*; 2: *Hypothyris semifulva*; 3: *Hypoleria lavinia*; 4: *Pteronymia tucuna*; 5: *Lycorea halia*, Danainae).

52. *Last instar rests in a "J" posture*: (0) present (Fig. 9V); (1) absent (Fig. 9N). This characteristic resting posture occurs throughout the Ithomiinae with the exception of a handful of species in which it has apparently been lost.

53. *Last instar leaf-shelter building behavior*: (0) absent (Fig. 9V); (1) a single leaf is bent (early instars) or rolled (later instars) and fastened loosely with silk (Fig. 10-AA,AB); (2) several leaves are loosely fastened together with silk. State 1 is an apparent synapomorphy for *Dircenna* + *Hyalenna*, while state 2 has been observed only in *Episcada clausina*.

Pupa

54. *Pupal angle*: (0) 180° (Fig. 10G); (1) 120° (Fig. 10E); (2) 90° (Fig. 10J). There is much variation between, but not within clades, in the extent to which the pupa is angled at the abdomen/thorax suture. Most of the more primitive species have a slight angle (state 1), most of the more derived species have a sharper angle (state 2), and small groups of species (*Methona*, some Mechanitini and *Placidina*) have a straight pupa (state 0).

55. *Dorsal edge of abdomen in posterior half to cremaster with a pronounced curve*: (0) absent (Fig. 10E); (1) present (Fig. 10H).

56. *Dorsal edge of abdomen at thorax/abdomen suture*: (0) slightly indented (120–180°) (Fig. 10E); (1) deeply indented (90°) (Fig. 10F).

57. *Abdominal segment 1 in comparison with segment 2*: (0) of similar width (Fig. 10N); (1) constricted to half or less width (Fig. 10O); (2) absent (Fig. 10R). *Epityches eupompe* is difficult to evaluate because of fusion between abdominal segments, but segment 1 appears to be state 0.

58. *Protuberances at the base of the cremaster stalk in dorsal view*: (0) absent or vestigial (Fig. 10N); (1) conspicuous (Fig. 10O,P).

59. *Dorsal edge of abdomen at third abdominal segment*: (0) slightly protruding (Fig. 10M); (1) smooth (Fig. 10K).

60. *If dorsal edge of abdomen is protruding at third segment (Char. 59:0), then protrusion is*: (0) broad across the abdomen, like a "shelf" (Fig. 10M); (1) a bump at the middle of the abdomen only (Fig. 10J).

61. *Lateral tubercles at junction between wing base and posterior edge mesothorax*: (0) absent (Fig. 10Q); (1) present (Fig. 10R). In dorsal view, two (one each side) more or less pointed lateral projections are visible in all species near the junction of the wing base and anterior edge of the mesothorax. In a number of species an additional pair of tubercles (again one each side) are also present in a more posterior position at the posterior edge of the mesothorax. In *Dircenna dero* both pairs of tubercles are present, though the posterior pair is rather reduced.

62. *Ocular caps*: (0) rounded (Fig. 10R); (1) pointed (Fig. 10Q). The ocular caps are blunt, short projections that may either be rounded or pointed.

63. *Ground color of pupa*: (0) yellow to greenish (Fig. 10P); (1) light green (Fig. 10J); (2) strong green (Fig. 10L); (3) cream white to light brown (Fig. 10K); (4) dark brown (Fig. 10E); (5) orange (Fig. 10F).

64. *Brown coloration in pupal skins after eclosion*: (0) absent (Fig. 10Y); (1) present (Fig. 10Z). In the majority of species the pupal cases after eclosion are colorless, with the exception of black spots or markings. In some species, notably in the Dircennini, there is an additional brown coloration present, especially along the edges of the wing cases, abdomen and cephalic region, sometimes occurring over the entire pupa.

65. *Reflective areas*: (0) absent (Fig. 10R); (1) small stripes at edges of wing cases and wing veins (Fig. 10Q); (2) covering most of wing case and abdomen (Fig. 10T); (3) diffuse scattered areas throughout pupa (Fig. 10S); (4) pupa totally reflective (Fig. 10M). Many ithomiine pupae have areas that are brilliantly reflective gold, silver or other colors.

66. *Color of the cremaster stalk*: (0) black (Fig. 10P); (1) red to pinkish (Fig. 10N); (2) colorless (Fig. 10O).

67. *Central dorsal black spot on abdominal segment 3*: (0) absent (Fig. 10S); (1) present (Fig. 10Q). This spot is positioned on the abdominal segment 3 protrusion (Char. 59:0), when that is present.

68. *Paired dorso-lateral patterned bands on abdomen*: (0) unmarked/same color as rest of pupa (Fig. 10T); (1) with mottled brown pattern (Fig. 10S); (2) with an even brown pattern (Fig. 10N); (3) absent except single spot on segment 2 (Fig. 10R). Distinct dorso-lateral bands are visible in most species, and in some (e.g., *Episcada*) they merge to form a single dorsal band. They may be marked with various darker colors or be visible as distinct, unmarked ground color between reflective areas. In *Melinaea menophilus* these bands are absent except for a single mid-dorsal spot in segment 2 formed by their fusion (inferred from examination of other species in which fusion also occurs, e.g., *Episcada*).

69. *If paired dorso-lateral bands on abdomen have mottled brown pattern present (Char. 68:1), then pattern*: (0) confined to bands (Fig. 10S); (1) spread as speckling over abdomen (Fig. 10U); (2) broken into isolated spots scattered over abdomen (Fig. 10G).

70. *Lateral dark spot on abdominal segment 2 surrounding or dorsal of spiracle*: (0) absent (Fig. 10L); (1) present (Fig. 10K). A number of species have brownish coloration in this area and elsewhere on the pupa (see Char. 64), but this is regarded as distinct from the black spots coded here.

71. *Lateral black spot in section between end of abdominal segment 1 and wing margin*: (0) absent (Fig. 10L); (1) present (Fig. 10I).

72. *Dorsal black stripe on suture between eighth and ninth abdominal segments*: (0) present (Fig. 10P); (1) absent (Fig. 10Q).

73. *Dark markings on wing cases*: (0) large black spots (Fig. 10H); (1) parallel thin black lines (Fig. 10M); (2) two ''v''-shaped discal marks, shading more or less along postdiscal veins and a line of submarginal dark spots (Fig. 10F); (3) fine, irregular lateral parallel lines (Fig. 10G); (4) diffuse irregular markings (Fig. 10K); (5) tiny black dots (Fig. 10I); (6) absent (Fig. 10L).

74. *Exuvial holdfast tubercles (EHTs)*: (0) strongly sclerotized with black markings (Fig. 10W); (1) unmarked (Fig. 10V).

75. *If EHTs are marked (Char. 74:0), then dark markings*: (0) cover EHTs only (Fig. 10W); (1) join the EHTs to one another and to the cremaster stalk (Fig. 10X).

Adult

Ecology and chemistry

76. *Male attraction to pyrrolizidine alkaloid (PA) sources*: (0) absent/low; (1) high (Fig. 10AC,AD). PAs play a crucial role in the ecology of Danainae (for references see Ackery and Vane-Wright, 1984) and Ithomiinae, being the precursors for defensive chemicals (Brown, 1984) as well as male-disseminated sexual pheromones (Edgar et al., 1976). PAs are obtained by adults feeding at various sources (pharmacophagy), mainly Asteraceae flowers (Fig. 10AC) (and, rarely, leaf stems and/or branches) as well as dried or withered plants in the Boraginaceae (Fig. 10AD). In the Ithomiinae, species that show low attraction also tend to have females as well as males visiting PA sources; in species that have strong attraction it is almost exclusively males that visit such sources, because PAs are transferred to the female in the spermatophore (Brown, 1985). Therefore, although sexual dimorphism in pharmacophagy was initially coded as a character, it was excluded because it is strongly correlated with this character. Coding of this and the following character is based on several decades of field observations by KSB and AVLF, during which time baits of dried *Heliotropium* (Boraginaceae) were used extensively to attract ithomiines. Some additional Andean species are coded for this character based on observations of KRW of flower-feeding, but as baits were not used these species are coded as unknown for Char. 77.

77. *If male attraction to PA sources is high (Char. 76:1), then PA sources are*: (0) diverse, including Boraginaceae baits (Fig. 10AD); (1) mainly flowers of Eupatoriae (Fig. 10AC).

78. *Level of PA storage in adults*: (0) low (< 1% dry weight); (1) high (1–20% dry weight). Basal Ithomiinae tend to store PAs from larval hostplants, and adults are generally not strongly attracted to PA sources, resulting in low levels of PA storage in adults (Brown, 1985; Trigo et al., 1996).

79. *3-OH-kynurenine in adults*: (0) absent; (1) present. The yellow pigment in the scales of many Ithomiinae is derived from 3-OH-kynurenine (Brown, 1967).

80. *Male attraction to red flowers*: (0) frequent; (1) rare. Coding of this character is based mainly on extensive observations of ithomiine populations by KSB and AVLF in Brazil (São Paulo and other south-eastern states and Acre). The ecological significance of this behavior is unknown, but the lack of attraction to red flowers (unlike many other nymphalids) may be linked with the dependence of most species coded state 1 on the predominantly white flowers of Asteraceae as a PA source.

81. *Male attraction to rotting fish bait*: absent or very rare (0); common (1). A large proportion of all Nymphalidae are strongly attracted to baits of rotting carrion, as well as to feces and damp sand or mud, especially when urine is present. These food substrates attract similar species and most likely provide sodium ions, among other possible nutrients (Arms et al., 1974). Feeding behavior is apparently related to adult morphology and ecology (Hall and Willmott, 2000), and very probably also to larval hostplants. Among the Ithomiinae only *Elzunia* and *Tithorea* are regularly attracted to rotting fish bait, based on 26 months of field work in Ecuador by KRW with extensive trapping in virtually all habitats where ithomiines occur. Outgroup behavior (*Tellervo*) is unknown, but species in the only neotropical forest danaine genus *Lycorea* Doubleday [1847] are also strongly attracted to fish baits.

Male body

Antenna

The following two characters are based on an unpublished study by A. Brower (pers. comm.). There is substantial variation in the extent to which antennae are scaled, ranging from dense scales from the antennal base to the base of the club in some *Episcada* and *Aeria*, to only sparse scaling on the basal antennomeres in, for example, some *Oleria*. This variation is correlated to some extent with antennal color, with yellow antennae lacking scales, but not entirely, as *Oleria* antennae are black. There is also significant variation in the morphology of the carinae, the three ridges on the ventral surface of the antenna common to all Nymphalidae. These are almost absent in some Mechanitini, Ithomiini and Dircennini, and more marked in Oleriini. Some species (e.g., *Olyras* and Mechanitini) have more closely spaced carinae, with the lateral carinae about half way between the medial carina and antenna edge, while in others (e.g., Oleriini) the lateral carinae are placed at the

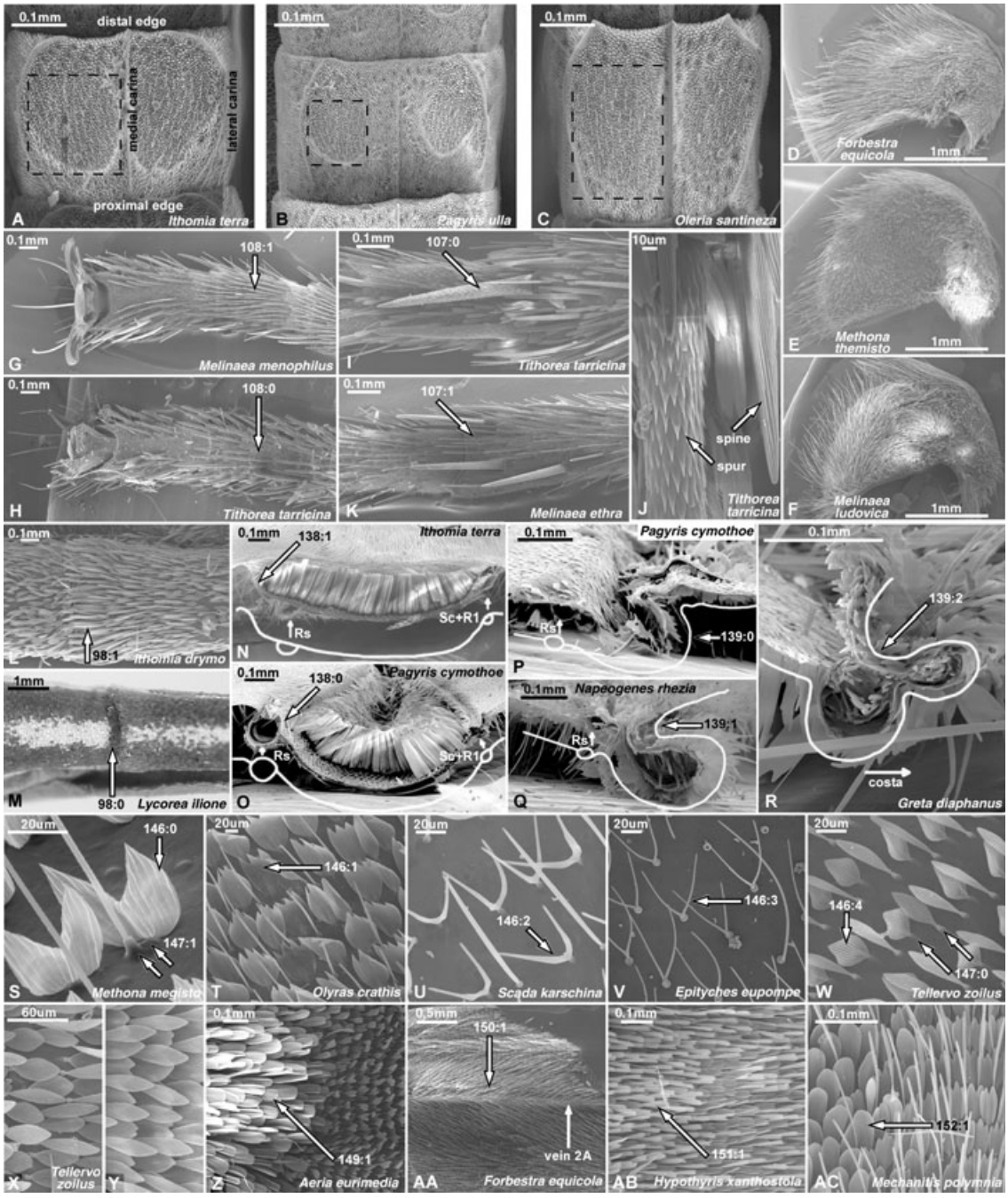

Fig. 11. Female antenna, fourth antennomere, ventral view (limits of sulci marked with dashed line): (A) *Ithomia t. terra*; (B) *Pagyris u. ulla*; (C) *Oleria s. santineza*. Male left tegula, lateral view: (D) *Forbestra e. equicola*; (E) *Methona themisto*; (F) *Melinaea l. ludovica*. Legs: (G) *Melinaea m. menophilus*, female mid-leg tarsus, ventral view; (H) *Tithorea tarricina pinthias*, same as G; (I) *Tithorea tarricina pinthias*, female mid-leg tibia and spurs; (J) same as I, tibial spur (left) and spine (right); (K) *Melinaea ethra*, female mid-leg tibia. Male ventral abdomen, junction tergites 2 (right) and 3 (left): (L) *Ithomia drymo*; (M) *Lycorea ilione*. Male hindwing anterior edge, cross-section through androconial scale patch between veins Sc + R1 and Rs, looking distally: (N) *Ithomia t. terra*; (O) *Pagyris cymothoe cymothoe*. Male hindwing anterior edge near apex, cross-section through androconial scale patch between veins Sc + R1 and Rs, looking basally: (P) *Pagyris c. cymothoe*; (Q) *Napeogenes r. rhezia*; (R) *Greta diaphanus*. Wing scales: (S) *Methona megisto*, male DHW transparent area; (T) *Olyras c. crathis*, male DFW yellow tornal spot; (U) *Scada k. karschina*, male DFW translucent area; (V) *Epityches eupompe*, male DHW transparent area; (W) *Tellero; zoilus*, male DFW translucent white area. Androconial wing scales: (X) *Tellero; zoilus*, male DFW tornus, light basal area; (Y) as X, dark distal area; (Z) *Aeria e. eurimedia*, male DFW discal cell, androconial (left) and wing (right) scales; (AA) *Forbestra e. equicola*, male DFW elongate androconial scales lining vein 2A; (AB) *Hypothyris xanthostola*, male DHW cell 2A-Cu2, androconial (left) and non-androconial (right) scales; (AC) *Mechanitis p. polymnia*, male DHW anterior edge cell Cu1-M3, androconial (left) and non-androconial (right) scales.

distal edge of the antenna. Unfortunately, across the range of taxa studied here, it proved difficult to define character states and therefore to code much of this variation.

82. *Sulci (ventral depressions containing sensory hairs) on fourth from terminal antennomere of female antenna*: (0) equidistant from medial and lateral carinae (Fig. 11A); (1) nearer to lateral carinae (Fig. 11B). There is variation in the size, depth, definition and position of sulci among the Ithomiinae. Sulci range from a shallow, smooth scoop in more primitive species (e.g., Melinaeini, *Tithorea*) to well-marked depressions (e.g., *Pteronymia*, *Episcada*, *Ceratinia*). Owing to continuous variation, however, it proved difficult to code sulci shape, and only two characters, based on sulci position, were defined.

83. *Sulci on fourth from terminal antennomere of female antenna*: (0) equidistant from distal and proximal edges of antennomere (Fig. 11A); (1) nearer proximal edge of antennomere (Fig. 11C).

Labial palpus and head

The third palpal segment is variable in size, but due to continuous variation no character was coded.

84. *Labial palpus color in lateral view*: (0) black at tip (segment 3) and on ventral half on segment 2 (dorsally white) (Fig. 12B); (1) black at tip and extending medially into segment 2 (Fig. 12A); (2) entirely black (Fig. 12C).

85. *Labial palpus with long blade and/or hair-like scales ventrally*: (0) present (Fig. 12B); (1) absent (Fig. 12A). These elongate scales are noticeably distinct from the scales clothing the sides of the palpus.

86. *Frons*: (0) black with ventrally tapering white borders (Fig. 12E); (1) black with white border restricted to dorsal half (Fig. 12F); (2) entirely black (Fig. 12D).

87. *Dorsal head with pale central marking*: (0) a small dash posterior of antennae bases (Fig. 12H); (1) a line extending from posterior edge of head to ventral edge of frons (Fig. 12G).

Patagia, tegula, thorax and abdomen

88. *Patagia with outer half of lobes*: (0) largely reddish orange (Fig. 12H); (1) white to cream (Fig. 12I); (2) black (Fig. 12J); (3) yellow (Fig. 12K).

89. *Patagia with inner part of lobes, if different from outer half*: (0) black (Fig. 12I); (1) white (Fig. 12J); (2) reddish brown (Fig. 12L). Species with uniformly colored patagia are coded as equivocal, to avoid duplicating the previous character.

90. *Anterior ventral projection of tegula*: (0) pale yellow to white (Fig. 12N); (1) partially pale in center (Fig. 12P); (2) dark brown/black (Fig. 12O); (3) reddish brown (Fig. 12M).

91. *Scale direction on tegula*: (0) posterior, except more or less radiating from a posterio-ventral point (Figs 11D and 12M); (1) anticlockwise (right tegula) around a central point (Figs 11E and 12P); (2) clockwise (right tegula) and converging on center (Figs 11F and 12N). Scales typically lie flat against the tegula and all point in a certain direction.

92. *Pale continuous central band on tegula*: (0) absent (Fig. 12O); (1) present (Fig. 12N).

93. *Dorsal thorax with pale midline*: (0) even in width (Fig. 12Q); (1) tapering posteriorly (Fig. 12R); (2) reduced to posterior third (Fig. 12S); (3) an elongate central dash (Fig. 12T); (4) a small central spot (Fig. 12U); (5) absent (Fig. 12V). Because this character essentially codes reduction in the thoracic midline, "absent" was logically included as a state rather than a separate character.

94. *Scales on dorsal metathorax pointing*: (0) anteriorly (Fig. 13A); (1) anteriorly, except at apex where vertical (Fig. 13B); (2) vertically, except anteriorly at posterior edge (Fig. 13C); (3) vertically (Fig. 13D); (4) in circular pattern on either side of thorax, pointing anteriorly in center (Fig. 13E); (5) posteriorly, except anteriorly at posterior edge (Fig. 13F); (6) in circular pattern on either side of thorax, pointing posteriorly in center (Fig. 13G). This character was occasionally difficult to assess in museum specimens, especially as the metathorax is often damaged by the pin and may have scales rubbed off. Scales either lie flat against the metathorax or nearly vertically.

95. *Dorsal abdomen color*: (0) dark brown (Fig. 12W); (1) orange-brown (Fig. 12X); (2) dark brown, yellow laterally towards the base (Fig. 12Y); (3) dark brown with lateral orange-brown smudges in the middle of each tergite (Fig. 12Z); (4) dark brown, with the ventral half of tergites white posteriorly (Fig. 12AA); (5) dark brown with the edges of tergites lined with pale gray (Fig. 12AB); (6) dark brown with white spots in the middle of the posterior edge of each tergite (Fig. 12AC); (7) dark brown with white spots at the anterior corner ventral edge of tergites (Fig. 12AD); (8) dark brown with white spots at posterior corner ventral edge of tergites (Fig. 12AE); (9) black with white lateral spots at the middle ventral edge of each tergite and a white dorsal line of spots in the middle of each tergite (Fig. 12AF); (A) dark brown with a pale, broken dorsolateral line (Fig. 12AG); (B) dark brown with a continuous pale dorsolateral line (Fig. 12AH). Like the following two characters, the dorsal abdomen color pattern is to some extent affected by mimicry. Nevertheless, despite often similar appearances, the precise position of pattern elements with respect to body sclerites provides evidence as to homology in pattern development.

96. *Ventral thorax pale stripes*: (0) continuous from coxa to wing base on meso- and metathoraces (Fig. 12AI); (1) broken at dorsal edge of meron 3 (Fig. 12AJ); (2) broken at meron 3 (Fig. 12AK); (3)

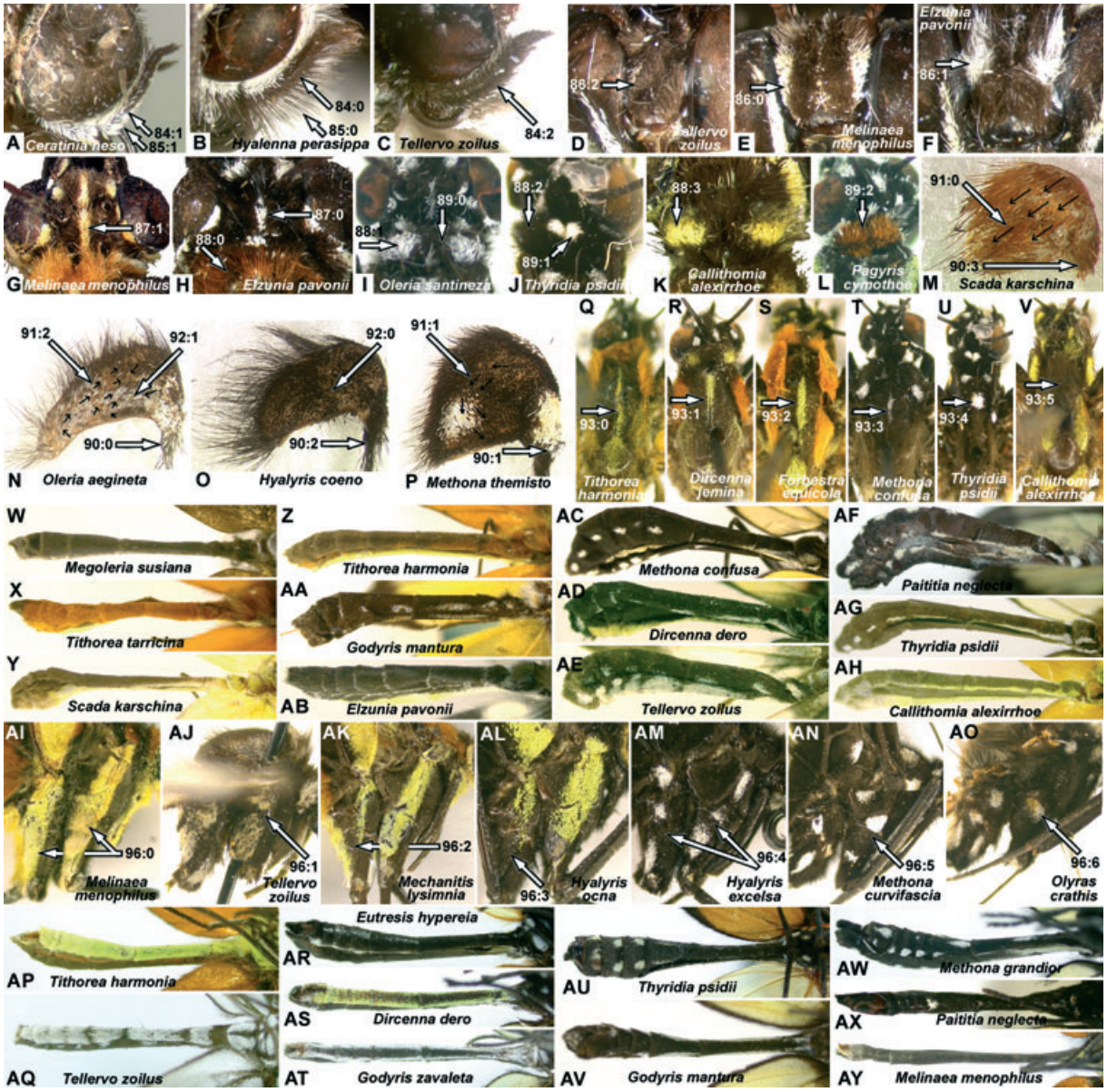

Fig. 12. Labial palpi: (A) *Ceratinia n. neso*; (B) *Hyalenna perasippa* ssp. n.; (C) *Tellervo z. zoilus*. Frons: D, *Tellervo z. zoilus*; (E) *Melinaea menophilus zaneka*; (F) *Elzunia pavonii*. Head and patagia, dorsal view: G, *Melinaea menophilus zaneka*; (H) *Elzunia pavonii*; (I) *Oleria s. santineza*; (J) *Thyridia psidii aedesia*; (K) *Callithomia alexirrhoe butes*; (L) *Pagyris cymothoe cymothoe*. Right tegula: M, *Scada k. karschina*; (N) *Oleria aegineta inelegans*; (O) *Hyalyris c. coeno*; (P) *Methona themisto*. Dorsal thorax: (Q) *Tithorea harmonia manabiana*; (R) *Dircenna jemina visina*; (S) *Forbestra equicola equicoloides*; (T) *Methona c. confusa*; (U) *Thyridia psidii aedesia*; (V) *Callithomia alexirrhoe butes*. Abdomen, dorsolateral view: (W) *Megoleria s. susiana*; (X) *Tithorea tarricina bonita*; (Y) *Scada karschina*; (Z) *Tithorea harmonia hermias*; (AA) *Godyris mantura honrathi*; (AB) *Elzunia pavonii*; (AC) *Methona c. confusa*; (AD) *Dircenna dero* ssp. n.; (AE) *Tellervo z. zoilus*; (AF) *Paititia neglecta*; (AG) *Thyridia psidii ino*; (AH) *Mechanitis polymnia chimborazona*. Ventral thorax, lateral view: (AI) *Melinaea menophilus zaneka*; (AJ) *Tellervo z. zoilus*; (AK) *Mechanitis lysimnia menecles*; (AL) *Hyalyris ocna* ssp. n.; (AM) *Hyalyris excelsa* ssp. n.; (AN) *Methona c. curvifascia*; (AO) *Olyras c. crathis*. Abdomen, ventrolateral view: (AP) *Tithorea harmonia hermias*; (AQ) *Tellervo z. zoilus*; (AR) *Eutresis hypereia banosana*; (AS) *Dircenna dero* ssp. n.; (AT) *Godyris zavaleta telesilla*; (AU) *Thyridia psidii aedesia*; (AV) *Godyris mantura honrathi*; (AW) *Methona grandior* ssp. n.; (AX) *Paititia neglecta*; (AY) *Melinaea menophilus zaneka*.

absent on meron 3 (Fig. 12AL); (4) broken on meron 2 and 3 (Fig. 12AM); (5) broken into white spots on ventral edge of meron and between meron and episternum (Fig. 12AN); (6) broken into white spots at dorsal edge of meron, episternum (Fig. 12AO). The ventral thorax has lateral pale white to yellow stripes immediately basal of black stripes where the legs fold against the body. Among members of a mimicry ring containing

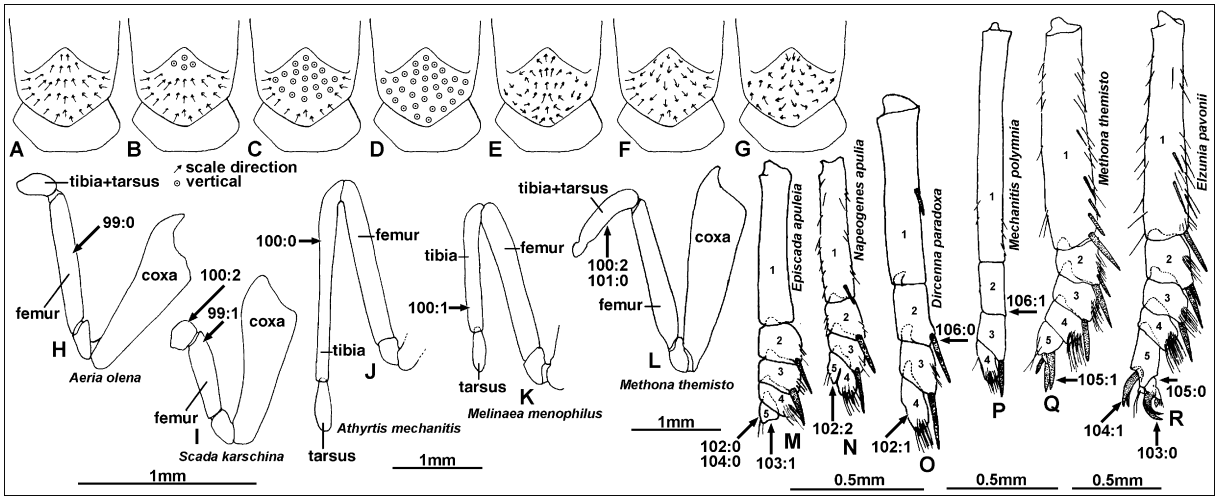

Fig. 13. Direction of scales on dorsal metathorax, representing Char. 95, states 0–6, respectively: (A–G). Male foreleg, lateral view: (H) *Aeria olena*; (I) *Scada k. karschina*; (J) *Athyrtis m. mechanitis*; (K) *Melinaea menophilus zaneka*; (L) *Methona themisto*. Female foreleg, lateral view: (M) *Episcada a. apuleia*; (N) *Napeogenes a. apulia*; (O) *Dircenna paradoxa praestigiosa*; (P) *Mechanitis p. polymnia*; (Q) *Methona themisto*; (R) *Elzunia pavonii*.

Methona and similar species, these stripes are usually broken to form a similarly appearing pattern of a black body with white dots.

97. *Ventral abdomen and sides*: (0) pale yellow to white (Fig. 12AP); (1) white, with segment borders dark brown (Fig. 12AQ); (2) dark brown with yellowish white dorsal edges to sternites and a yellow-white ventral midline in the posterior half (Fig. 12AR); (3) yellow with a dark brown midline (Fig. 12AS); (4) white with a dark brown midline (Fig. 12AT); (5) dark brown, with a pale yellowish dorsolateral line broken at the anterior edge of sternites (Fig. 12AU); (6) dark brown, except white in the dorsal half posteriorly (Fig. 12AV); (7) dark brown with a white midline and white spots at dorso-posterior edge of sternites (Fig. 12AW); (8) black, except for white spots at middle at posterior edge of sternites, line of broken white dorso-lateral spots near dorsal edge of sternite (Fig. 12AX); (9) dark brown (Fig. 12AY).

98. *Abdominal sternites with elongate scales at posterior edge*: (0) absent (Fig. 11M); (1) present (Fig. 11L). State 1 is an apparent synapomorphy for *Tellervo* + Ithomiinae. In Danainae the scales at the posterior edges of each sternite are similar morphologically to the rest of the sternite, but in *Tellervo* and Ithomiinae they are distinctly elongate.

Male foreleg

99. *Male foreleg with femur*: (0) equal or longer than coxa (Fig. 13H); (1) shorter than coxa (Fig. 13I). Fox and Real (1971) stated that Napeogenini had state 0 and Ithomiini state 1 for this character. However, we found the differences between these tribes to be very small, and often difficult to see, if apparent at all. Only a small number of primitive species show the femur substantially shorter than the coxa, and only these were coded state 1.

100. *Male foreleg with tibia + tarsus*: (0) unfused, longer than femur (Fig. 13J); (1) unfused, shorter or equal to femur (Fig. 13K); (2) fused, shorter than femur (Fig. 13L).

101. *If male foreleg tibia and tarsus are fused (Char. 100:2), then they are*: (0) elongate (Fig. 13L); (1) rounded (Fig. 13I). The fused tibia and tarsus is typically rounded or "pear"-like, except in *Methona themisto*. In *Episcada* and related genera the fused tibia and tarsus may be flattened against the femur and so triangular in outline, but given significant variation even within species this character was not coded.

Female legs

More primitive species tend to have denser tarsal trichoid sensillae.

102. *Female foreleg fourth and fifth tarsal segments*: (0) distinct (Fig. 13M); (1) fifth fused with fourth or absent (Fig. 13O); (2) fifth partially fused with fourth, visible as a bump (Fig. 13N).

103. *Female foreleg fifth tarsal segment claws*: (0) present (Fig. 13R); (1) absent (Fig. 13M). This and the next two characters were coded as equivocal for species where the fifth tarsal segment is absent or fused with the fourth (Char. 102:1).

104. *Female foreleg tarsus with paired "spurs" dorsally on fifth segment*: (0) absent (Fig. 13M); (1) present (Fig. 13R). Spurs are elongate, articulating spine-like projections, of similar color to other leg segments,

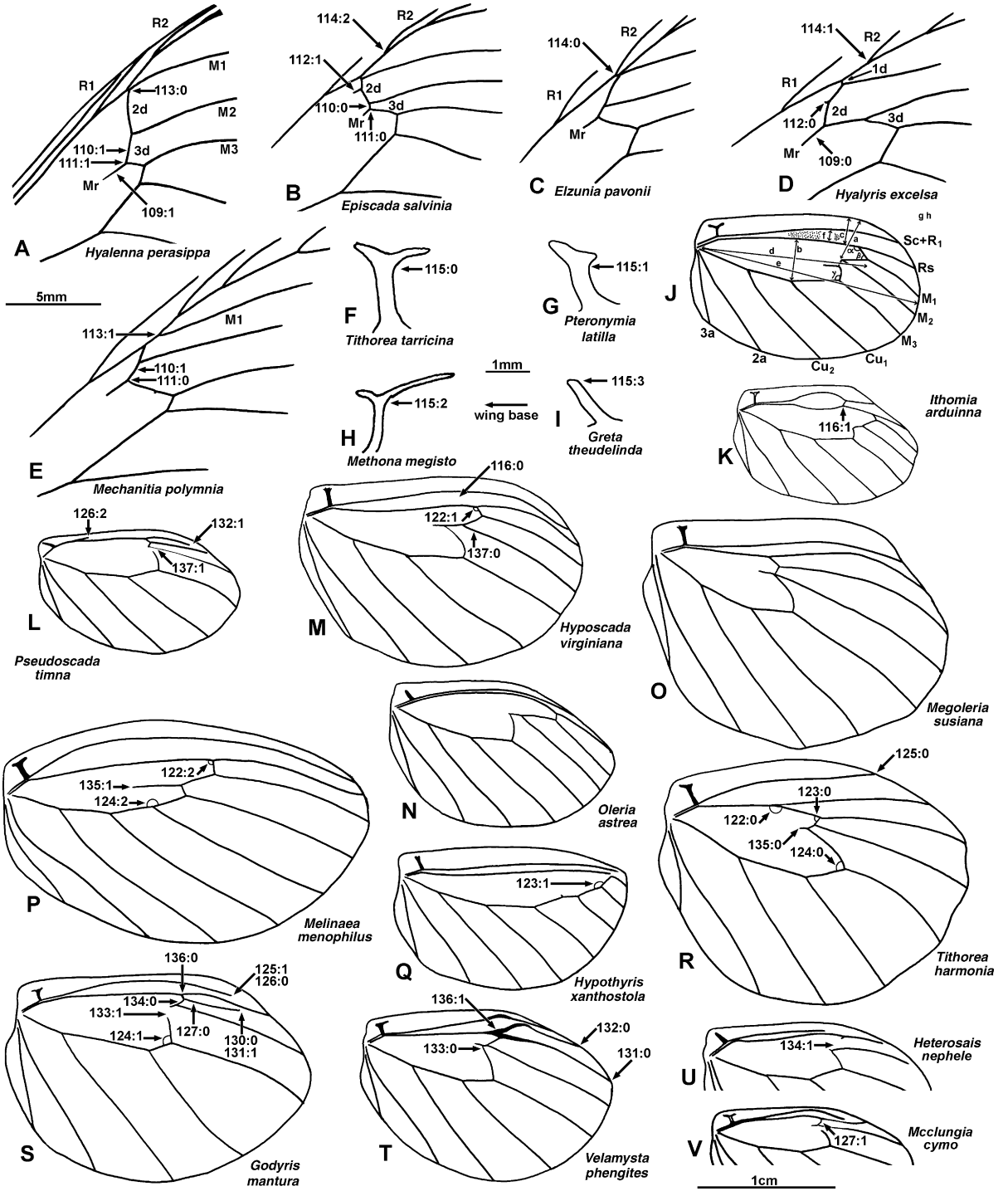

Fig. 14. Male forewing venation, discal area: (A) *Hyalenna perasippa* ssp. n.; (B) *Episcada s. salvinia*; (C) *Elzunia pavonii*; (D) *Hyalyris excelsa decumana*; (E) *Mechanitis p. polymnia*. Male VHW humeral vein: (F) *Tithorea tarricina duenna*; (G) *Pteronymia latilla fulvescens*; (H) *Methona megisto*; (I) *Greta t. theudelinda*. Male hindwing venation: (J) generalized diagram showing venation and measured shape variables; (K) *Ithomia a. arduinna*; (L) *Pseudoscada timna pusio*; (M) *Hyposcada virginiana adelphina*; (N) *Oleria astrea burchelli*; (O) *Megoleria s. susiana*; (P) *Melinaea m. menophilus*; (Q) *Hypothyris xanthostola*; (R) *Tithorea harmonia megara*; (S) *Godyris mantura honrathi*; (T) *Velamysta p. phengites*; (U) *Heterosais n. nephele*; (V) *Mcclungia cymo salonina*.

compared with the very dark brown, smaller and morphologically distinct spines that are also present on all legs (see Fig. 11J).

105. *Female foreleg tarsus with paired "spurs" ventrally on fifth segment*: (0) absent (Fig. 13R); (1) present (Fig. 13Q).

106. *Female foreleg with paired spurs at ventral distal edge of*: (0) third, second (sometimes first) tarsal segments (Fig. 13O); (1) third segment only (Fig. 13P).

107. *Female mid- and hindleg tibial spurs*: (0) present (Fig. 11I,J); (1) absent (Fig. 11K). Tibial spurs are absent in all Ithomiinae except *Tithorea* and *Elzunia*. The distinction between spurs and spines is discussed under Char. 104 and illustrated in Fig. 11(J).

108. *Female foretarsus segment 4 ventral surface*: (0) with sparse, thick spines similar to other segments (Fig. 11H); (1) with dense, thin spines differing from other segments (Fig. 11G). State 1 is a synapomorphy for *Melinaea*.

Wing venation

Male forewing

109. *Male FW with medial recurrent vein Mr on*: (0) 2d (Fig. 14D); (1) 3d (Fig. 14A).

110. *If male FW with Mr on 3d (Char. 109:1), then upper arm of 3d is*: (0) approximately half or less the length of 2d (Fig. 14B); (1) about the same length as 2d, or greater (Fig. 14A,E). In *Dircenna paradoxa* there is geographic variation in the relative lengths of 3d and 2d. Individuals from northern Ecuador and Colombia have the upper arm of 3d similar in length to 2d, thus very closely resembling the venation of *Hyalenna*, while individuals from central and southern Ecuador to Peru have state 0. There are no other morphological differences between individuals from these regions (Willmott and Lamas, 2006).

111. *If male FW with Mr on 3d (Char. 109:1), then Mr positioned*: (0) nearer the base of vein M2 than M3 (Fig. 14B,E); (1) nearer the base of vein M3 than M2 (Fig. 14A). State 1 occurs exclusively in all *Hyalenna*.

112. *Male FW with additional medial recurrent vein anterior of Mr*: (0) absent or weak (about half size of Mr) (Fig. 14D); (1) strong, about the same size as Mr (Fig. 14B).

113. *Male FW with M1 originating*: (0) at or on discocellular veins (Fig. 14A); (1) distal of the discal cell end (Fig. 14E). *Mechanitis lysimnia* shows significant variation in forewing venation, even between wings of the same individual. It was therefore coded as polymorphic.

114. *Male FW with origin of vein R2*: (0) basal of discal cell end (Fig. 14C); (1) distal of but near discal cell end [ratio of cell end-R1/cell end-R2 > 1.3] (Fig. 14D); (2) distal of and far from cell end (ratio of cell end-R1/cell end-R2 < 1.3) (Fig. 14B).

Male hindwing

115. *Male hindwing humeral vein*: (0) "forked" with distal and basal arms similar in length (Fig. 14F); (1) forked with distal arm reduced to a bump or absent (Fig. 14G); (2) forked with basal arm reduced to a bump or absent (Fig. 14H); (3) unforked (both arms apparently absent) (Fig. 14I). Fox (1940) placed a great emphasis on whether or not the VHW humeral vein was "forked" in his taxonomy. However, there is substantial variation even within single individuals (comparing both wings) in the extent of the "arms" arising from the tip of the humeral vein, and as these fade gradually into the surrounding wing, assessing the shape of the vein is often rather subjective. The state "unforked" of Fox may arise either through loss of one or other of the arms at the tip or through loss of both (in which case a slight double bump is sometimes visible at the tip). These different possibilities have therefore been coded as distinct states.

116. *Male hindwing with cross-vein joining Sc + R1 and Rs*: (0) absent (Fig. 14M); (1) present (Fig. 14K). State 1 is a synapomorphy for *Ithomia*.

117. *Male hindwing with ratio of distance between base of vein M2 and costa/maximum discal cell width,* r *(= a/b, Fig. 14J)*: (0) $r < 0.75$ (Fig. 14M); (1) $r > 0.75$ (Fig. 14N). State 0 represents the discal cell being placed placed more anteriorly in the wing, nearer the costa, and occurs in most species in the tribes Godyridini and Dircennini.

118. *Male hindwing with ratio of distance between costa and anterior edge discal cell opposite end of vein M2/distance between base of vein M2 and costa,* r *(= c/a, Fig. 14J)*: (0) $r < 1.07$ (Fig. 14L); (1) $1.07 < r < 1.23$ (Fig. 14K); (2) $1.23 < r$ (Fig. 14P). Higher numbered character states represent species in which the base of vein M2, which typically meets the discal cell near the medial recurrent vein, is positioned nearer the middle, rather than anterior edge, of the discal cell.

119. *Male hindwing with ratio of anterior cell length (base of discal cell to base of vein M1 or Rs, whichever further)/maximum wing length,* r *(= d/e, Fig. 14J)*: (0) $r < 0.56$ (Fig. 14R); (1) $0.56 < r < 0.69$ (Fig. 14P); (2) $0.69 < r$ (Fig. 14Q). Species with higher numbered states have relatively longer discal cells in comparison with overall, wing width, occurring especially in the Napeogenini and Oleriini.

120. *Male hindwing with ratio of maximum cell width/anterior cell length (base of discal cell to base of vein M1 or Rs, whichever further),* r *(= b/d, Fig. 14J)*: (0) $r < 0.28$ (Fig. 14R); (1) $0.28 < r$ (Fig. 14Q). Species with state 0 have relatively narrower discal cells.

121. *Male hindwing with ratio of distance between discal cell and Sc + R1 at maximum width of androconial scale patch/maximum cell width,* r *(= f/b, Fig. 14J)*: (0) $r < 0.2$ (Fig. 14N); (1) $0.2 < r < 0.3$ (Fig. 14O);

(2) $0.3 < r$ (Fig. 14R). Species with higher numbered character states have a broader patch of androconial scales between veins Sc + R1 and Rs because these veins are further apart. Primitive species tend to have higher states. *Pseudoscada timna*, *P. erruca* and *P. florula* were coded as unknown because vein Sc + R1 does not extend to the broadest part of the androconial scale patch.

122. *Male hindwing with angle between veins Rs (in discal cell) and 1d (= α, Fig. 14J)*: (0) greater than 140° (Fig. 14R); (1) between 110 and 139° (Fig. 14M); (2) less than 110° (Fig. 14P).

123. *Male hindwing with angle between veins 1d and 2d (= β, Fig. 14J)*: (0) acute or nearly right angle (Fig. 14R); (1) about 140° (Fig. 14Q). State 1 is an autapomorphy for *Hypothyris xanthostola*.

124. *Male hindwing with angle between veins 3d and Cu1-M3 (= γ, Fig. 14J)*: (0) less than or equal to 90° (Fig. 14R); (1) between 90 and 145° (Fig. 14S); (2) greater than 145° (Fig. 14P).

125. *Male hindwing with vein Sc + R1*: (0) reaching margin (Fig. 14R); (1) not reaching margin (Fig. 14S).

126. *If male hindwing with vein Sc + R1 not reaching margin (Char. 125:1)*: (0) Sc + R1 ends near or distal of cell end (Fig. 14S); (1) Sc + R1 ends about halfway along the cell (Fig. 15B); (2) Sc + R1 almost absent (Fig. 14L).

127. *Male hindwing with vein M1*: (0) present (Fig. 14S); (1) absent (Fig. 14V). State 1 occurs only in *Mcclungia cymo*, in which absence of M1 is inferred from the apparent presence of both 1d and 2d at the end of the discal cell, which lie anterior and posterior of the end of M1. Presence of both 1d and 2d is inferred from a kink in the discocellular vein lying between veins Rs and M2, which apparently represents the junction between these two veins. In the derived state of the following Char. 127:1, in contrast, the discocellular vein is straight between Rs and and M2, suggesting that M1 and Rs are fused in species where only a single one of these veins is apparent.

128. *Male hindwing with veins M1 and Rs basally*: (0) distinct (Fig. 15B); (1) fused (Fig. 15C). Fusion of these veins is inferred from the straight discocellular vein between veins Rs and M2, and related species in which the veins are partially fused. In *Heterosais* the discocellular vein attached to Rs is partially visible with the basal angle between it and vein Rs distinctly acute (Fig. 14U). As all other species in the Godyridini have the angle between Rs and 1d greater than 110° (Char. 122:0,1), the inference is that this vein represents vein 2d, in which case veins M1 and Rs are fused.

129. *If male hindwing with veins M1 and Rs basally fused (Char. 128:1), remainder of veins are*: (0) partially fused (Fig. 15C); (1) entirely fused (Fig. 15A).

130. *Male hindwing with veins M1and Rs distally*: (0) separate (Fig. 14S); (1) almost or actually touching at tip (Fig. 15B). Species with these veins entirely fused (Char. 129:1) are coded equivocal.

131. *Male hindwing with vein M1*: (0) reaching margin (Fig. 14T); (1) not reaching margin (Fig. 14S). Species with veins M1 and Rs entirely fused (Char. 129:1) are coded equivocal.

132. *Male hindwing with vein Rs*: (0) reaching margin (Fig. 14T); (1) not reaching margin (Fig. 14L). Species with veins M1 and Rs entirely fused (Char. 129:1) are coded equivocal.

133. *Male hindwing with anterior tip of 3d*: (0) present (Fig. 14T); (1) absent (Fig. 14S). State 1 is exclusive to all Godyridini except for *Velamysta*, *Veladyris* and *Heterosais*. In the former two genera state 0 may be a symplesiomorphy, in *Heterosais* it appears to be a reversal and synapomorphy.

134. *Male hindwing with vein 2d*: (0) complete (Fig. 14S); (1) incomplete (Fig. 14U). This is a synapomorphy for *Heterosais*.

135. *Male hindwing with vein Mr on*: (0) 3d (Fig. 14R); (1) 2d (Fig. 14P). Species with Mr at the junction of 3d and 2d are coded equivocal. Most Godyridini are also coded equivocal as the anterior portion of 2d is absent (Char. 134:1).

136. *Male hindwing with base of veins M1, Rs and neighboring Sc + R1*: (0) of similar width to rest of vein (Fig. 14S); (1) swollen to about three times usual width (Fig. 14T). State 1 is a synapomorphy for *Velamysta*.

137. *Male hindwing with vein M2*: (0) of similar width to other veins (Fig. 14M); (1) very narrow or absent basally (Fig. 14L).

138. *Male hindwing androconial scales beneath hair pencil*: (0) on flat wing membrane or in a curved channel running between Sc + R1 and Rs (Fig. 11O); (1) in a curved channel extending posteriorly beyond vein Rs (Fig. 11N). Most species have the wing membrane beneath the androconial scales between veins Sc + R1 and Rs more or less curved to accommodate these enlarged scales. In *Ithomia* this curved channel is of a particular form, which extends posteriorly beyond vein Rs.

139. *Male hindwing fold in cell Sc + R1-Rs near margin*: (0) absent or simple "U"-shape (Fig. 11P); (1) "S"-shape (Fig. 11Q); (2) double "S"-shape (Fig. 11R). A number of other species have the wing folded between Sc + R1 and Rs to form a half-tube with parallel sides. In species in several genera in the Napeogenini the wing is even more strongly folded, so that vein Sc + R1 almost touches vein Rs (state 1), enclosing the androconial scales between these two veins, while in *Greta diaphanus* it is doubly folded (state 2).

Female hindwing

140. *Female hindwing with vein Sc + R1*: (0) meeting vein Rs at base of humeral vein (Fig. 15G); (1) meeting

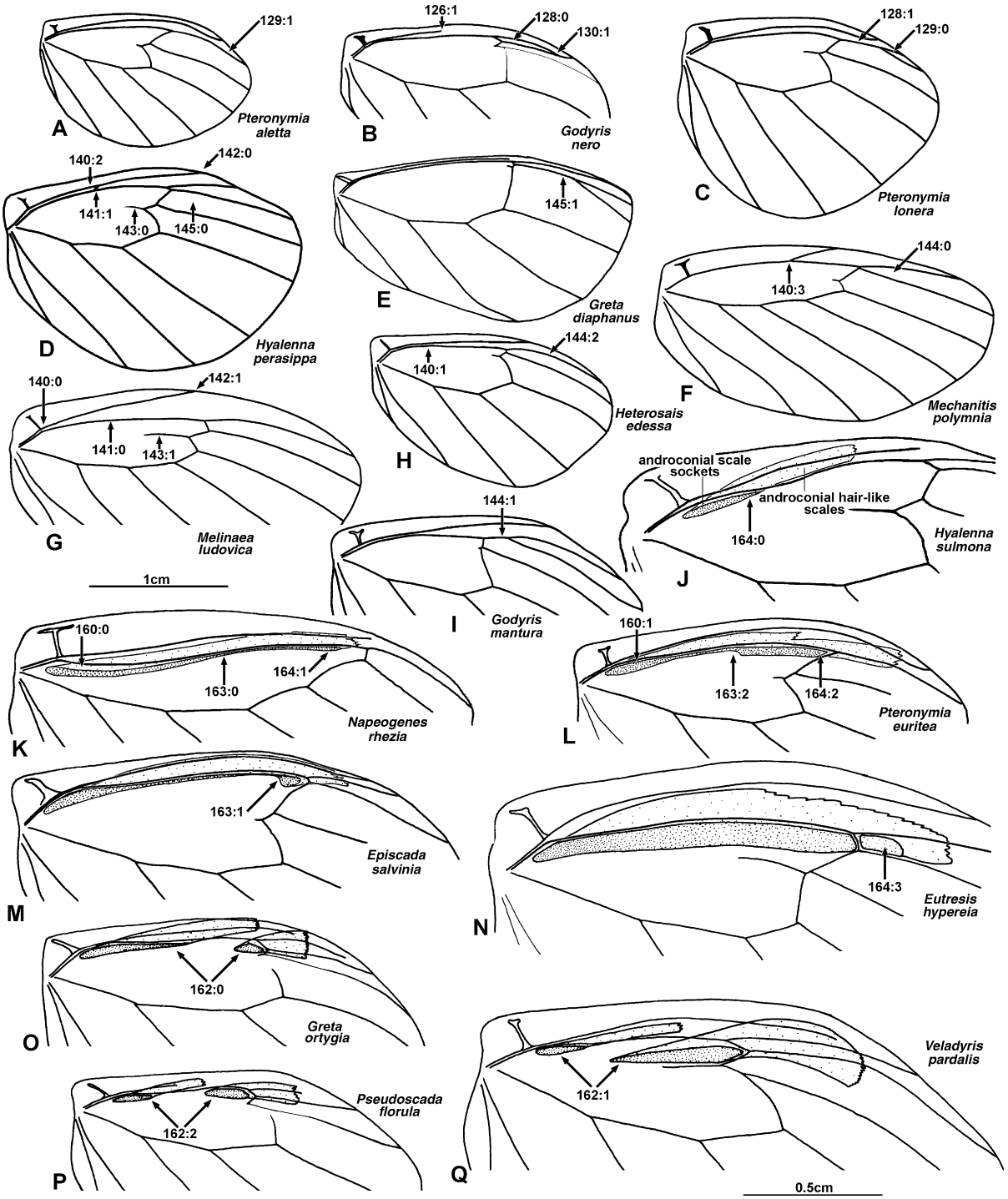

Fig. 15. Female hindwing venation: (A) *Pteronymia a. aletta*; (B) *Godyris nero*; (C) *Pteronymia lonera*; (D) *Hyalenna perasippa* ssp. n.; (E) *Greta diaphanus*; (F) *Mechanitis p. polymnia*; (G) *Melinaea l. ludovica*; (H) *Heterosais edessa*; (I) *Godyris mantura honrathi*. Male DHW discal cell, distribution of androconial hair-like scales (''hair pencil''): (J) *Hyalenna sulmona lobusa*; (K) *Napeogenes r. rhezia*; (L) *Pteronymia euritea*; (M) *Episcada s. salvinia*; (N) *Eutresis hypereia theope*; (O) *Greta o. ortgyia*; (P) *Pseudoscada florula aureola*; (Q) *Veladyris p. pardalis*.

and running alongside vein Rs between humeral vein and point opposite base of vein Cu2 (Fig. 15H); (2) meeting and running alongside vein Rs distal of point opposite base of vein Cu2 (Fig. 15D); (3) fused with vein Rs to distal of point opposite base of vein Cu2 (Fig. 15F).

141. *Female hindwing with cross-vein between vein Sc + R1 and discal cell*: (0) absent (Fig. 15G); (1) present (Fig. 15D). This cross-vein varies somewhat in development, being a clear vein similar in thickness to Sc + R1 in some species (e.g., *Hyalenna perasippa*) to slight bumps, which just merge with one another, only visible in cleared specimens. A slight indentation in vein Sc + R1 usually indicates where the cross-vein originates, if present.

142. *Female hindwing with vein Sc + R1 ending at anal margin*: (0) distal of cell end (1d) (Fig. 15D); (1) basal of cell end (Fig. 15G). If vein Sc + R1 is incomplete (coded for males in Char. 125:1) then this character is coded as equivocal.

143. *Female hindwing with vein Mr*: (0) on 3d (Fig. 15D); (1) 2d (Fig. 15G). Despite some correlation with Char. 135, sexes differ in the position of Mr in a number of species, and in most Godyridini males cannot be coded (see Discussion under Char. 135).

144. *Female hindwing with veins M1 and Rs*: (0) distinct (Fig. 15F); (1) partially fused (Fig. 15I); (2) entirely fused (Fig. 15H).

145. *Female hindwing with veins M2 and M1*: (0) separate (Fig. 15D); (1) partially fused (Fig. 15E).

Scales

Main wing scales

146. *Transparent areas of wing with ground scales*: (0) flat crescents (Fig. 11S); (1) flat, leaf-shaped with multiple scalloped distal edge (Fig. 11T); (2) ''U''-shaped hairs (Fig. 11U); (3) pitchfork-shaped hairs (Fig. 11V); (4) flat, leaf-shaped (Fig. 11W). Two types of scales are present on the main wing areas, one longer and narrower (cover scales) and the other shorter and broader (ground scales). Many ithomiines have areas of the wing translucent or transparent, through narrowing of both types of scale to reveal the transparent wing membrane. Typically cover scales are hair-like, while ground scales occur in various different forms, coded here.

147. *Wing with cover and ground scale bases*: (0) dispersed, or in lines (Fig. 11W); (1) almost touching (Fig. 11S). Cover and ground scales on the main wing areas (see Char. 146) are typically arranged in alternating, irregular lines (e.g., Fig. 11Y) or more randomly dispersed. In *Athesis*, *Patricia* and *Methona* the scales are arranged in pairs, one of each type of scale in each, with the bases immediately adjacent.

Androconial scales (not DHW costal region)

148. *Male DFW with reduced scale density in a patch from anal margin to posterior edge discal cell*: (0) absent; (1) present (Fig. 11X,Y). State 1 is an autapomorphy for *Tellervo*. Examination of this part of the wing shows no evidence of modified, androconial scales, despite the sexual dimorphism in this character. The paler area on the male DFW results from slightly more dispersed and narrower wing scales.

149. *Male DFW with patch of spatulate, silky black androconial scales in anterior half discal cell to base cells M3–M2 and M2–M1*: (0) absent; (1) present (Fig. 11Z). State 1 is an autapomorphy for *Aeria eurimedia*.

150. *Male DFW with dense, elongate androconial scales lining vein 2A*: (0) absent; (1) present (Fig. 11AA). State 1 is a synapomorphy for *Forbestra + Mechanitis*.

151. *Male DHW with dense, elongate triangular scales in discal area*: (0) absent; (1) present (Fig. 11AB). State 1 is an autapomorphy for *Hypothyris xanthostola*.

152. *Male DHW with dense, rounded androconial scales in postdiscal band*: (0) absent; (1) present (Fig. 11AC). State 1 is an autapomorphy for *Mechanitis polymnia*.

153. *If male DHW hair pencil present (Char. 156:1), then VFW anal margin cell 2A-Cu2 is*: (0) entirely covered with narrow hair-like to broader leaf-like scales (Fig. 17A); (1) devoid of scales in basal half of cell at anterior edge (Fig. 17C); (2) devoid of scales in an elongate patch in basal half of cell in middle (Fig. 17D); (3) devoid of scales in an elongate patch in basal half bordering on vein 2A (Fig. 17E); (4) devoid of scales in an ovoid patch in basal half extending across into anal margin-2 A (Fig. 17F); (5) devoid (or nearly so) of scales from near base to past base vein Cu2 (Fig. 17G). Cell 2A-Cu2 on the VFW of male ithomiines is clothed with variously modified scales, the distribution of which is correlated with the position of androconial scales on the dorsal hindwing. *Tellervo* (the outgroup), which lacks hindwing androconial hair-like scales, is coded as equivocal. In some ithomiine species part of this cell is devoid of scales, or has only a very sparse scattering of needle-like scales. The extent of this bare area varies between genera and is coded here. State 5 is a synapomorphy for Godyridini + Dircennini.

154. *Male VFW cubital vein with elongate hairs extending posteriorly*: (0) absent (Fig. 16A); (1) present in basal half of vein only (Fig. 17E); (2) present throughout vein (Fig. 16B).

155. *Male VFW with scales around vein 2A*: (0) absent or barely differentiated from scales in remainder of cell (Fig. 17C); (1) yellow, sparse, distinct from surrounding scales (Figs 16C and 17A); (2) yellow, very dense, elongate, distinct from surrounding scales (Figs 16D and 17B).

Male DHW androconial ''hair pencil''

156. *Male DHW with a linear band of androconial erectile, piliform scales (''hair pencil'') at anterior edge of discal cell*: (0) absent (Fig. 17H); (1) present (Fig. 16E). State 1 is a universal synapomorphy for the Ithomiinae. The sockets are highly modified from usual scale sockets

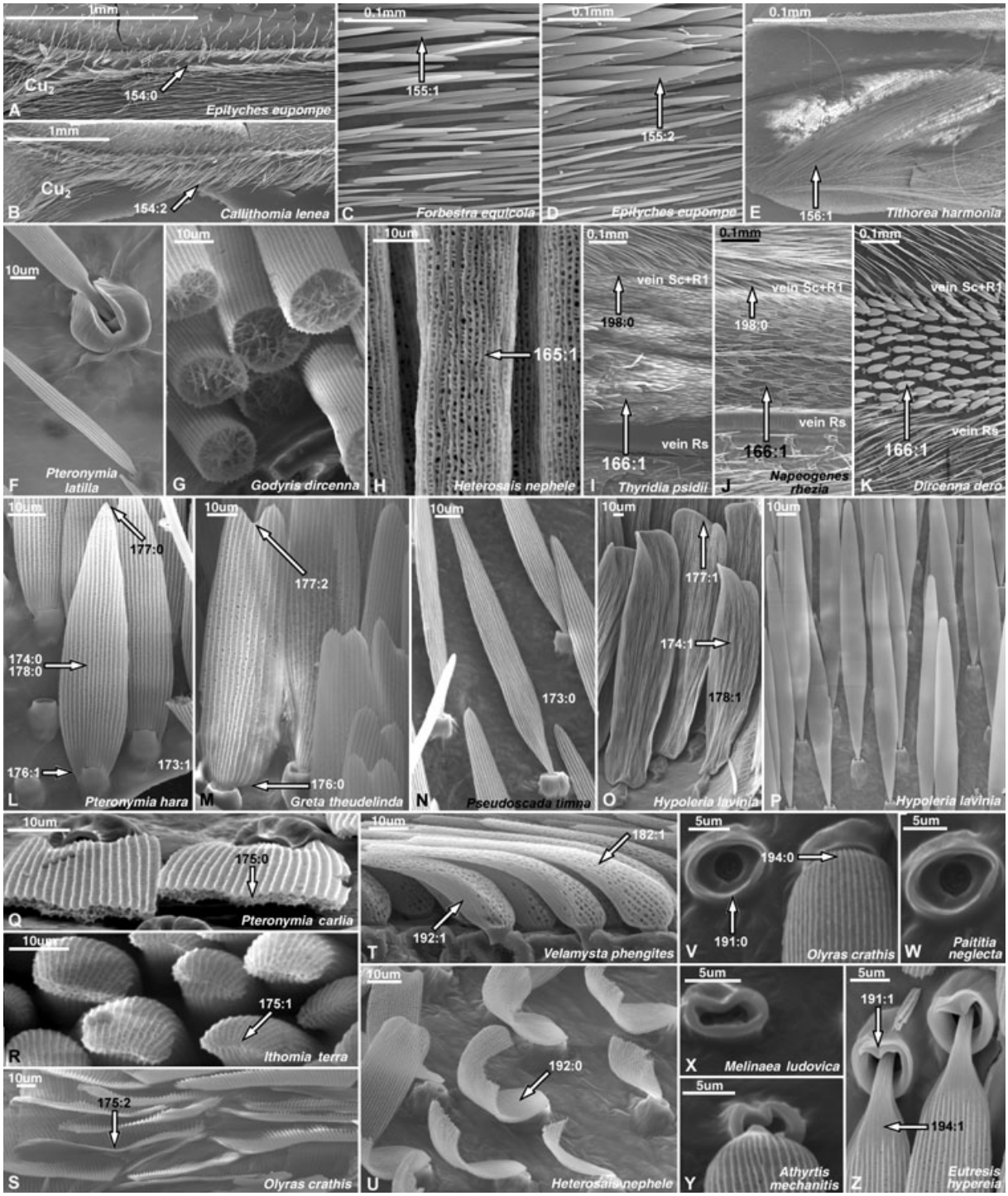

Fig. 16. Male androconial scales. VFW cubital vein: (A) *Epityches eupompe*; (B) *Callithomia lenea zelie*. VFW vein 2A androconial (upper) and wing (lower) scales: C, *Forbestra e. equicola*; (D) *Epityches eupompe*. (E) *Tithorea harmonia megara*, male DHW androconial hair-like scales (''hair pencil'') and underlying androconial scale patch. (F) *Pteronymia l. latilla*, DHW hair pencil scale and socket (upper), wing scale and socket (lower); (G) *Godyris dircenna*, cross-section through DHW hair pencil scales; (H) *Heterosais n. nephele*, thickened androconial hair-like scales underlying DHW hair pencil. DHW androconial scale patch between veins Sc + R1 and Rs: (I) *Thyridia psidii psidii*; (J) *Napeogenes r. rhezia*; (K) *Dircenna dero celtina*. DHW androconial scales in cell Rs-Sc + R1, basal (B) and distal (D): (L) *Pteronymia h. hara* (B); (M) *Greta t. theudelinda* (B); (N) *Pseudoscada timna pusio* (B); (O) *Hypoleria lavinia riffarthi* (B); (P) *Hypoleria lavinia riffarthi* (D); (Q) *Pteronymia carlia* (B), cross-section; (R) *Ithomia t. terra* (B), scale tips; (S) *Olyras c. crathis* (B), scale tips; (T) *Velamysta p. phengites* (B), lateral view; (U) *Heterosais n. nephele* (B), torn scales underlying thickened hair pencil scales (H); (V) *Olyras c. crathis* (B), socket and base scale; (W) *Paititia neglecta* (B), socket; (X) *Melinaea l. ludovica* (B), socket; (Y) *Athyrtis mechanitis salvini* (B), socket and base scale; (Z) *Eutresis hypereia theope* (B), socket and base scale.

Fig. 17. Male wing androconia and markings. VFW anal margin: (A) *Forbestra equicola equicoloides*, note androconial scales along vein 2A; (B) *Epityches eupompe*, note androconial scales along vein 2A; (C) *Paititia neglecta*; (D) *Aeria eurimedia agna*; (E) *Melinaea l. ludovica*; (F) *Tithorea tarricina duenna*; (G) *Callithomia lenea zelie*. DHW costa and discal cell: (H) *Tellervo z. zoilus*; (I) *Tithorea harmonia hippothous*; (J) *Aeria eurimedia agna*; (K) *Melinaea m. menophilus*; (L) *Epityches eupompe*; (M) *Pseudoscada florula aureola*; (N) *Hyalenna p. perasippa*; (O) *Methona themisto*; (P) *Episcada hemixanthe*; (Q) *Tithorea harmonia manabiana*; (R) *Pseudoscada t. timna*; (S) *Melinaea l. ludovica*; (T) *Elzunia pavonii*; (U) *Velamysta p. phengites*; (V) *Megoleria* s. *susiana*; (W) *Olyras c. crathis*; (X) *Pteronymia h. hara*. DHW androconial scales in cell Rs-Sc + R1: (Y) *Godyris mantura honrathi*, basal scales; (Z) as X, distal scales. VHW discal cell and costa: (AA) *Tithorea harmonia manabiana*; (AB) *Eutresis hypereia banosana*; (AC) *Paititia neglecta*; (AD) *Veladyris p. pardalis*.

(see Fig. 16F) permitting the hairs to be raised in a fan-shape when pheromones are disseminated.

157. *Male DHW hair pencil present*: (0) in males only; (1) in both sexes (Fig. 17O). State 1 occurs in several *Methona* species only.

158. *Male DHW hair pencil scales*: (0) uniformly dense (Fig. 17I); (1) dense at base, much sparser towards cell end (Fig. 17K).

159. *Male DHW hair pencil color*: (0) uniform (Fig. 17K); (1) darker at base, paler distally (Fig. 17L);

(2) paler at base, darker distally (Fig. 17I). *Elzunia* is coded as equivocal as, in comparison with the morphologically similar and closely related *Tithorea*, it has apparently lost the distal hair pencil.

160. *Male DHW hair pencil "footprint"*: (0) roughly equidistant from vein Rs throughout length (Fig. 15L); (1) displaced posteriorly from vein Rs towards base of wing (Fig. 15K). The sockets in which the androconial hair scales are inserted are enlarged and hemispherical, clearly visible on the wing membrane on cleared specimens and forming a distinct "footprint" where the hairs are attached. In most Ithomiinae the hairs are attached in a band close to the edge of the discal cell (vein Rs) and parallel with this vein throughout the length of the hair pencil; in the Napeogenini the hair pencil is displaced away from vein Rs at the base of the hair pencil.

161. *Male DHW hair pencil in a*: (0) single patch (Fig. 17N); (1) double patch (Fig. 17K); (2) triple patch (Fig. 17J). The hair pencil may be continuous or broken into distinct patches. Most genera contain species with both single and double hair pencils (only *Aeria eurimedia* has a third hair pencil). State 0 is either a result of the hair pencil being unbroken (e.g., *Oleria*) or the loss of the distal hair pencil (e.g., *Elzunia*), but no attempt was made to distinguish between these origins due to substantial variation in hair pencil extent.

162. *When male DHW hair pencil is double (Char. 161:1)*: (0) basal patch is larger than distal (Figs 15O and 17L); (1) distal patch is larger than basal (Figs 15Q and 17K); (2) both patches are equal in size (Figs 15P and 17M).

163. *Male DHW hair pencil "footprint"*: (0) even in width or tapering distally (Fig. 15K); (1) tapering distally then ending in an expanded circle (Fig. 15M); (2) constricted in middle (Fig. 15L). If the hair pencil is broken into distinct patches (Char. 161:2,3), then this character is coded as equivocal.

164. *Male DHW hair pencil "footprint"*: (0) less than half width of discal cell (Fig. 15J); (1) not reaching end of discal cell, but greater than half width of discal cell (Fig. 15K); (2) reaching end of discal cell (Fig. 15L); (3) greater than discal cell width, extending into cell M1-Rs (Fig. 15N).

165. *Male DHW hair pencil*: (0) of a single scale type lying above scales and depression in cell Sc + R1-Rs (Fig. 16E); (1) differentiated into paler dorsal hairs and darker, thicker ventral hairs, latter lying within depression in cell Sc + R1-Rs (Fig. 16H). State 1 is a synapomorphy for *Heterosais*. The thickened hairs have a distinct ultrastructure, being strongly perforated with the vanes sinuate (Fig. 16H), rather than unperforated with parallel vanes (see Fig. 16G), and in all examined specimens were loosely cemented together into a solid mass. In several examined specimens of *Heterosais nephele* these thickened hairs appeared to have abraded the underlying androconial scales, curling them about the lateral axis and bending them backwards at the pedicel, and tearing a number of scales in half (Fig. 16U).

Male DHW androconial scales beneath hair pencil

166. *Male DHW androconial scales beneath hair pencil*: (0) undifferentiated from those anterior of vein Sc + R1; (1) differentiated from those anterior of vein Sc + R1 (Fig. 16I–K). All male ithomiines have modified, acicular or ovate lamellar androconial scales in the distal half of the discal cell, surrounding the sockets of the hair pencil, and extending anteriorly to the costa. The scales that lie beneath the hair pencil scales (when not erected) are further modified from surrounding wing scales. In *Sais* and *Scada* veins Sc + R1 and Rs are very close together with few scales between these veins, but nevertheless those that are present are slightly broader than those outside this area. In the following characters "androconial scales' refers to the modified androconial scales that underly the hair pencil only.

167. *Male DHW androconial scales (Char. 166:1) beneath hair pencil*: (0) in cell Rs-Sc + R1 only (Fig. 17P); (1) in cell Rs-Sc + R1 and extending midway into cell M1-Rs (Fig. 17Q); (2) in cell Rs-Sc + R1 and M1-Rs, reaching vein M1 (Fig. 17R); (3) in cells Rs-Sc + R1, M1-Rs, and reaching to vein M1, extending into anterior portion discal cell among bases of androconial hairs (Fig. 17S). In *Paititia*, *Olyras*, *Athyrtis* and *Melinaea* there is a basal patch of androconial scales in cell Sc + R1-Rs, while the remainder of the cell contains a dense, tiny androconial scale. This type of scale further extends among the bases of the hair pencil scales in the discal cell, and into cell M1-Rs, a distinctive distribution. This type of scale apparently represents the usual modified scales that occur between veins Sc + R1 and Rs, as in *Melinaea* it is confined in cell Sc + R1-Rs to a distal patch directly beneath the hair pencil. In *Godyris* and relatives the androconial scales in cell M1-Rs represent an expansion of the scales usually in cell Sc + R1-Rs, and are distinct from scales in adjacent areas. *Brevioleria* and *Heterosais edessa* are coded equivocal as absence of androconial scales distally is believed correlated with absence of the distal portion of the hair pencil, coded in Char. 168.

168. *Male DHW androconial scales (Char. 166:1) beneath hair pencil*: (0) present throughout (Fig. 17Q); (1) absent in basal area (Fig. 17U); (2) absent in distal area (Fig. 17T). The distribution of androconial scales varies between taxa, but in *Elzunia* and *Brevioleria* the absence of a distal hair pencil (inferred from comparison with close relatives in which it is present) is correlated with the absence of a distal patch of androconial scales, which are replaced by typical wing scales (state 2). In *Velamysta* the basal area of Sc + R1-Rs contains apparently typical wing scales, similar to those anterior

and posterior of this cell, and this species is thus coded 1. In *Ithomia* a cross-vein closes cell Sc + R1-Rs immediately distal of the basal androconial scale patch and species were coded equivocal, as the wing area usually occupied by the distal part of the androconial scale patch is absent.

169. *Male DHW androconial scales (Char. 166:1) beneath hair pencil*: (0) differentiated into patches of two distinct types of scale, one basal and one distal (Fig. 17Q); (1) undifferentiated, basal scale-type apparently absent (distal dominant) (Fig. 17P). The androconial scales beneath the DHW hair pencil may be uniform throughout, or differentiated, with those nearer the wing base different in color and/or morphology from those more distal (compare Figs 16O and Q, 18A and B, 18C and D). In species with a single type of scale this may result from the entire loss of the other patch (i.e., no androconial scales are present in part of the wing: Char. 168) or from expansion of one or other patch at the expense of the other. Comparison of scale morphology in closely related species, where one bears differentiated scales and the other not, shows that in almost all cases the scales of the species with a single patch correspond to those of the distal patch in the other species. For *Methona* and Mechanitini there are no obvious close relatives, but the scales in most species more resemble the distal patch scales in other primitive ithomiines. Scales in species with only one type of scale were therefore coded as distal scales and basal scale characters were left equivocal. This character was coded equivocal for species lacking part of the androconial patch (Char. 168) and for *Ithomia*, for the reasons discussed under Char. 168. Note that scales in *Heterosais edessa* are coded as distal patch scales even though the distal part of the androconial scale patch is absent, because scales are undifferentiated in the closely related *Heterosais nephele* and coded there as distal scales.

170. *Male DHW androconial scale patch (Char. 166:1) beneath hair pencil*: (0) continuous (Fig. 17P); (1) broken (Fig. 17Q). Species coded state 1 may have the two patches differing in scale morphology (e.g., *Hypoleria lavinia*) or the same (e.g., *Episcada hymenaea*).

171. *Male DHW basal androconial scale patch beneath hair pencil with distal border*: (0) approximately perpendicular to veins Sc + R1 and Rs or inclined with anterior edge more distal (Fig. 17S); (1) border much more distal posteriorly, with scale patch extending along posterior half of cell Sc + R1-Rs to just opposite discocellular veins (Fig. 17W). State 1 is a synapomorphy for *Olyras* + *Paititia*. *Pteronymia hara* is coded equivocal as there is no clear boundary between basal and distal scale types.

172. *Male DHW basal androconial patch scales beneath hair pencil*: (0) white (Fig. 17X); (1) whitish cream to gray buff (Fig. 17V); (2) brown (Fig. 17T); (3) mixed light and darker gray-brown (Fig. 17Y).

173. *Male DHW basal androconial patch scales beneath hair pencil, density*: (0) sparse, with little overlap between adjacent scales, sockets of at least some scales visible (Fig. 16N); (1) dense, with much overlap (< 70%) between adjacent scales, sockets not visible (Fig. 16L); (2) very dense (> 70% overlap), sockets not visible, stacked almost vertically (Fig. 16O). Although occasionally basal and distal androconial patches share the same character state (for this and other following characters), in most cases this is not so, and no cases were found where a possible synapomorphy in the distal patch might be duplicated by coding the same feature in the basal patch.

174. *Male DHW basal androconial patch scales beneath hair pencil*: (0) flat or lightly curving throughout scale (Fig. 16L); (1) curled longitudinally at edges and wrinkled (Fig. 16O).

175. *Male DHW basal androconial patch scales beneath hair pencil, thickness*: (0) similar in thickness to normal wing scales, width > 3 × height of vanes (Fig. 16Q); (1) very thin, similar width to height of vanes, translucent (Fig. 16R); (2) tubular, hollow in cross-section (Fig. 16S).

176. *Male DHW basal androconial patch scales beneath hair pencil, base of blade*: (0) with shallow angle at pedicel (> 90°) (Fig. 16M); (1) "auriculate", with sharp angle at pedicel (< 90°) (Fig. 16L). Species with rectangular scales (Char. 178:1) are coded state 0 and have an angle of approximately 90°.

177. *Male DHW basal androconial patch scales beneath hair pencil, tip*: (0) tapering or rounded (Fig. 16L); (1) flat to indented (Fig. 16O); (2) bifurcate (Fig. 16M).

178. *Male DHW basal androconial patch scales beneath hair pencil, overall shape*: (0) broader in basal half and tapering distally (Fig. 16L); (1) rectangular (Fig. 16O).

179. *Male DHW distal androconial patch scales beneath hair pencil, color*: (0) white (Fig. 17U); (1) whitish cream to gray buff (Fig. 17V); (2) brown (Fig. 17Q); (3) whitish gray with brown tips (Fig. 17Z); (4) black.

180. *Male DHW distal androconial patch scales beneath hair pencil, density*: (0) sparse, with little overlap between adjacent scales, sockets of at least some scales visible (Fig. 18B); (1) dense, with much overlap (< 70%) between adjacent scales, sockets not visible (Fig. 18F); (2) very dense (> 70% overlap), sockets not visible, stacked almost vertically (Fig. 18Q).

181. *Male DHW distal androconial patch scales beneath hair pencil*: (0) straight about longitudinal axis (Fig. 18F); (1) curled at edges longitudinally (Fig. 18T). State 1 is a synapomorphy for *Forbestra* + *Mechanitis*. Coded equivocal for species with non-lamellar scales.

182. *Male DHW distal androconial patch scales beneath hair pencil in lateral view*: (0) straight; (1)

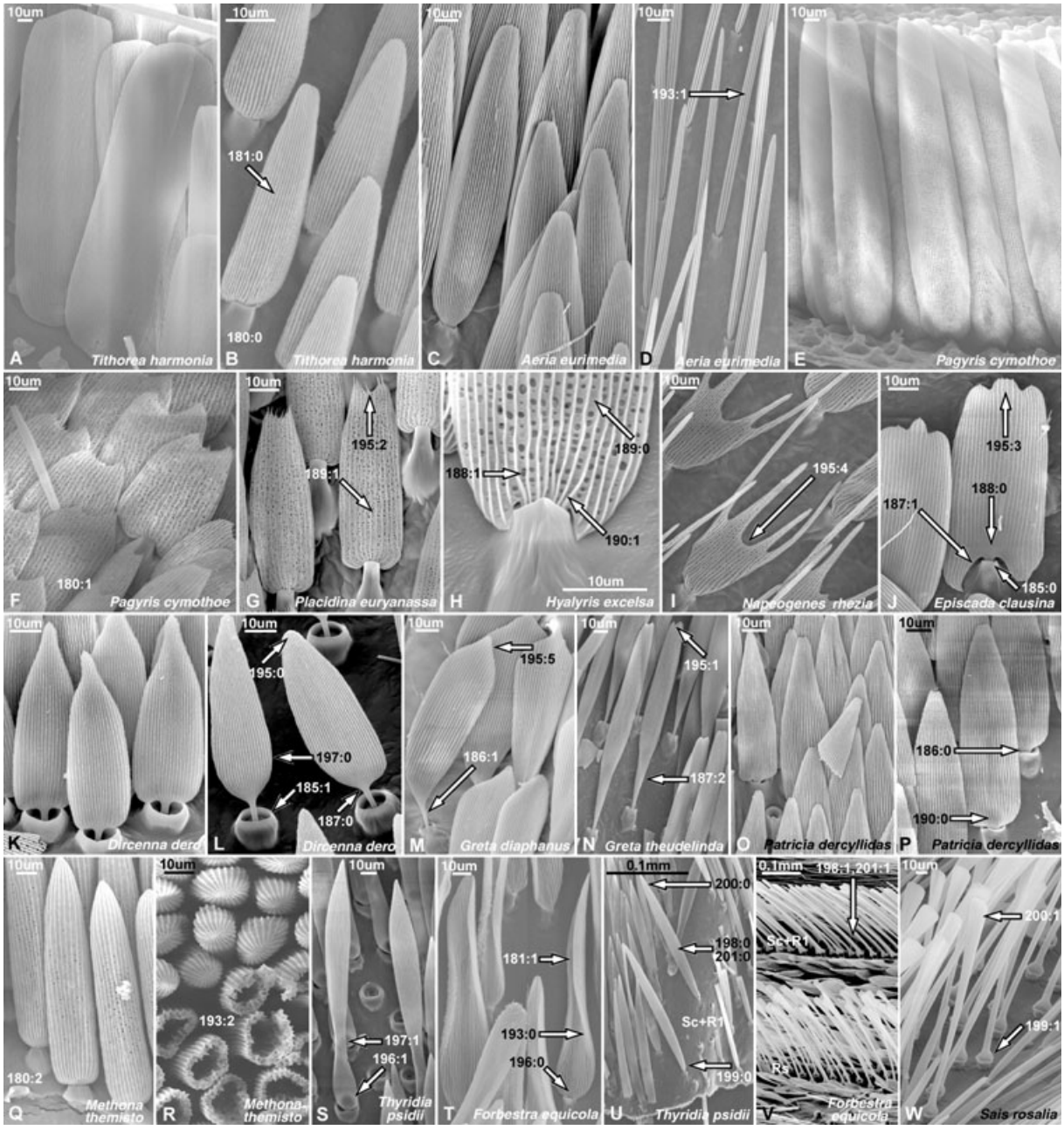

Fig. 18. Male DHW androconial scales in cell Rs-Sc + R1, basal (b), distal (d) or distal where undifferentiated (du), homologous to distal: (A) *Tithorea harmonia megara* (b); (B) *Tithorea harmonia megara* (d); (C) *Aeria e. eurimedia* (b); (D) *Aeria e. eurimedia* (d); (E) *Pagyris c. cymothoe* (b); (F) *Pagyris c. cymothoe* (d); (G) *Placidina euryanassa* (du); (H) *Hyalyris e. excelsa* (du), socket and base of scale; (I) *Napeogenes r. rhezia* (du); (J) *Episcada clausina striposis* (du); (K) *Dircenna dero* (b); (L) *Dircenna dero celtina* (d); (M) *Greta diaphanus* (du); (N) *Greta t. theudelinda* (d); (O) *Patricia dercyllidas hazelea* (b); (P) *Patricia dercyllidas hazelea* (d); (Q) *Methona themisto* (du); (R) *Methona themisto* (du), cross-section and scale tips; (S) *Thyridia p. psidii* (du); (T) *Forbestra e. equicola* (du); (U) *Thyridia p. psidii*, scales lining vein Sc + R1; (V) *Forbestra e. equicola*, spatulate androconial scales lining veins Sc + R1 and Rs; (W) *Sais r. rosalia*, spatulate androconial scales lining vein Sc + R1.

curving (Fig. 16T). State 1 is a synapomorphy for *Velamysta*.

183. *If male DHW androconial scales beneath hair pencil are differentiated (Char. 169:1), patch with longer scales is*: (0) neither (equal in size) (Fig. 18C,D); (1) basal (< twice length of distal) (Fig. 16O,P); (2) basal (> twice length of distal) (Fig. 18A,B); (3) basal (> three times length of distal) (Fig. 18E,F); (4) distal (Figs 16M and 18N).

184. *If male DHW androconial scales beneath hair pencil are differentiated (Char. 169:1), patch with proportionally broader scales is*: (0) neither (Fig. 18O,P);

(1) basal (< twice width of distal) (Figs 16M and 18N); (2) basal (> twice width of distal) (Fig. 18C,D); (3) distal (Fig. 18A,B).

185. *Male DHW distal androconial patch scales beneath hair pencil, socket*: (0) upright to reclining, bottle-shape to short tube, with collar opening not greater than 3 × pedicel width (Fig. 18J); (1) a short, rounded cup, collar opening approximately 5 × pedicel width (Fig. 18L). There is substantial variation in the morphology of androconial scale sockets, but only a single character state discrete from others could be defined. State 1 is a synapomorphy for *Dircenna* + *Hyalenna*, being lost in *H. perasippa*.

186. *Male DHW distal androconial patch scales beneath hair pencil, pedicel*: (0) short, not extending beyond collar (Fig. 18P); (1) elongate (Fig. 18M). Some *Godyris* species have the pedicel and blade smoothly merging, but the pedicel is still noticeably more elongate than in all other species coded as state 0.

187. *Male DHW distal androconial patch scales beneath hair pencil base of blade*: (0) with shallow angle at pedicel (> 90°) (Fig. 18L); (1) auriculate, with sharp angle at pedicel (< 90°) (Fig. 18J); (2) flat, merging smoothly with pedicel (Fig. 18N). A few species show variation between scales, with some scales angled and others auriculate, and were coded as dimorphic.

188. *Male DHW distal androconial patch scales beneath hair pencil, basal area of scale blade*: (0) smooth or with windows reduced (Fig. 18J); (1) with windows (Fig. 18H). In most species the androconial scale blade is unperforated or perforated with windows mainly in the distal portion. In the Ithomiini + Napeogenini the blade has windows right to the very base (state 1).

189. *Male DHW distal androconial patch scales beneath hair pencil, ultrastructure*: (0) with flutes parallel and not prominent (Fig. 18H); (1) with flutes prominent and not parallel (Fig. 18G). Flutes are raised ridges running across the channels between vanes, and are typically less prominent than and oriented at right angles or nearly so to vanes. State 1 occurs only in *Pagyris* + *Placidina*, although this character could not be coded for Ithomiini because the distal scales are absent.

190. *Male DHW distal androconial patch scales beneath hair pencil, vanes at base of scale*: (0) parallel or smoothly converging (Fig. 18P); (1) wrinkled (Fig. 18H). In Ithomiini + Napeogenini the vanes are distinctly pinched together and wrinkled at the base of the scale, as if the scale has been constricted at this point.

191. *Male DHW distal androconial patch scales beneath hair pencil, sockets*: (0) round (Fig. 16V,W); (1) "U"-shaped (Fig. 16X–Z). State 1 occurs only in *Melinaea*, *Athyrtis* and *Eutresis*.

192. *Male DHW distal androconial patch scales beneath hair pencil with vanes on lower surface*: (0) similar to upper surface (Fig. 16U); (1) much reduced or absent (Fig. 16T). Unlike most butterfly scales (Downey and Allyn, 1975), but like those of some Danainae (Ackery and Vane-Wright, 1984), almost all ithomiines have scales with vanes on both surfaces of the blade, except in *Velamysta* in which they are distinctly reduced on the lower surface, probably because these scales seem to be rigidly inserted into their sockets.

193. *Male DHW distal androconial patch scales beneath hair pencil*: (0) lamellar (Fig. 18T); (1) acicular (Fig. 18D); (2) tubular (Fig. 18R).

194. *Male DHW distal androconial patch scales beneath hair pencil with basal area*: (0) with vanes (Fig. 16V); (1) lacking vanes (Fig. 16Z). This character was coded equivocal for most Godyridini, which lack vanes in the basal area because the pedicel is elongated, a character already coded elsewhere. The vanes are reduced in the middle of the scale towards the base in some Dircennini, but still present at the edges of the scale. In *Eutresis*, *Athyrtis* and *Melinaea* the vanes are absent across the entire scale in the basal part, and these taxa were coded state 1.

195. *Male DHW distal androconial patch scales beneath hair pencil, tip*: (0) pointed to rounded to blunt (Fig. 18L); (1) indented (Fig. 18N); (2) bifurcate (Fig. 18G); (3) trifurcate (Fig. 18J); (4) deeply dentate (Fig. 18I); (5) pointed and attenuated at tip (Fig. 18M). State 4 is a synapomorphy for *Napeogenes*.

196. *Male DHW distal androconial patch scales beneath hair pencil, base*: (0) tapering or similar width to rest of scale (Fig. 18T); (1) swollen (Fig. 18S).

197. *Male DHW distal androconial patch scales beneath hair pencil*: (0) broadest at some point between base and tip (Fig. 18L); (1) constricted near base (Fig. 18S). Scales in most species broaden from the base then taper distally, except in *Thyridia*, in which they are medially constricted.

198. *Male DHW with differentiated scent scales lining veins Sc + R1 and Rs on DHW*: (0) absent (Figs 16I,J and 18 U); (1) present (Fig. 18V). In most ithomiines the androconial scales lining vein Rs are similar in form to these scales anterior of this vein, while vein Sc + R1 has very few or no scales. In *Sais*, *Scada*, *Forbestra* and *Mechanitis* the scales on these veins are dense, strongly modified and distinct from surrounding areas. In *Thyridia* the base of the androconial scales between veins Sc + R1 and Rs is swollen and the overall shape of the scale is spatulate, both characters of the scales lining veins Sc + R1 and Rs in remaining Mechanitini. Thus the latter may be homologous to the typical androconial scales between Sc + R1 and Rs, but given the different position on the wing, and presence of scales otherwise typical of primitive species between Sc + R1 and Rs, we code these two types of scale separately. State 1 is a synapomorphy for *Sais* + *Scada* + *Forbestra* + *Mechanitis*.

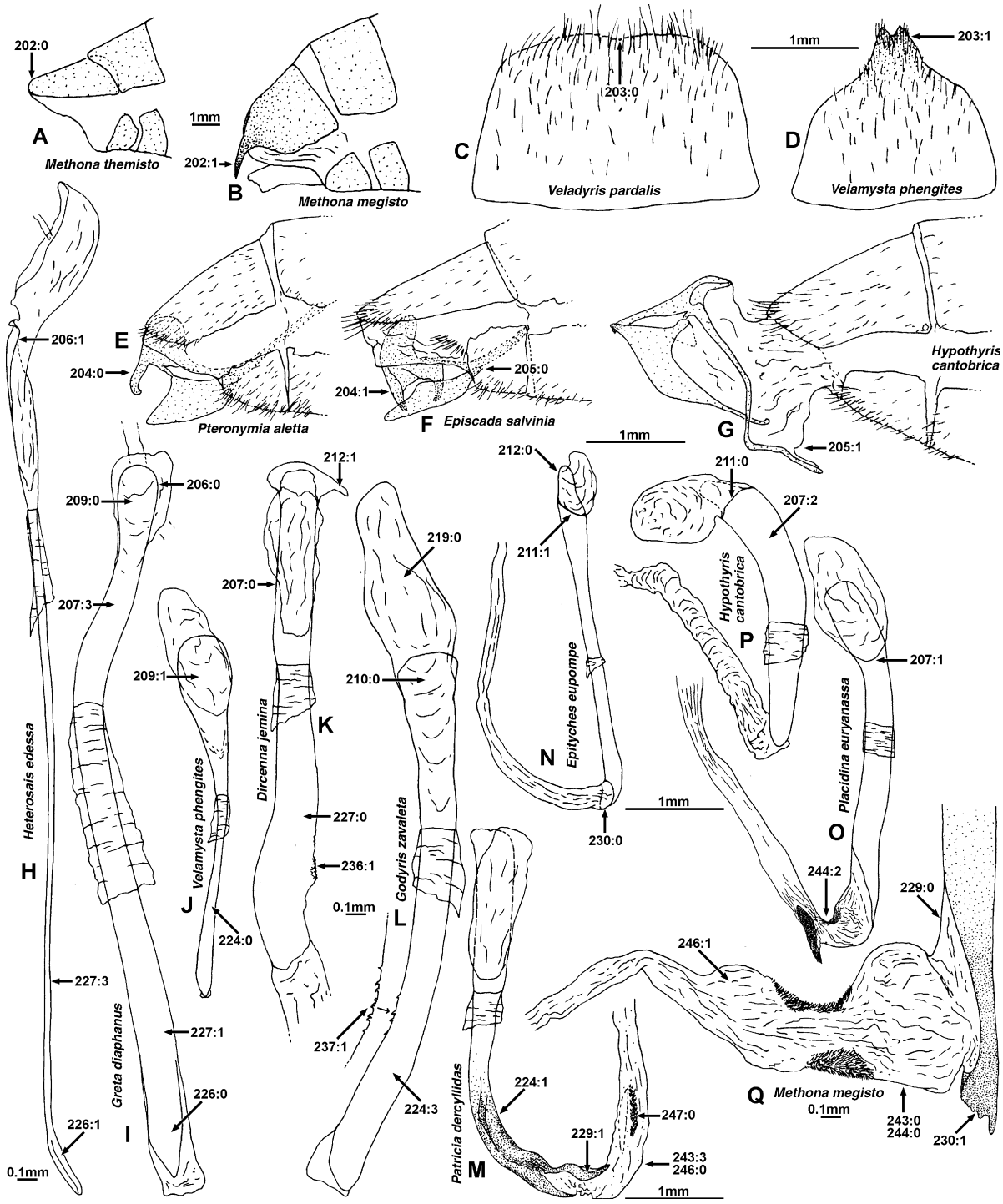

Fig. 19. Male genitalia and abdomen. Posterior abdomen tip, lateral view: (A) *Methona t. themisto*; (B) *Methona megisto*. Terminal (posterior) tergite, dorsal view: (C) *Veladyris p. pardalis*; (D) *Velamysta p. phengites*. Posterior abdomen tip, lateral view, genitalic capsule everted: (E) *Pteronymia a. aletta*; (F) *Episcada s. salvinia*; (G) *Hypothyris* (*Rhodussa*) *c. cantobrica*. Aedeagus, dorsal view: (H) *Heterosais edessa*; (I) *Greta diaphanus*; (J) *Velamysta p. phengites*; (K) *Dircenna j. jemina*; (L) *Godyris zavaleta rosata*. Aedeagus, dorsal view, vesica everted: (M) *Patricia d. dercyllidas*; (N) *Epityches eupompe*; (O) *Placidina euryanassa*; (P) *Hypothyris* (*Rhodussa*) *c. cantobrica*; (Q) *Methona t. themisto*, posterior tip only.

199. *Male DHW androconial scales on veins Sc + R1 and Rs with*: (0) base tapering (Fig. 18U); (1) base sharply expanded (Fig. 18W). State 1 is a synapomorphy for *Sais + Scada + Forbestra + Mechanitis*.

200. *Male DHW androconial scales on veins Sc + R1 and Rs*: (0) tapering distally (Fig. 18U); (1) spatulate (Fig. 18W). State 1 is a synapomorphy for *Sais + Scada + Forbestra + Mechanitis*.

201. *Male DHW androconial scales on veins Sc + R1 and Rs*: (0) lying flat against vein (Fig. 18U); (1) erect, pointing inwards to form a channel (Fig. 18V). State 1 is a synapomorphy for *Sais + Scada + Forbestra + Mechanitis*.

Male genitalia and abdomen

Abdomen and genitalic capsule

202. *Male terminal tergite in lateral view*: (0) rounded or slightly lobed (Fig. 19A); (1) with pointed lateral projections (Fig. 19B). State 1 occurs only in *Eutresis hypereia* and *Methona megisto*.

203. *Male terminal tergite in dorsal view*: (0) rounded or slightly indented in middle (Fig. 19C); (1) produced into a sclerotized "beak" with two prongs (Fig. 19D). State 1 is a synapomorphy for *Velamysta*.

204. *Male genitalic capsule when extruded from abdomen*: (0) approximately horizontal (Fig. 19E); (1) vertical, with dorsal edge of uncus vertical (Fig. 19F). State 1 occurs in *Dircenna*, *Hyalenna*, *Ceratinia*, *Episcada* and related genera.

205. *Base of vinculum when genitalic capsule everted from abdomen*: (0) remains inside/at edge last sternite (Fig. 19F); (1) completely everted (Fig. 19G). State 1 is an autapomorphy for *Tellervo* and *Hypothyris cantobrica*.

Aedeagus

206. *Anterior section of aedeagus (ductus ejaculatorius area) in dorsal view*: (0) straight (Fig. 19I); (1) rotated to right (Fig. 19H). State 1 is a synapomorphy for *Heterosais*.

207. *Anterior section of aedeagus in dorsal view, ignoring zone*: (0) straight (Fig. 19K); (1) bent sharply to left at ductus ejaculatorius (Fig. 19O); (2) curving evenly to left (Fig. 19P); (3) kinked slightly right then left (Fig. 19I). Initial attempts to code overall aedeagus shape produced so many character states that resultant coding contained little phylogenetic information. However, much of the variation between species occurs through the aedeagus being bent at the zone. This variation was therefore disregarded, thus greatly reducing the number of coded states.

208. *Aedeagus ventral edge below ductus ejaculatorius in lateral view*: (0) straight (Fig. 20L); (1) angled at middle (Fig. 20G).

209. *Aedeagus width in anterior section in dorsal view*: (0) approximately even throughout or broadening anteriorly to up to twice width (Fig. 19I); (1) broadening anteriorly to four times width (Fig. 19J). State 1 is an synapomorphy for *Velamysta*.

210. *Aedeagus anterior section in dorsal view*: (0) of even width or gradually broadening throughout anteriorly (Fig. 19L); (1) abruptly broadening at anterior tip like a mallet (Fig. 20E).

211. *Dorsal junction of aedeagus with posterior edge of ductus ejaculatorius in dorsal view*: (0) symmetrical (Fig. 19P); (1) asymmetrical (Fig. 19N). State 1 is an autapomorphy for *Epityches*.

212. *Aedeagus with lateral projections at anterior tip*: (0) absent (Fig. 19N); (1) present (Fig. 19K).

213. *Aedeagus base with paired, broad rounded lateral lobes*: (0) absent (Fig. 20C); (1) present (Fig. 20A). State 1 is an autapomorphy for *Hyposcada virginiana*.

214. *Anterior dorsal edge of aedeagus forming a support for ductus ejaculatorius*: (0) absent (Fig. 21A); (1) present (Fig. 21G). State 1 is an autapomorphy for *Pteronymia hara*.

215. *Aedeagus base with anterior edge of ductus ejaculatorius located on a forward fold*: (0) absent (Fig. 20I); (1) present (Fig. 20J). State 1 is an autapomorphy for *Hyposcada virginiana*.

216. *Anterior end of aedeagus*: (0) opening dorsally (Fig. 21G); (1) opening to right-hand side (Fig. 21D); (2) opening ventrally (Fig. 21B). In most species the anterior section of the aedeagus opens dorsally into the ductus ejaculatorius. In *Hypoleria adasa*, *Mcclungia*, *Brevioleria* and *Godyris mantura* the aedeagus is rotated to the right 90° and opens into the ductus ejaculatorius to the right, and in *Callithomia* it is rotated 180° and thus opens ventrally.

217. *Anterior end of aedeagus opening into ductus ejaculatorius*: (0) vertically, with anterior tip of aedeagus forming a sclerotized rounded lobe equal in height to remainder of aedeagus (Fig. 20G); (1) subvertically, similar to state 0 but with sclerotized lobe at anterior tip absent (Fig. 20O); (2) subhorizontally, with no sclerotized anterior lobe and broad, semisclerotized edges basal of ductus ejaculatorius (Fig. 20K); (3) horizontally, with no sclerotized anterior lobe and ventral edge of aedeagus and ductus ejaculatorius making a straight line (Fig. 20M). In more primitive species the ductus ejaculatorius arises vertically from the anterior section of the aedeagus but posterior of the tip (state 0). In a number of more derived species it is shifted anteriorly so that the sclerotized anterior tip of the aedeagus is absent and the ductus ejaculatorius opens subhorizontally.

218. *Ductus ejaculatorius*: (0) unsclerotized, soft tissue (Fig. 20J); (1) semisclerotized (Fig. 20H). State 1 is a synapomorphy for *Haenschia* also occurring in *Hypoleria adasa*.

219. *Ductus ejaculatorius*: (0) lying in a flat plane (Fig. 19K); (1) bent and twisted to right (Fig. 20G); (2)

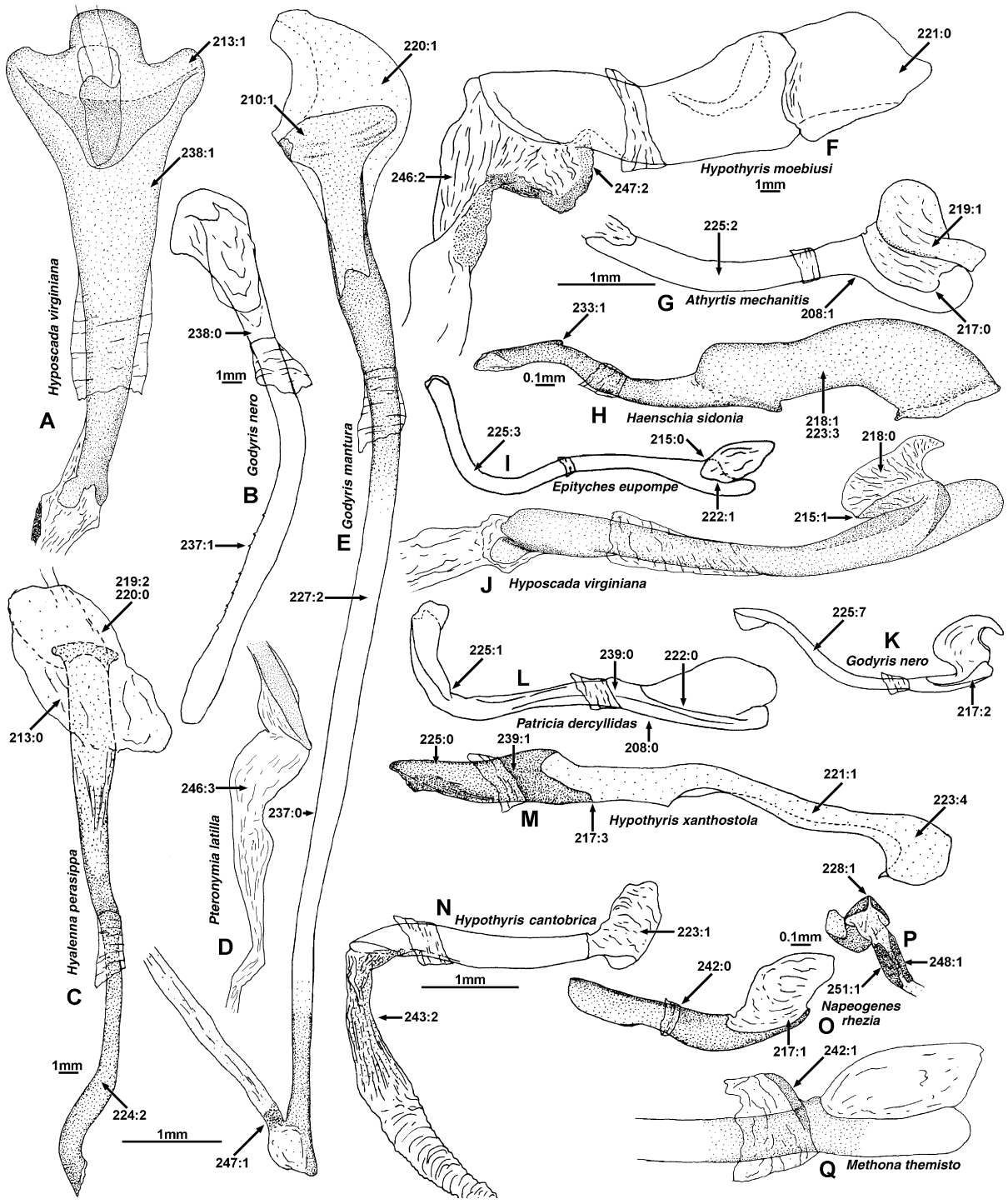

Fig. 20. Male genitalia. Aedeagus, dorsal view: (A) *Hyposcada v. virginiana*, vesica everted; (B) *Godyris nero*; (C) *Hyalenna p. perasippa*; (D) *Pteronymia l. latilla*, tip only, vesica everted; (E) *Godyris mantura honrathi*, vesica everted. Aedeagus, lateral view: (F) *Hypothyris m. moebiusi*, vesica everted; (G) *Athyrtis mechanitis salvini*; (H) *Haenschia sidonia*; (I) *Epityches eupompe*; (J) *Hyposcada v. virginiana*, vesica everted; (K) *Godyris nero*; (L) *Patricia d. dercyllidas*; (M) *Hypothyris* (*Garsauritis*) *x. xanthostola*; (N) *Hypothyris* (*Rhodussa*) *c. cantobrica*, vesica everted; (O) *Napeogenes rhezia cyrianassa*. (P) *Napeogenes rhezia cyrianassa*, posterior view, vesica everted. (Q) *Methona t. themisto*, lateral view of basal section.

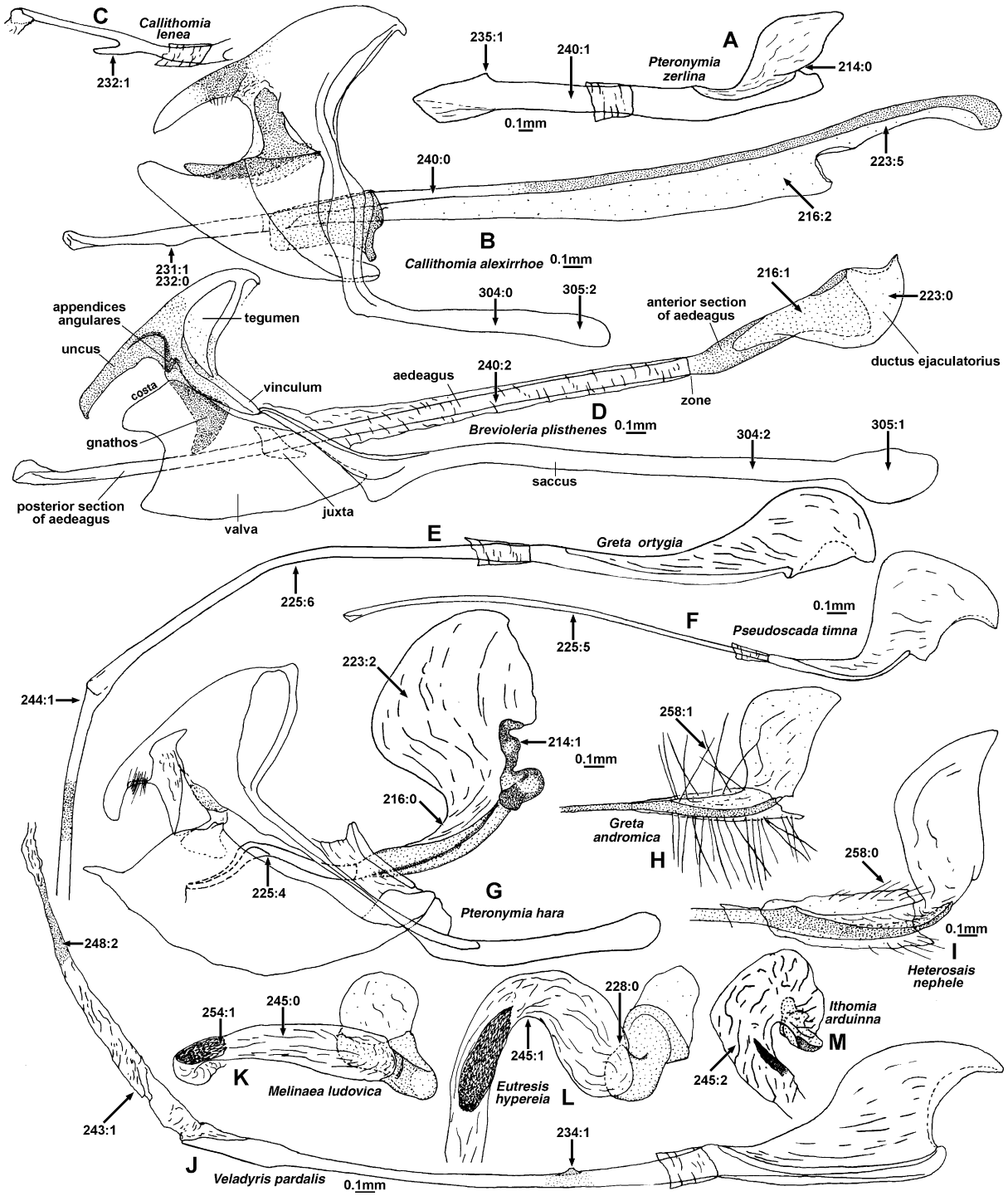

Fig. 21. Male genitalia. (A) *Pteronymia z. zerlina*, aedeagus, lateral view. (B) *Callithomia alexirrhoe zeuxippe*; (C) *Callithomia lenea zelie*, aedeagus posterior tip, lateral view; (D) *Brevioleria plisthenes*; (E) *Greta o. ortygia*, aedeagus, lateral view, vesica everted; (F) *Pseudoscada timna pusio*, aedeagus, lateral view; (G) *Pteronymia h. hara*; (H) *Greta andromica andania*, aedeagus, lateral view of basal section; (I) *Heterosais nephele*, aedeagus, lateral view of basal section; (J) *Veladyris p. pardalis*, aedeagus, lateral view, vesica everted. Aedeagus and everted vesica, posterior view: (K) *Melinaea l. ludovica*; (L) *Eutresis h. hypereia*; (M) *Ithomia a. arduinna*.

twisted to left in dorsal view (Fig. 20C). This character refers to the shape of the ductus ejaculatorius, whereas Char. 220 refers to its orientation with respect to the aedeagus base.

220. *Ductus ejaculatorius emerging*: (0) perpendicularly from aedeagus (Fig. 20C); (1) rotated to the right to lie flat against aedeagus (Fig. 20E). State 1 is a synapomorphy for *Hypoleria adasa*, *Mcclungia*, *Brevioleria* and *Godyris mantura*. The ductus ejaculatorius is similar in shape to related species but is rotated 90° so to lie flat against the aedeagus, opening to the left.

221. *Extension of ductus ejaculatorius anteriorly beyond aedeagus*: (0) shorter than anterior section of aedeagus (Fig. 20F); (1) longer than anterior extension of aedaegus (Fig. 20M). State 1 is a synapomorphy for *Haenschia*, also occurring in some *Hypothyris*.

222. *Ductus ejaculatorius opening into aedeagus*: (0) just slightly less to about half length of anterior section (Fig. 20L); (1) less than half length of anterior section (Fig. 20I).

223. *Ductus ejaculatorius shape*: (0) a simple ''hood'', greater or equal in width to height (Fig. 21D); (1) a vertically expanded ''hood'', height greater than width (Fig. 20N); (2) a vertically expanded ''hood'' wider dorsally than at base (Fig. 21G); (3) a tube, greatly elongated anteriorly (Fig. 20H); (4) an anteriorly elongated sickle shape (Fig. 20M); (5) elongate with small opening posterior of anterior end of aedeagus (Fig. 21B). In all states except 4 and 5 the ductus ejaculatorius opens at its anterior edge; in 4 it opens ventrally and in 5 dorsally but in the middle of the ductus ejaculatorius.

224. *Posterior section of aedeagus in dorsal view, ignoring zone*: (0) straight (Fig. 19J); (1) bent to right near tip (Fig. 19M); (2) bent to left near tip (Fig. 20C); (3) evenly curving to left (Fig. 19L). See Discussion under Char. 207.

225. *Posterior section of aedeagus in lateral view, ignoring zone*: (0) straight (Fig. 20M); (1) curving upwards near tip (Fig. 20L); (2) curving slightly and evenly upwards (Fig. 20G); (3) curving sharply upwards (Fig. 20I); (4) bent downwards near tip (Fig. 21G); (5) curving evenly downwards (Fig. 21F); (6) bent downwards at middle (Fig. 21E); (7) kinked up near middle then down at tip (Fig. 20K).

226. *Aedeagus posterior section*: (0) of even width (Fig. 19I); (1) broadening at posterior tip (Fig. 19J).

227. *Ratio of length of posterior section of aedeagus divided by minimum width of posterior section,* r: (0) $r < 13$ (Fig. 19K); (1) $13 < r < 34$ (Fig. 19I); (2) $34 < r < 67$ (Fig. 20E); (3) $67 < r$ (Fig. 19H). If the aedeagus is evenly tapering throughout, the average width was measured. Higher states indicate a relatively longer and thinner aedeagus.

228. *Aedeagus posterior tip in posterior view*: (0) rounded in cross-section (Fig. 21L); (1) with a dorsal ''peak'' (Fig. 20P). State 1 is a synapomorphy for *Napeogenes*.

229. *Aedeagus posterior tip with a sclerotized ''ribbon'' on right side extending on to base of vesica*: (0) absent (Fig. 19Q); (1) present (Fig. 19M). State 1 is a synapomorphy for *Athesis* + *Patricia*.

230. *Aedeagus posterior tip with a flat, serrate heavily sclerotized flange*: (0) absent (Fig. 19N); (1) present (Fig. 19Q). State 1 is a synapomorphy for *Methona*.

231. *Aedeagus with dorsolateral projection on left side near middle posterior section*: (0) absent; (1) present (Fig. 21B). State 1 is a synapomorphy for *Callithomia*.

232. If aedeagus has a dorsolateral projection on left side near middle posterior section (Char. 231:1), then projection is: (0) a bump (Fig. 21B); (1) a spine (Fig. 21C).

233. *Aedeagus posterior tip with a rounded, anteriorly curved and posteriorly straight projection*: (0) absent; (1) present (Fig. 20H). State 1 is a synapomorphy for *Haenschia*.

234. *Aedeagus with small dorsal flange about a quarter way along posterior section*: (0) absent; (1) present (Fig. 21J). State 1 is an autapomorphy for *Veladyris pardalis*.

235. *Aedeagus with flat, pointed dorsal projection near posterior tip*: (0) absent; (1) present (Fig. 21A). State 1 occurs here only in *P. zerlina*, but is a synapomorphy for a clade of eight *Pteronymia* species.

236. *Aedeagus with serrate right lateral edge near posterior tip*: (0) absent; (1) present (Fig. 19K). State 1 is a synapomorphy for *Dircenna* (excluding *D. paradoxa*).

237. *Aedeagus posterior tip with line of small teeth along left lateral edge near tip*: (0) absent (Fig. 20E); (1) present (Figs 19L and 20B). State 1 is a synapomorphy for *Godyris* (excluding *G. mantura* and relatives).

238. *Aedeagus in dorsal view*: (0) even in width or broadening in part of anterior or posterior section only (Fig. 20B); (1) broadening evenly throughout (Fig. 20A). State 1 is an autapomorphy for *Hyposcada virginiana*.

239. *Aedeagus in lateral view*: (0) little varying in width (Fig. 20L); (1) tapering continuously from anterior to posterior tip (Fig. 20M).

240. *Ratio of length of posterior section of aedeagus to anterior section,* r: (0) $r < 0.5$ (Fig. 21B); (1) $0.5 < r < 1.58$ (Fig. 21A); (2) $1.58 < r$ (Fig. 21D). State 0 indicates posterior section much shorter than anterior; state 1 indicates posterior and anterior sections more or less equal in length; state 2 indicates posterior section much longer than anterior.

241. *Total length of aedeagus divided by genitalic capsule height, r*: (0) $r < 1.22$ (Fig. 21G); (1) $1.22 < r < 1.8$; (2) $1.8 < r < 3$; (3) $3 < r$ (Fig. 21B). Genitalic capsule height is the distance from the top of the tegumen to the middle of the saccus, measured along the vinculum.

242. *Aedeagus with dorsal projection at base junction of anterior and posterior sections*: (0) absent (Fig. 20O); (1) present (Fig. 20Q). State 1 is a synapomorphy for *Methona*.

Vesica and cornuti

243. *With aedeagus anterior opening directly dorsally (''midnight''), vesica everts in posterior view*: (0) at 9–10.30 pm (to left) (Fig. 19Q); (1) at midnight (dorsally) (Fig. 21J); (2) at 6–7.30 pm (ventrally) (Fig. 20N); (3) at 3 pm (to right) (Fig. 19M). The vesica usually everts at an angle to the aedeagus, and the direction in which it everts varies between genera and species. To control for the rotation of the aedeagus with respect to the genitalic capsule in some species (Char. 216:1,2) the direction in which the vesica everts is measured relative to the anterior opening of the aedeagus into the ductus ejaculatorius. In species in which this opening is horizontal (Char. 217:3), the edge of the sclerotized part of the aedeagus at the junction to the ductus ejaculatorius in lateral view is inclined, indicating the vertical sense in which the ductus ejaculatorius opened in ancestors. Some species coded state 1 for Char. 244, in which the vesica everts in a direct line with the aedeagus, could still be coded for this character based on a slight angle between vesica and aedeagus.

244. *Vesica everting*: (0) at an angle to aedeagus (Fig. 19Q); (1) in a direct line with aedeagus (Fig. 21E); (2) recurved back towards anterior end of aedeagus (Fig. 19O). In many species the vesica is slightly curved back anteriorly throughout its length, but in species coded state 2 this curvature is sharp and occurs near the cornuti.

245. *Vesica in posterior view*: (0) straight (Fig. 21K); (1) curved with concave side down (Fig. 21L); (2) curved into a spiral (Fig. 21M).

246. *Base of vesica*: (0) of even width (Fig. 19M); (1) expanded then contracting (Fig. 19Q); (2) expanded into a parallelogram shape then narrowing (Fig. 20F); (3) expanded with a central constriction (Fig. 20D).

247. *Patches of cornuti placed*: (0) near middle of vesica (Fig. 19M); (1) near base (distance between cornuti and aedeagus much less than size of cornutus) (Fig. 20E); (2) extending into soft tissue in mouth of aedeagus (Fig. 20F); (3) right inside soft tissue in mouth of aedeagus (Fig. 25E). Because one or other of the two (primitive) patches of cornuti is sometime absent, and because these patches are placed more or less opposite one another, this character refers to the position of either or both of the patches of cornuti.

248. *Cornuti*: (0) in two distinct patches or on one side of aedeagus only (Fig. 25C); (1) in two distinct patches partially fused into a band (Fig. 20P); (2) completely fused into a uniform band (Fig. 21J).

249. *Patches of cornuti*: (0) directly opposite (Fig. 25C); (1) with outer patch at distal edge of inner patch (Fig. 25A). In most species the vesica everts at an angle to the aedeagus, with one patch of cornuti on the side nearer the aedeagus (anterior) and the other on the farther side (posterior). These patches are referred to as the ''inner'' and ''outer'' patches, respectively. In almost all species the posterior tip of the aedeagus is more strongly sclerotized and distally extended on one side, with this corresponding directly to the ''outer'' side of the vesica. The position of the patches of cornuti with respect to the aedeagus tip is thus used to infer whether patches are inner or outer in species where the vesica everts in a direct line with the aedeagus (Char. 244:1).

250. *Cornuti of inner patch (see Discussion for Char. 249)*: (0) distinct, large spines (Fig. 25C); (1) tiny spines to faint heavier sclerotization (Fig. 25F); (2) absent (Fig. 25B).

251. *Cornuti of outer patch (see Discussion for Char. 249)*: (0) distinct, large spines (Fig. 25C); (1) tiny spines to faint heavier sclerotization (Fig. 20P); (2) absent (Fig. 25D); (3) very elongate spines (Fig. 25H). If the two patches of cornuti are fused completely into a band (Char. 248:2), then this character is coded as equivocal, as both patches of cornuti are morphologically the same and Char. 227 would otherwise be duplicated.

252. *Cornuti of inner patch (see Discussion for Char. 249) forming*: (0) a V-shape (Fig. 25C); (1) oval to thin line (Fig. 25E); (2) two parallel narrow bands (Fig. 25G); (3) a broad rectangular band (Fig. 25F). If the two patches of cornuti are fused completely into a band (Char. 248:2), this character is coded as equivocal.

253. *Cornuti of outer patch (see Discussion for Char. 249) forming*: (0) an approximate oval or rounded rectangle (Fig. 25C); (1) a thin line (Fig. 25H). If the two patches of cornuti are fused completely into a band (Char. 248:2), this character is coded as equivocal.

254. *Cornuti of outer patch (see Discussion for Char. 249)*: (0) even (Fig. 25H); (1) strongly differentiated with basal cornuti much larger than distal (Fig. 21K).

Juxta

255. *Juxta*: (0) present (sclerotized) (Fig. 23C); (1) absent (unsclerotized) (Fig. 23D). State 1 is an autapomorphy for *Ithomia drymo*.

256. *In lateral view juxta placed*: (0) about level with vinculum (Fig. 25M); (1) level with posterior edge of valvae (Fig. 25N). State 1 is a synapomorphy for *Godyris dircenna* and *G. nero*.

257. *Juxta*: (0) varying from a ''U''- to ''V''-shaped strip to plate in ventral view, straight and narrow or moderately (no more so than juxta height) broad in lateral view (Fig. 24E); (1) a narrow strip with dorsal tips curved posteriorly in lateral view (Fig. 25O); (2) a small round plate in ventral view (Fig. 24G); (3) a highly elongate plate in ventral view (Fig. 24A); (4) an elongate tube rectangular in lateral and ventral view (twice as

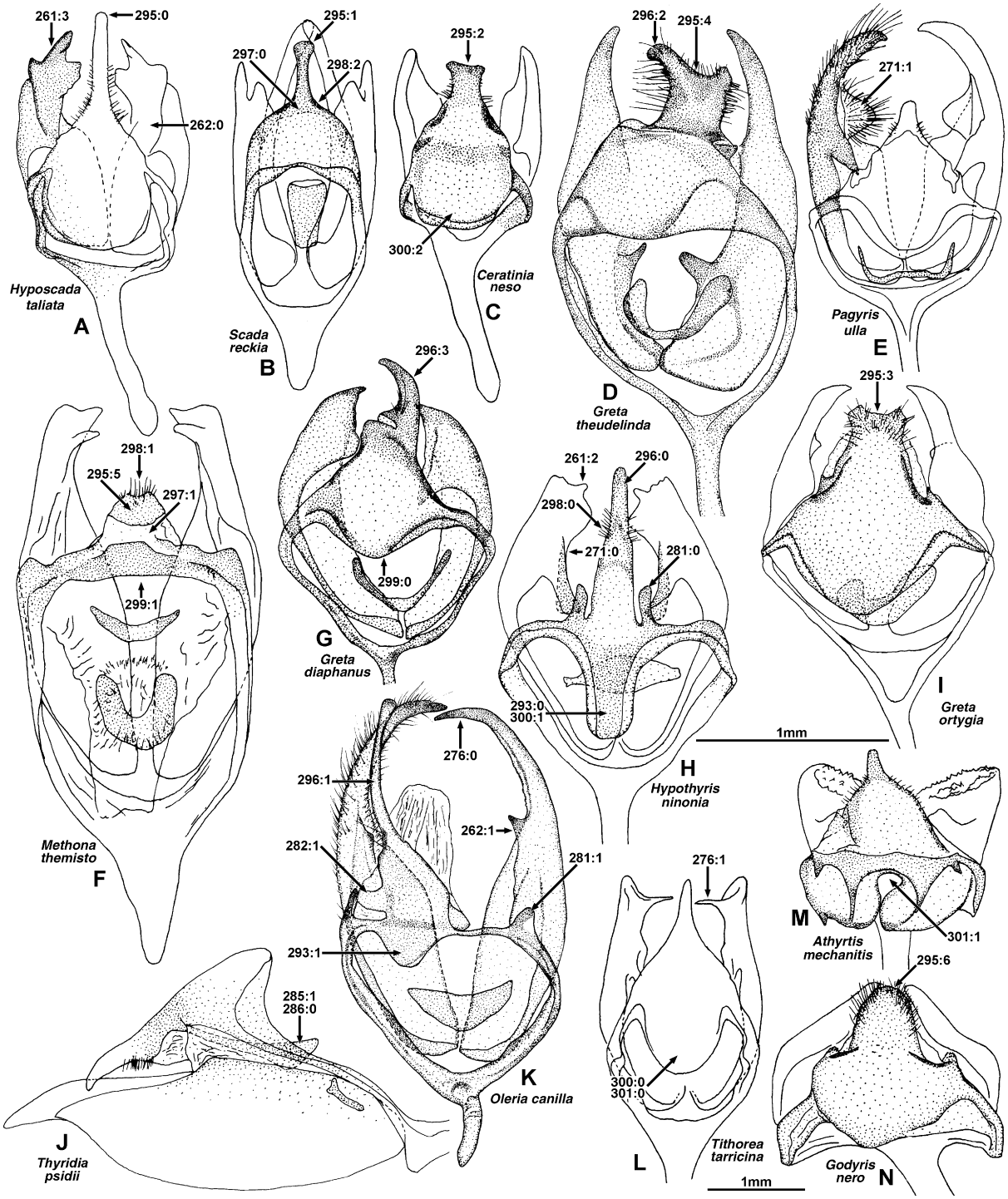

Fig. 22. Male genitalia, dorsal view, aedeagus removed, setae on valvae omitted except on right valva E and K. (A) *Hyposcada taliata*; (B) *Scada reckia theaphia*; (C) *Ceratinia n. neso*; (D) *Greta t. theudelinda*; (E) *Pagyris u. ulla*; (F) *Methona t. themisto*; (G) *Greta diaphanus*; (H) *Hypothyris n. ninonia*; (I) *Greta o. ortygia*; (J) *Thyridia p. psidii*; (K) *Oleria canilla*; (L) *Tithorea tarricina parola*; (M) *Athyrtis mechanitis salvini*; (N) *Godyris nero*.

long as wide) (Fig. 24I). There is substantial variation in juxta shape but much of this proved too continuous to be coded, with the exception of several particularly distinctive morphologies.

258. *Manica*: (0) with or without hairs (Fig. 21I); (1) with very long hairs (Fig. 21H). The manica is the membrane folded around and connected to the aedeagus at the zone, the junction between the basal and distal

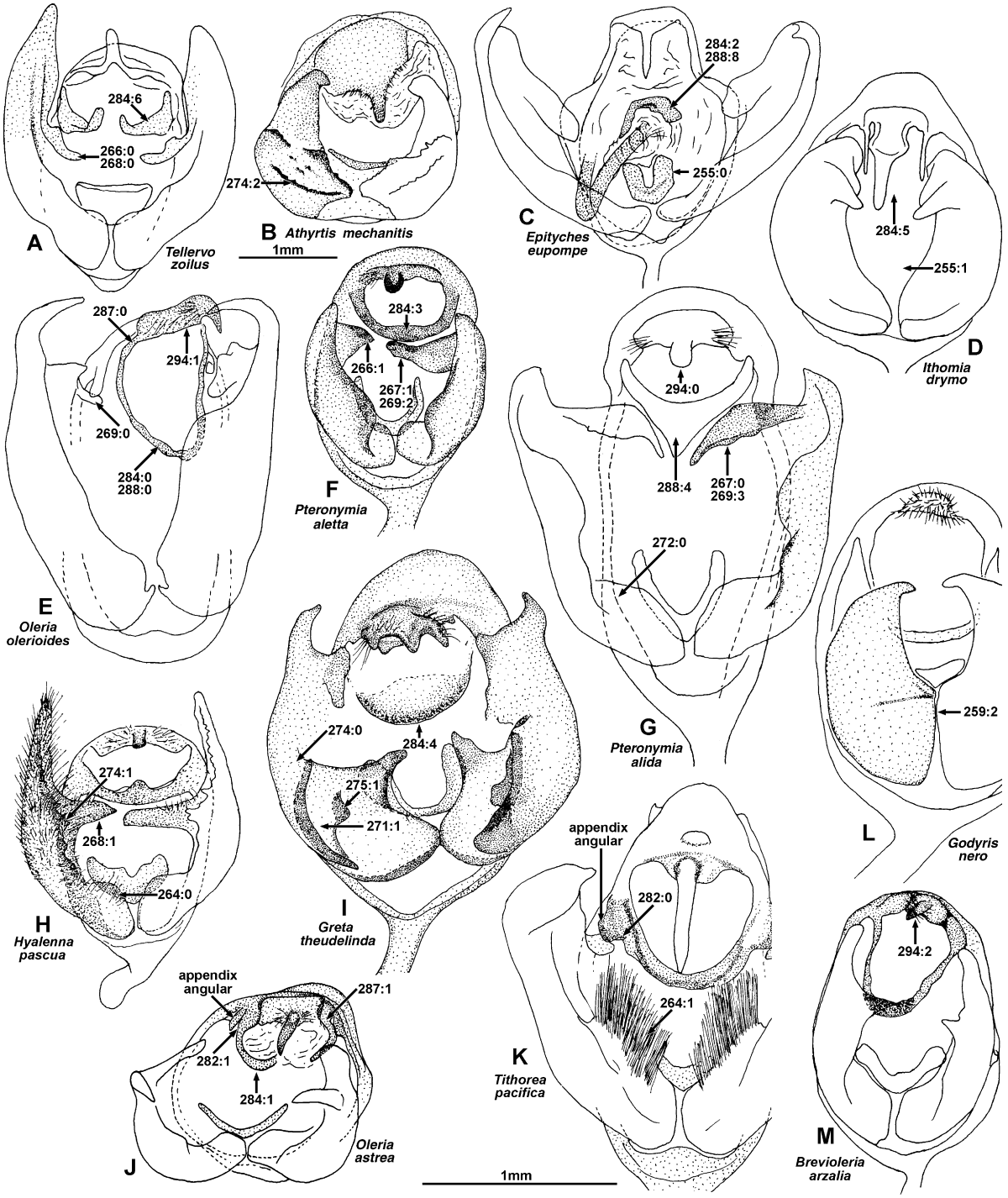

Fig. 23. Male genitalia, posterior view, aedeagus removed except C, setae on valvae omitted except on right valva H. (A) *Tellervo z. zoilus*; (B) *Athyrtis mechanitis salvini*; (C) *Epityches eupompe*; (D) *Ithomia drymo*; (E) *Oleria olerioides*; (F) *Pteronymia a. aletta*; (G) *Pteronymia a. alida*; (H) *Hyalenna pascua*; (I) *Greta t. theudelinda*; (J) *Oleria astrea burchelli*; (K) *Tithorea p. pacifica* Willmott & Lamas, 2004; (L) *Godyris nero*; (M) *Brevioleria arzalia* ssp. n.

sections. In most species there are scattered hairs on the inside surface of this membrane, visible when the aedeagus is extruded. In *Pseudoscada* and certain *Greta* these hairs are substantially longer than in all other species.

Valvae

259. *Valvae*: (0) meeting at very base only (Fig. 24A); (1) partially joined in base by soft tissue (Fig. 24H); (2) closely appressed/fused at base (Fig. 23L); (3) fused

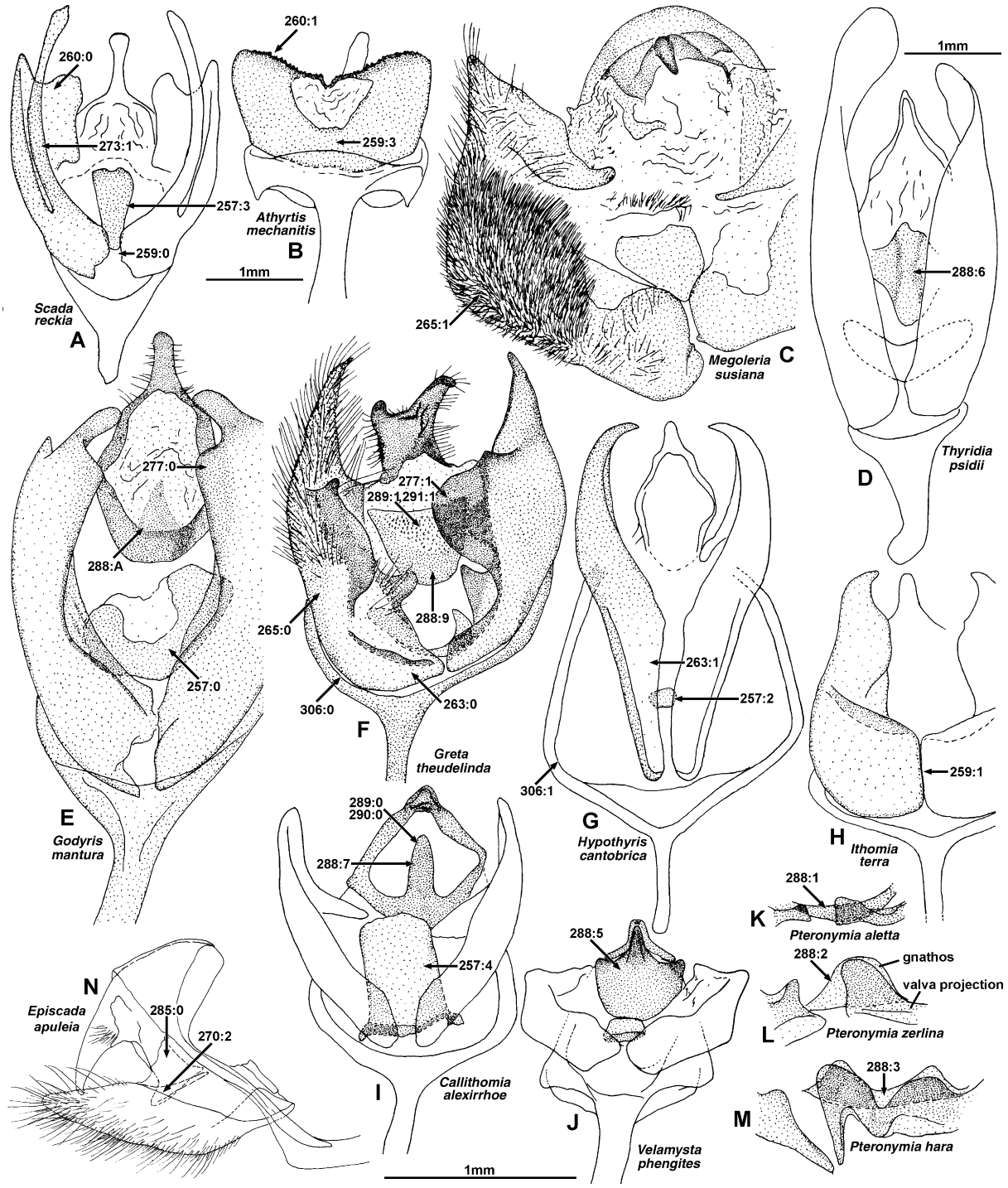

Fig. 24. Male genitalia, ventral view (except C,N), aedeagus removed, setae on valvae omitted except on right valva C and F. (A) *Scada reckia theaphia*; (B) *Athyrtis mechanitis salvini*; (C) *Megoleria* s. *susiana*, posterior view; (D) *Thyridia p. psidii*; (E) *Godyris mantura honrathi*; (F) *Greta t. theudelinda*; (G) *Hypothyris* (*Rhodussa*) *c. cantobrica*; (H) *Ithomia t. terra*; (I) *Callithomia alexirrhoe zeuxippe*; (J) *Velamysta p. phengites*. Gnathos and inner dorsal projection from costa of valva, ventral view: (K) *Pteronymia a. aletta*; (L) *Pteronymia z. zerlina*; (M) *Pteronymia h. hara*. Lateral view: (N) *Episcada a. apuleia*.

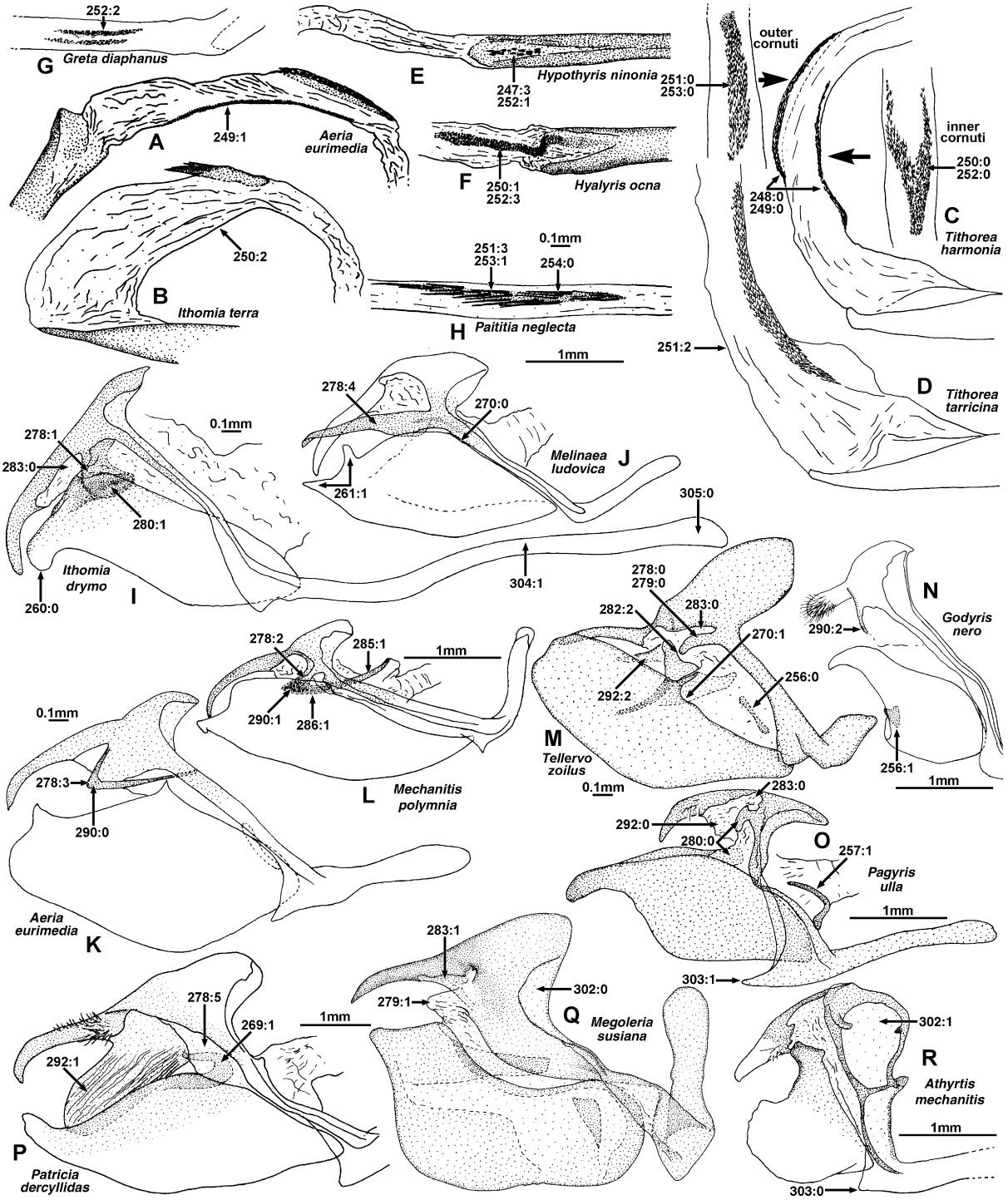

Fig. 25. Male genitalia. Aedeagus posterior tip and everted vesica, dorsal view: (A) *Aeria e. eurimedia*; (B) *Ithomia t. terra*; (C) *Tithorea harmonia manabiana*; (D) *Tithorea tarricina parola.* Aedeagus tip and everted vesica, view perpendicular t; cornuti: (E) *Hypothyris n. ninonia*; (F) *Hyalyris ocna* ssp. n. Vesica, view perpendicular t; cornuti: (G) *Greta diaphanus*; (H) *Paititia neglecta.* Male genitalia, lateral view: (I) *Ithomia drymo*; (J) *Melinaea l. ludovica*; (K) *Aeria eurimedia negricola*; (L) *Mechanitis p. polymnia*; (M) *Tellervo z. zoilus* ; (N) *Godyris nero*; (O) *Pagyris u. ulla*; (P) *Patricia d. dercyllidas*; (Q) *Megoleria* s. *susiana*; (R) *Athyrtis mechanitis salvini.*

entirely at base and with soft tissue in middle (Fig. 24B).

260. *Inner faces of valvae*: (0) approximately parallel when valvae are closed (Fig. 24A); (1) divergent (Fig. 24B). State 1 is an autapomorphy for *Athyrtis*.

261. *Valva posterior tip*: (0) ending in a smoothly rounded point or lobe (that may be bifurcate at very tip, as in *Hyposcada anchiala*) (Fig. 25I); (1) with a single dorso-lateral, inner lobe or projection (Fig. 25J); (2) tripartite (Fig. 22H); (3) with a lobe and a "cup" (Fig. 22A). Most primitive species of Ithomiinae have the posterior section of the valvae bifurcate, although the upper projection (state 1) is variously modified, forming an inner ridge in *Tithorea* (Char. 276:1). It is possible that the "tripartite" posterior tip in some Napeogenini also represents a similar state to 1, but as this is rather unclear and primitive Napeogenini have a simple valva (state 0) it was coded as a distinct state. Similarly, it also seems possible (but less likely) that the projecting dorsal, basal edge of the valva (Char. 262:1) may be homologous with Char. 261:1, but because of the different position (only *Scada* is ambiguous) it is coded as a distinct character.

262. *Valva basal costa in dorso-lateral view*: (0) rounded, not projecting inwards beyond rest of valva (Fig. 22A); (1) a smooth plate, projecting inwards and sometimes posteriorly (Fig. 22K). See Discussion under Char. 261; although *Scada* are coded 1 and appear similar to *Oleria*, the state is independently derived and in *Scada* may represent a modification of Char. 261:1. This is the dorsal edge of the valva, not the inner, dorso-basal portion that articulates with the vinculum (Char. 266–269).

263. *Basal portion of valva*: (0) similarly sclerotized to remainder of valva (Fig. 24F); (1) very elongate and weakly sclerotized (Fig. 24G). State 1 is an autapomorphy for *Hypothyris cantobrica*.

264. *Thick, long, dense hairs on inner basal edge of valva*: (0) absent (Fig. 23H); (1) present (Fig. 23K).

265. *Thick, short, dense hairs on ventral posterior part of valva*: (0) absent (Fig. 24F); (1) present (Fig. 24C). State 1 is a synapomorphy for *Megoleria*.

266. *Valva dorsal inner projection from costa (articulating with vinculum) sclerotized*: (0) similar to rest of valva (Fig. 23A); (1) more heavily than rest of valva (Fig. 23F).

267. *Valvae dorsal inner projections from costa (Char. 266)*: (0) approximately even in size (Fig. 23G); (1) larger on right-hand side (Fig. 23F).

268. *Valva dorsal inner projection from costa (Char. 266)*: (0) in line with more posterior valva edge (Fig. 23A); (1) angled inwards (Fig. 23H).

269. *Shape of valvae dorsal inner projections from costa (Char. 266)*: (0) varying from smoothly rounded to a slightly elongate, even lobe (Fig. 23E); (1) curving inwards and ending in an expanded rounded lobe (Fig. 25P); (2) right projection is a vertically broad then horizontally broad plate (Fig. 23F); (3) pointed, downward curving plate (Fig. 23G). State 2 occurs only in some *Pteronymia* and *Haenschia*. In *Haenschia* the right projection is a plate twisted through 90°, so that it is vertical at the base and horizontal at the tip. The right projection is similar in some *Pteronymia* except the tip is more heavily sclerotized and rounded, and the states in both these genera are interpreted as homologous.

270. *Valvae with ratio of distance between anterior edge and vinculum in line with dorsal edge of valva, and valva maximum height,* r: (0) $r < 0.55$ (Fig. 25J); (1) $0.55 < r < 1.1$ (Fig. 25M); (2) $r > 1.1$ (Fig. 24N). Species with higher states have the anterior edge of the valva further from the vinculum (relative to the valva width), resulting in valvae that can be opened to a greater extent.

271. *Broad, rounded, flat, weakly sclerotized lobe on dorsal inner edge of valva*: (0) absent (Fig. 22H); (1) present (Fig. 22E). State 1 occurs only in *Placidina* and *Pagyris*, and is either a synapomorphy for these two genera or has been subsequently lost in *Ithomia*.

272. *Inner face of valva in basal half with a broad, curving concavity*: (0) absent (Fig. 23G); (1) present (Fig. 23I). This concavity is shaped like a "suction cup" on the inner face of the valva, producing a notch or cleft at its dorsal edge around the middle of the valva, visible in posterior view.

273. *Valva ventral base with a very elongate, narrow projection extending posteriorly beyond valva*: (0) absent; (1) present (Fig. 24A). State 1 occurs only in several *Scada* species.

274. *Inner face of valva*: (0) smooth (Fig. 23I); (1) with spiny projections along the middle of the ventral edge (Fig. 23H); (2) with spiny projections in lines across the basal half of the valva (Fig. 23B). State 1 occurs here in *H. pascua* and is a synapomorphy for four *Hyalenna* species. State 2 is an autapomorphy for *Athyrtis*. In *Haenschia*, and to a lesser extent some other species (e.g., *Dircenna paradoxa*), the inner face of the valva is marked with numerous small "warts' which represent the expanded bases of hairs; in states 1 and 2 the projections do not terminate in hairs.

275. *Inner face of valva with small ridges near base*: (0) absent; (1) present (Fig. 23I).

276. *Valva with a vertical ridge on inner face just anterior of tip*: (0) absent (Fig. 22K); (1) present (Fig. 22L).

277. *Valvae ventral projections*: (0) symmetrical (Fig. 24E); (1) strongly asymmetrical (Fig. 24F). The ventral base of the valvae in a number of species, especially in the Godyridini, has various flat or elongate projections, which may be more or less symmetrical or strongly asymmetrical.

Gnathos and appendices angulares

278. *Appendices angulares*: (0) moderately sized projection on vinculum (similar in size to vinculum thickness) (Fig. 25M); (1) curved, vertical plates (Fig. 25I); (2) moderately posteriorly elongate projections (Fig. 25L); (3) large, triangular projections (Fig. 25K); (4) long, hollow tubes similar in length to valvae (Fig. 25J); (5) absent or tiny bumps on vinculum (Fig. 25P).

279. *Appendices angulares*: (0) sclerotized (Fig. 25M); (1) unsclerotized (Fig. 25Q). State 1 occurs only in *Megoleria susiana*, in which the appendices angulares are visible as unsclerotized projections.

280. *Appendices angulares*: (0) do not overlap in lateral view with valva dorsal inner projections (Char. 266) (Fig. 25O); (1) do overlap (Fig. 25I). The appendices angulares are usually dorsal of the dorsal edge of the valva and inner dorsal projections, but in a number of Napeogenini they extend ventrally to lie close beside these projections. If the appendices angulares are absent (some species coded 278:6) then this character is coded as equivocal.

281. *Appendices angulares positioned with respect to tegumen*: (0) equidistant (Fig. 22H); (1) further away on left side (Fig. 22K). Some species coded 278:6 were coded for this character if some trace of the appendices angulares was visible. In the Godyridini some species have the edge of the vinculum produced posteriorly into a slight fold immediately adjacent to the gnathos, and this represents the appendices angulares.

282. *Gnathos*: (0) attached to uncus and appendices angulares (Fig. 23J); (1) attached to uncus only (Figs 22K and 23J); (2) attached to uncus and tegumen by unsclerotized tissue (Fig. 25M). The ''gnathos' refers to any sclerotized band or ring that encircles the tuba analis and extends from near the junction of the vinculum and base of the uncus. The gnathos is highly variable in form and in many cases these different forms are not anatomically homologous. However, because of substantial variation between these forms, and because most seem to serve a similar purpose (supporting the tuba analis), for simplicity they are coded as single characters. In most Ithomiinae the gnathos attaches to the base of the uncus and the appendices angulares, which themselves arise from the upper part of the vinculum. In the Oleriini (*Megoleria*, *Hyposcada* and *Oleria*), the gnathos is attached to the base of the uncus only, and quite distinct from the appendices angulares.

283. *Appendices angulares and expanded base of uncus*: (0) separated by soft tissue (Fig. 25I,M,O); (1) fused with semi or sclerotized tissue (Fig. 25Q). The uncus in primitive species consists of a tapering, pointed tube that broadens towards the base, where it usually bears lateral hairs, then narrows distinctly (in lateral view) before its connection with the tegumen. The narrow area lies dorsal of weakly sclerotized region between the appendices angulares/vinculum and the broad base of the uncus. In *Scada*, Oleriini, Dircennini and Godyridini, this intermediate region is also semi or completely sclerotized, forming the dorsal part of the gnathos (which is isolated from the appendices angulares in Oleriini, but fused to these in the remainder). This character is coded equivocal if the appendices angulares are absent.

284. *Gnathos form of sclerotization*: (0) a narrow, entire, weakly sclerotized strip (Fig. 23E); (1) a sclerotized strip near vinculum only, not complete (Fig. 23J); (2) a sclerotized strip above aedeagus only (Fig. 23C); (3) a very heavily sclerotized continuous band (Fig. 23F); (4) a heavily sclerotized scoop isolated from vinculum (Fig. 23I); (5) absent (Fig. 23D); (6) strongly sclerotized, posteriorly pointing tubes, not complete (Fig. 23A). Absent is included as a state of this character as other states involve reduction in the gnathos.

285. *Gnathos*: (0) more or less parallel to vinculum (Fig. 24N); (1) projecting anteriorly (Figs 22J and 25L). In most species in which the outline of the gnathos is visible in lateral view it is more or less parallel with the vinculum. In *Aeria* and the Mechanitini the gnathos is directed anteriorly, at a sharp angle to the vinculum.

286. *If gnathos arms in lateral view are projecting anteriorly (Char. 285:1), then arms are*: (0) straight (Fig. 22J); (1) bent at right angles near base (Fig. 25L).

287. *If gnathos is attached to uncus only (Char. 237:1), then base of gnathos arms in posterior view*: (0) evenly curving (Fig. 23E); (1) kinked (Fig. 23J). State 1 is a synapomorphy for *Oleria*.

288. *Gnathos ventral portion*: (0) of similar width to the base of gnathos arms or slightly broader (Fig. 23E); (1) about twice width of base of gnathos arms (Fig. 24K); (2) broadening posteriorly into a smooth projection (not narrow projection like state 7) (Fig. 24L); (3) with two posterior projections (Fig. 24M); (4) with a posterior broad, slight projection and larger broad, anterior projection (broader and shorter projections than 6) (Fig. 23G); (5) with long central posterior and broad anterior projection (6 has short posterior projection, 7 has short anterior projection) (Fig. 24J); (6) with a short central posterior and long anterior projection (Fig. 24D); (7) with a posteriorly pointing central projection (Fig. 24I); (8) slightly broader and concave ventrally forming a ''hood'' (Fig. 23C); (9) greatly broadened into a square shape (Fig. 24F); (A) a rectangular sclerotized band with a posteriorly pointing semisclerotized projection (Fig. 24E). If the gnathos is absent ventrally, this character is coded equivocal.

289. *Gnathos ventrally*: (0) uniformly sclerotized (Fig. 24I); (1) becoming less sclerotized posteriorly (Fig. 24F). State 1 is a synapomorphy for Godyridini exluding *Veladyris* and *Velamysta*, apparently being lost in *Hypoleria adasa*.

290. *Base of gnathos/appendices angulares*: (0) smooth (Fig. 25K); (1) with rounded bumps (Fig. 25L); (2) with tiny spines (Fig. 25N).

291. *Gnathos with tiny bumps at posterior edge in ventral view*: (0) absent (Fig. 24I); (1) present (Fig. 24F). State 1 is a synapomorphy for Godyridini excluding *Veladyris* and *Velamysta*, apparently being lost in *Hypoleria adasa*.

Tuba analis

292. *Male genitalia with tuba analis*: (0) weakly sclerotized (except for gnathos, if present) (Fig. 25O); (1) a sclerotized, wrinkled tube (Fig. 25P); (2) a semi-sclerotized flat plate (Fig. 25M). State 1 occurs only in *Patricia*, state 2 only in *Tellervo*.

Uncus and tegumen

293. *Uncus and tegumen in dorsal view*: (0) symmetrical (Fig. 22H); (1) strongly asymmetrical, with tegumen displaced to right (Fig. 22K).

294. *Uncus in posterior view*: (0) horizontal (Fig. 23G); (1) rotated slightly anticlockwise (Fig. 23E); (2) rotated slightly clockwise (Fig. 23M).

295. *Uncus in dorsal view*: (0) tapering to a single point (Fig. 22A); (1) slightly flared and bifid at tip (Fig. 22B); (2) broad and shallowly bifid at tip (Fig. 22C); (3) broad and deeply bifid at tip, flaring slightly laterally (Fig. 22I); (4) asymmetrical, bifid, right projection longer than left (Fig. 22D); (5) short, blunt, flat or slightly bifid at tip (Fig. 22F); (6) broad and rounded (Fig. 22N).

296. *Uncus in dorsal view perpendicular to base of uncus*: (0) straight (Fig. 22H); (1) curved to left near base of narrow distal portion (Fig. 22K); (2) bent at base to left (Fig. 22D); (3) curved to right (Fig. 22G). A straight uncus can appear bent or curved in dorsal view, if the entire uncus and tegumen are rotated in posterior view (Char. 294:1,2).

297. *Uncus*: (0) continuously connected to tegumen by sclerotized tissue (Fig. 22B); (1) isolated from tegumen by unsclerotized tissue at base (Fig. 22F). State 1 is a synapomorphy for *Methona*.

298. *Uncus with lateral hairs*: (0) near base and at sides only (Fig. 22H); (1) near base, at sides and extending on to tip (Fig. 22F); (2) lacking hairs (Fig. 22B).

299. *Tegumen*: (0) present (Fig. 22G); (1) absent (Fig. 22F). State 1 is a synapomorphy for *Methona*.

300. *Ratio of width of tegumen to length uncus + tegumen,* r: (0) $0.3 < r < 0.55$ (Fig. 22L); (1) $r < 0.3$ (Fig. 22H); (2) $r > 0.55$ (Fig. 22C). State 1 indicates a relatively narrow tegumen, state 2 indicates a relatively broad tegumen, in dorsal view.

301. *Tegumen*: (0) a rounded lobe (Fig. 22L); (1) deeply cleft (Fig. 22M). State 1 is an autapomorphy for *Athyrtis*.

302. *Weakly sclerotized tissue on anterio-ventral edge of tegumen in lateral view*: (0) equal or less in size than sclerotized dorsal portion (Fig. 25Q); (1) greatly expanded (Fig. 25R). State 1 is an autapomorphy for *Athyrtis*.

Saccus

303. *Saccus posterior edge protruding*: (0) not much beyond vinculum (Fig. 25R); (1) substantially beyond vinculum (Fig. 25O).

304. *Ratio of saccus length to length of uncus + tegumen,* r: (0) $r < 1.25$ (Fig. 21B); (1) $1.25 < r < 2.1$ (Fig. 25I); (2) $2.1 < r$ (Fig. 21D). Higher states indicate a relatively longer saccus. Saccus length is measured from the anterior tip to the midpoint of the saccus where it intersects a line parallel to and passing through the middle of the vinculum.

305. *Saccus width*: (0) approximately even throughout (ratio maximum width/minimum width, $r < 2.25$) (Fig. 25I); (1) broadening near anterior tip (ratio maximum width/minimum width, $r > 2.25$) (Fig. 21D); (2) broadening gradually throughout, towards anterior tip (ratio maximum width/minimum width, $r > 2.25$) (Fig. 21B). Most species have the saccus of even width, while many species in the Godyridini and *Callithomia* have the saccus enlarged at the anterior tip. The maximum saccus width therefore refers to the maximum width in the anterior portion of the saccus. In a few cases the saccus evenly tapers anteriorly, in which case a single average width was used for both maximum and minimum saccus width. In the Godyridini the saccus broadens noticeably only near the anterior tip, whereas in *Callithomia* it broadens gradually throughout its length.

Vinculum

306. *Vinculum*: (0) running close to or outside anterio-ventral portion of valvae (Fig. 24F); (1) far outside anterio-ventral portion of valvae (Fig. 24G). State 1 is an autapomorphy for *Hypothyris cantobrica*.

Female genitalia and abdomen

External

307. *Terminal (eighth) tergite in dorsal view*: (0) entirely sclerotized or with small unsclerotized area at indentation at middle of posterior edge (Fig. 26A); (1) like state 0, but with anterior half also weakly sclerotized (Fig. 26B); (2) with sclerotized halves medially divided by unsclerotized tissue (Fig. 26C).

308. *Pleural tissue connecting terminal (eighth) and penultimate (seventh) tergites*: (0) similar in width to tissue between other tergites (Fig. 26D); (1) much narrower than between adjacent tergites, with tergite edges adjacent (Fig. 26F).

309. *Eighth sternite*: (0) present (Fig. 26F); (1) absent, terminal tergite of similar height to remaining tergites (Fig. 26G); (2) absent, terminal tergite elongate ventrally (Fig. 26I). Character 320 codes the form of the

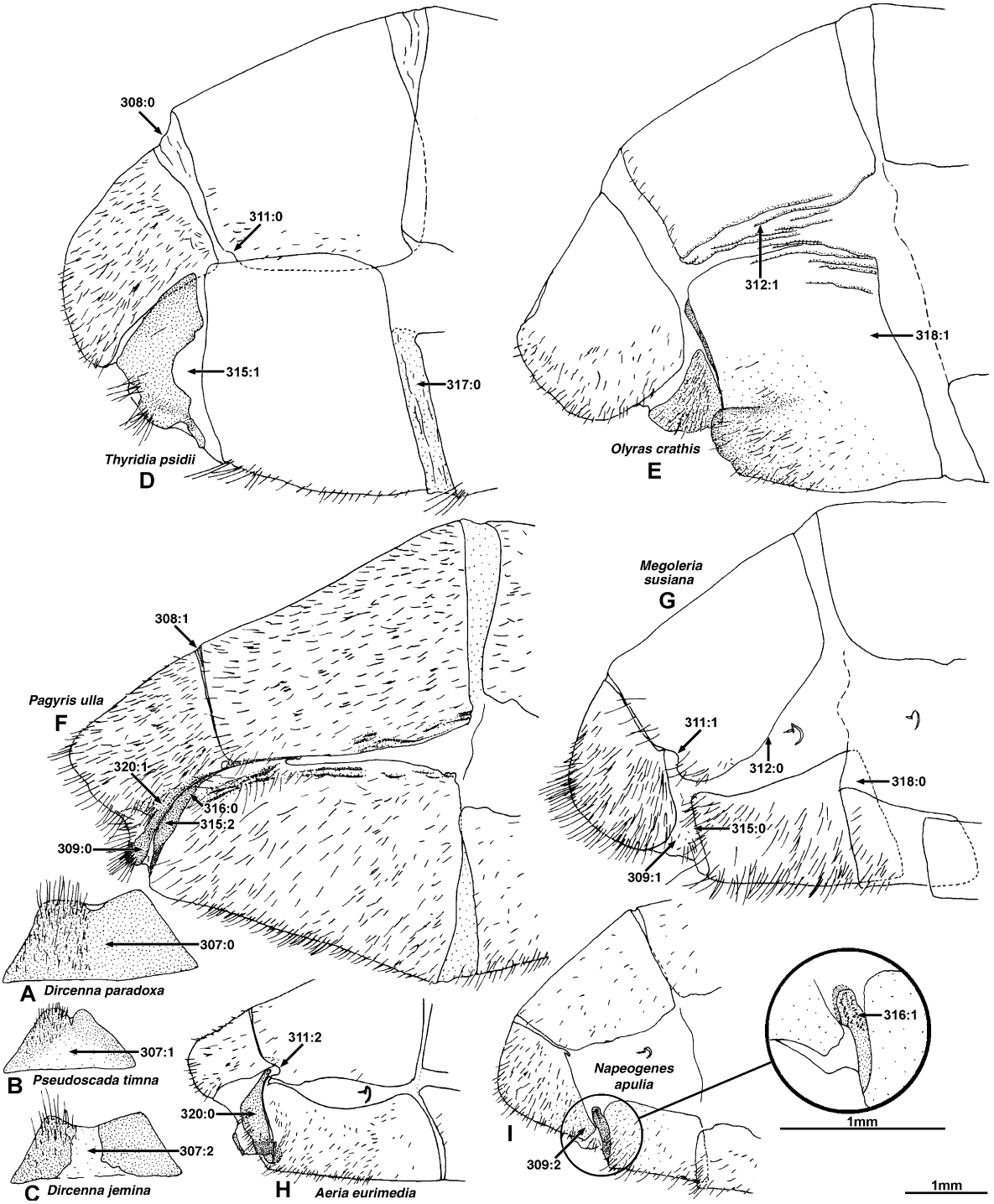

Fig. 26. Female abdomen. Terminal (posterior) tergite, dorsal view: (A) *Dircenna paradoxa praestigiosa*; (B) *Pseudoscada timna* ssp. n.; (C) *Dircenna j. jemina*. Abdomen posterior tip, lateral view: (D) *Thyridia p. psidii*; (E) *Olyras c. crathis*; (F) *Pagyris u. ulla*; (G) *Megoleria s. susiana*; (H) *Aeria e. eurimedia*; (I) *Napeogenes apulia* ssp. n.

eighth sternite, also known as the lamella postvaginalis, which is usually present as a pair of distinct, separate or fused plates ventral of the terminal (eighth) tergite. In some species these plates are visibly fused to the ventral edge of the terminal tergite (see Discussion under Char. 320), and in others they are apparently absent. This absence may be the result of loss of the eighth sternite or fusion with the terminal tergite; some species (e.g.,

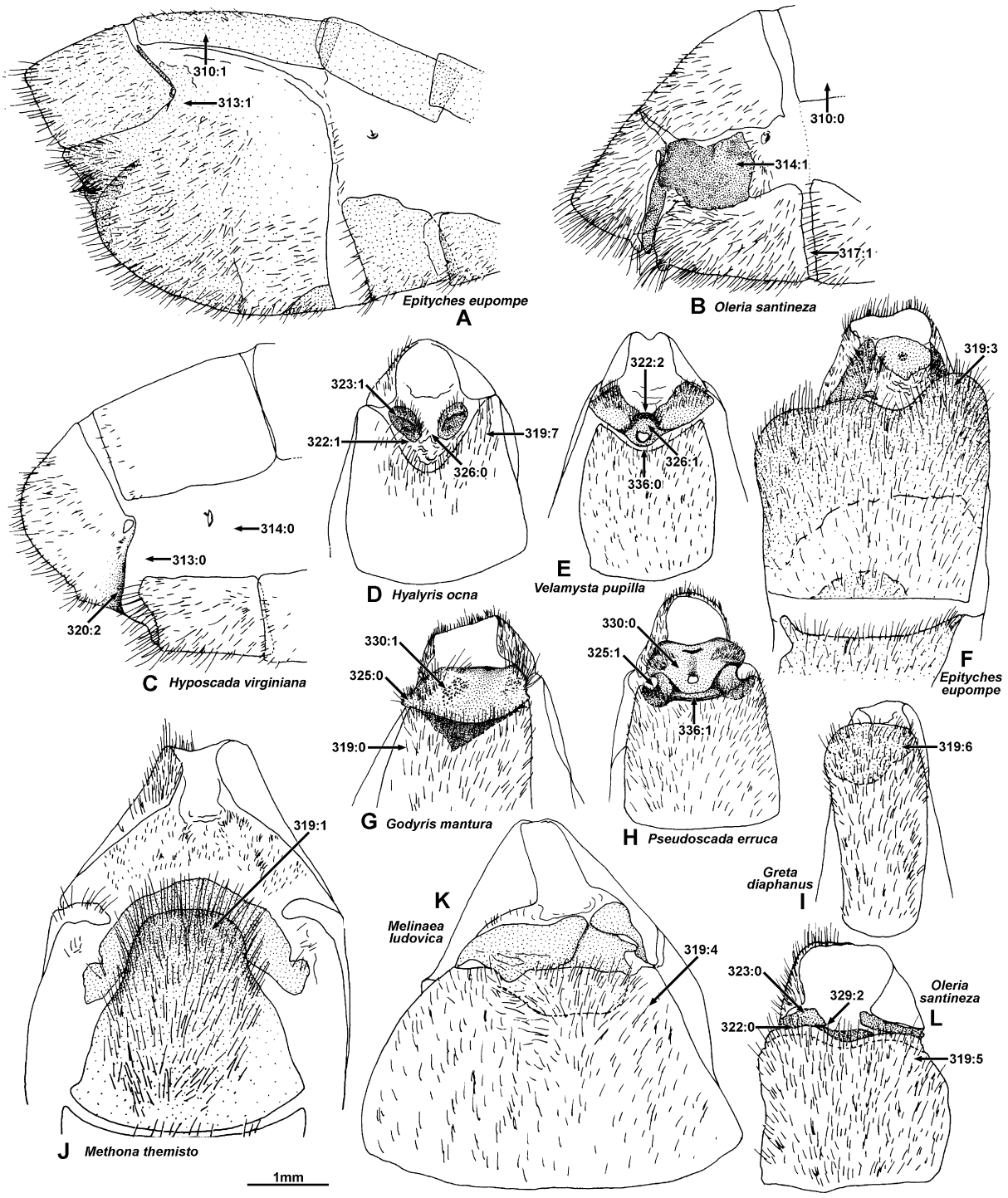

Fig. 27. Female abdomen. Abdomen posterior tip, lateral view: (A) *Epityches eupompe*; (B) *Oleria santineza* ssp. n.; (C) *Hyposcada virginiana evanides*. Abdomen posterior tip, ventral view: (D) *Hyalyris ocna* ssp. n.; (E) *Velamysta pupilla cruxifera* (Hewitson, 1877); (F) *Epityches eupompe*; (G) *Godyris mantura honrathi*; (H) *Pseudoscada erruca*; (I) *Greta diaphanus*; (J) *Methona t. themisto*; (K) *Melinaea l. ludovica*; (L) *Oleria santineza* ssp. n.

Tithorea tarricina) have the terminal tergite similar in size to remaining tergites, suggesting that the eighth sternite has simply been lost, whereas others have the terminal tergite elongated (e.g., *Napeogenes*), suggesting fusion with the eighth sternite. To avoid unnecessary inferences about whether or not the eighth sternite is present and fused or absent, we therefore coded instead the shape of the terminal tergite when the eighth sternite

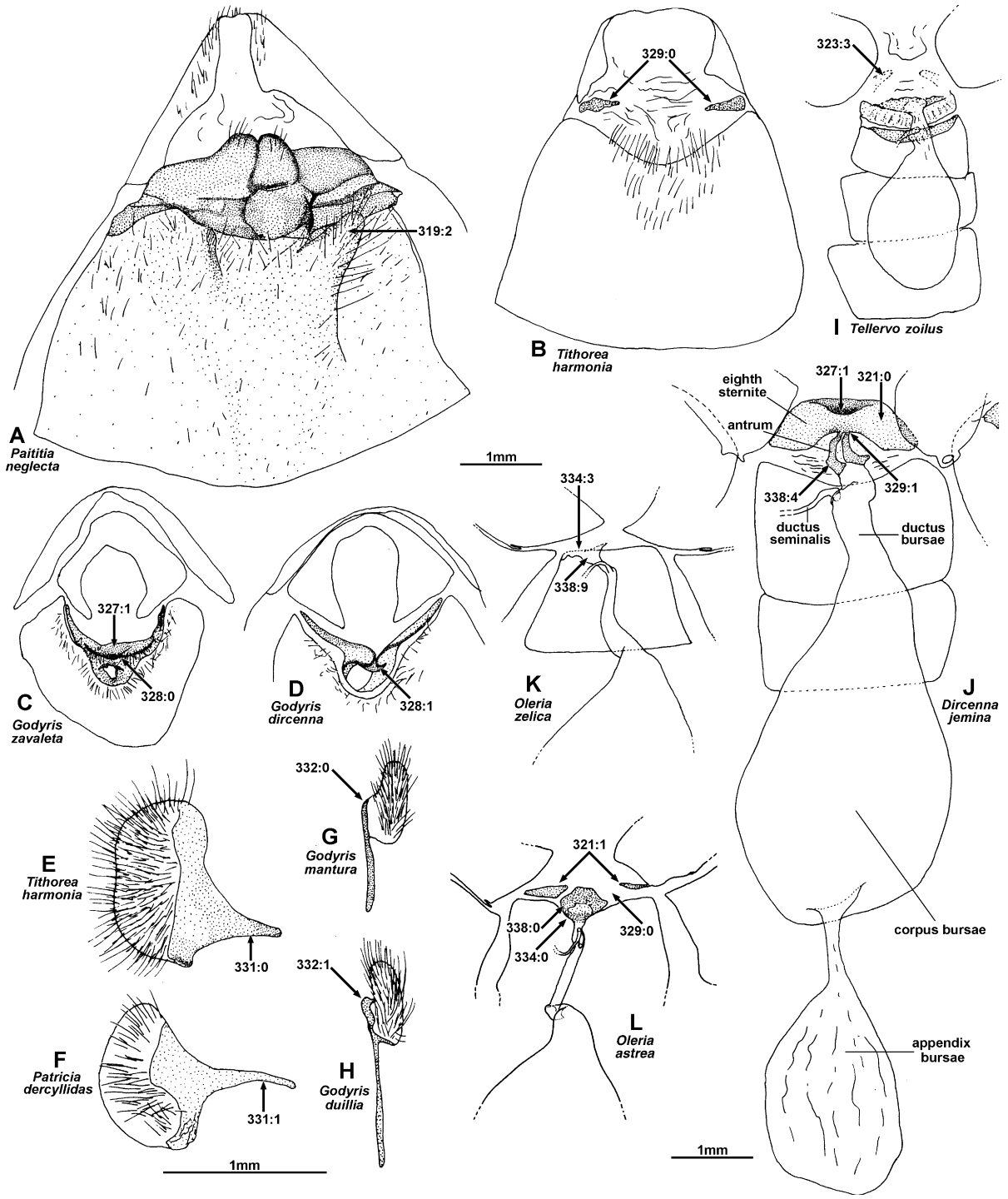

Fig. 28. Female abdomen and genitalia. Abdomen posterior tip, ventral view: (A) *Paititia neglecta*; (B) *Tithorea harmonia megara*. Abdomen posterior tip, posterior view: (C) *Godyris zavaleta telesilla*; (D) *Godyris dircenna*. Papilla analis, lateral view: E, *Tithorea harmonia megara*; (F) *Patricia d. dercyllidas*. Papilla analis, dorsal view: (G) *Godyris mantura honrathi*; (H) *Godyris duillia*. Genitalia, dorsal view: (I) *Tellervo z. zoilus*; (J) *Dircenna j. jemina*; (K) *Oleria z. zelica*; (L) *Oleria astrea burchelli*.

is apparently absent. Species coded for this character were therefore coded as equivocal for Char. 320.

310. *Penultimate (seventh) tergite*: (0) approximately same width as terminal (eighth) tergite, or larger (Fig. 27B); (1) about half the width of terminal tergite (Fig. 27A).

311. *Posterior edge of penultimate (seventh) tergite*: (0) straight (Fig. 26D); (1) weakly curved around

spiracle (Fig. 26G); (2) strongly curved around spiracle (Fig. 26H).

312. *Ventral edge of penultimate (seventh) tergite*: (0) smooth and uniformly sclerotized (Fig. 26G); (1) wrinkled and heavily sclerotized (Fig. 26E).

313. *Seventh sternite and terminal (eighth) tergite*: (0) distinct, separated by soft pleural tissue (Fig. 27C); (1) almost fused with semisclerotized intervening pleural tissue (Fig. 27A). State 1 is a synapomorphy for *Aremfoxia* + *Epityches*.

314. *Pleural tissue between right-hand penultimate (seventh) tergite and seventh sternite with a large, irregular, heavily sclerotized mass*: (0) absent (Fig. 27C); (1) present (Fig. 27B). State 1 is an autapomorphy for *Oleria santineza*.

315. *Pleural tissue at lateral posterior edge of seventh sternite*: (0) weakly sclerotized (Fig. 26G); (1) semisclerotized (Fig. 26D); (2) strongly sclerotized, forming a broad, smooth band (Fig. 26F).

316. *Sclerotized pleural tissue at lateral posterior edge of seventh sternite (Char. 315:1)*: (0) smooth (Fig. 26F); (1) with tiny studs (Fig. 26I). State 1 is a synapomorphy for *Napeogenes*.

317. *Pleural tissue between seventh and sixth sternites sclerotized*: (0) weakly (Fig. 27B); (1) strongly (Fig. 26D).

318. *Seventh sternite*: (0) similar in width to sixth (Fig. 26G); (1) about twice width (Fig. 26E).

319. *Seventh sternite overall shape*: (0) slightly indented or straight, smooth, uniformly sclerotized (Fig. 27G); (1) heavily sclerotized forming a rounded "keel" (Fig. 27J); (2) with a more heavily sclerotized, shallow, rounded projection on the right-hand side only (Fig. 28A); (3) asymmetrical, swollen, extended posteriorly on right side (Fig. 27F); (4) asymmetrical and folded inwards at posterior right end (Fig. 27K); (5) symmetrical and folded inwards with a heavily sclerotized lip (Fig. 27L); (6) elongate, rounded and folded inwards at posterior tip (Fig. 27I); (7) deeply invaginated at posterior edge forming a "U" shape in ventral view, as broad anteriorly as laterally (Fig. 27D).

320. *Eighth sternite lateral plates*: (0) distinct or fused to terminal (eighth) tergite only at spiracular opening (Fig. 26H); (1) fused to terminal (eighth) tergite in basal half (Fig. 26F); (2) entirely fused to terminal tergite (Fig. 27C). Entire fusion with the terminal tergite (state 2) is inferred from the ventral edge of the tergite being elongate, distinctly more heavily sclerotized and lacking in hairs than the remaining tergite, and/or with a notch at the posterior edge where the sternite and tergite are joined. If there is no such evidence of the eighth sternite plates the character is coded equivocal (and these species are coded 309:1,2).

321. *Basal attachment of eighth sternite plates*: (0) symmetrical (Fig. 28J); (1) asymmetrical, with left plate attached near base of tergite and right side more ventral (Fig. 28L).

322. *Eighth sternite lateral plates in ventral view with anterior edge*: (0) near or posterior of posterior edge of terminal sternite (Fig. 27L); (1) extending far anteriorly past posterior edge terminal sternite (Fig. 27D). State 1 is a synapomorphy for *Hypothyris* and *Hyalyris*, also recurring in *Methona megisto*.

323. *Shape of eighth sternite lateral plates*: (0) flat or concave plates (Fig. 27L); (1) slightly convex, wrinkled dish-like plates (Fig. 27D); (2) double curved plates, forming a protruding "snout" above ostium bursae (Fig. 27E); (3) slightly protruding rounded lobes (Fig. 28I). Many Godyridini have the eighth sternite plates pinched inwards just before the ostium bursae, then flared outwards to form a slightly protruding "snout" above the ostium bursae. In *Tellervo* the eighth sternite plates are visible only as weakly sclerotized, slightly protruding lobes.

324. *Edges of eighth sternite lateral plates*: (0) flat or lightly curved (Fig. 30D); (1) with ventro-inner edge recurved, forming a pouch from inside view (Fig. 30A). State 1 is a synapomorphy for Mechanitini excluding *Thyridia*.

325. *Anterior edge of eighth sternite plates*: (0) flat or convex (Fig. 27G); (1) formed into a broad, concave half-tube (Fig. 27H).

326. *Eighth sternite lateral plates*: (0) separate (Fig. 27D); (1) fused at ventral inner edges into a band (independent of whether or not also fused with antrum) (Fig. 27E).

327. *Tissue at ventral edge of mouth of oviduct, above eighth sternite plates*: (0) flat and unsclerotized (Fig. 30D); (1) a pouch, sclerotized on ventral edge (Fig. 28C,J). State 1 is a synapomorphy for Godyridini + Dircennini.

328. *Eighth sternite lateral plate edges*: (0) not pinched together forming an "x"-pattern in ventral view (Fig. 28C); (1) pinched together forming an "x"-pattern in ventral view (Fig. 28D). State 1 is a synapomorphy for *Godyris dircenna* + *G. nero*.

329. *Eighth sternite lateral plates*: (0) distinct from antrum (Fig. 28B,L); (1) fused to antrum (Fig. 28J); (2) fused on right side only (Fig. 27L). If the antrum is completely unsclerotized, this character is coded equivocal.

330. *Inside edge of antrum near dorsal edge*: (0) smooth (Fig. 27H); (1) heavily studded (Fig. 27G). State 1 is an autapomorphy for *Godyris mantura*.

Internal

331. *Anterior apophysis of papilla analis*: (0) short (Fig. 28E); (1) long (Fig. 28F). There is some variation in the length and shape of the anterior apophysis, but in *Tellervo*, *Tithorea*, *Elzunia* and *Methona* it is distinctly shorter than in other species.

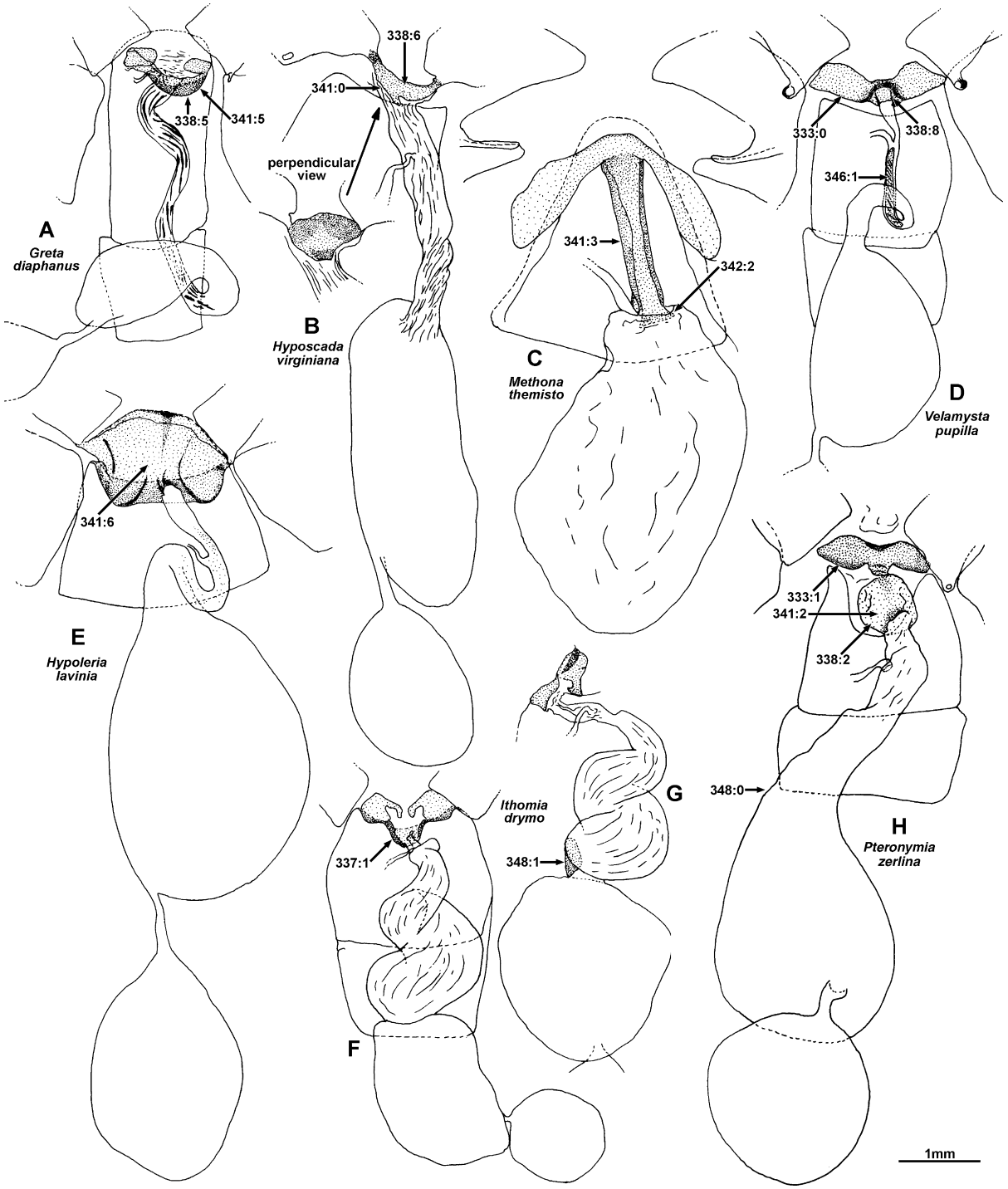

Fig. 29. Female genitalia, dorsal view (except G). (A) *Greta diaphanus*; (B) *Hyposcada virginiana evanides*; (C) *Methona t. themisto*; (D) *Velamysta pupilla cruxifera*; (E) *Hypoleria lavinia libera* Godman & Salvin, 1879; (F) *Ithomia drymo*; (G) *Ithomia drymo*, lateral view antrum, ductus bursae and corpus bursae; (H) *Pteronymia zerlina machay*.

332. *Papillae anales in dorsal view with outer edge of sclerotized basal part*: (0) contiguous with unsclerotized distal part (Fig. 28G); (1) forming a distinct "step" (Fig. 28H).

333. *Anterior edge of eighth sternite plates*: (0) no more heavily sclerotized than rest of plates (Fig. 29D); (1) more heavily sclerotized, forming a distinct band (Fig. 29H).

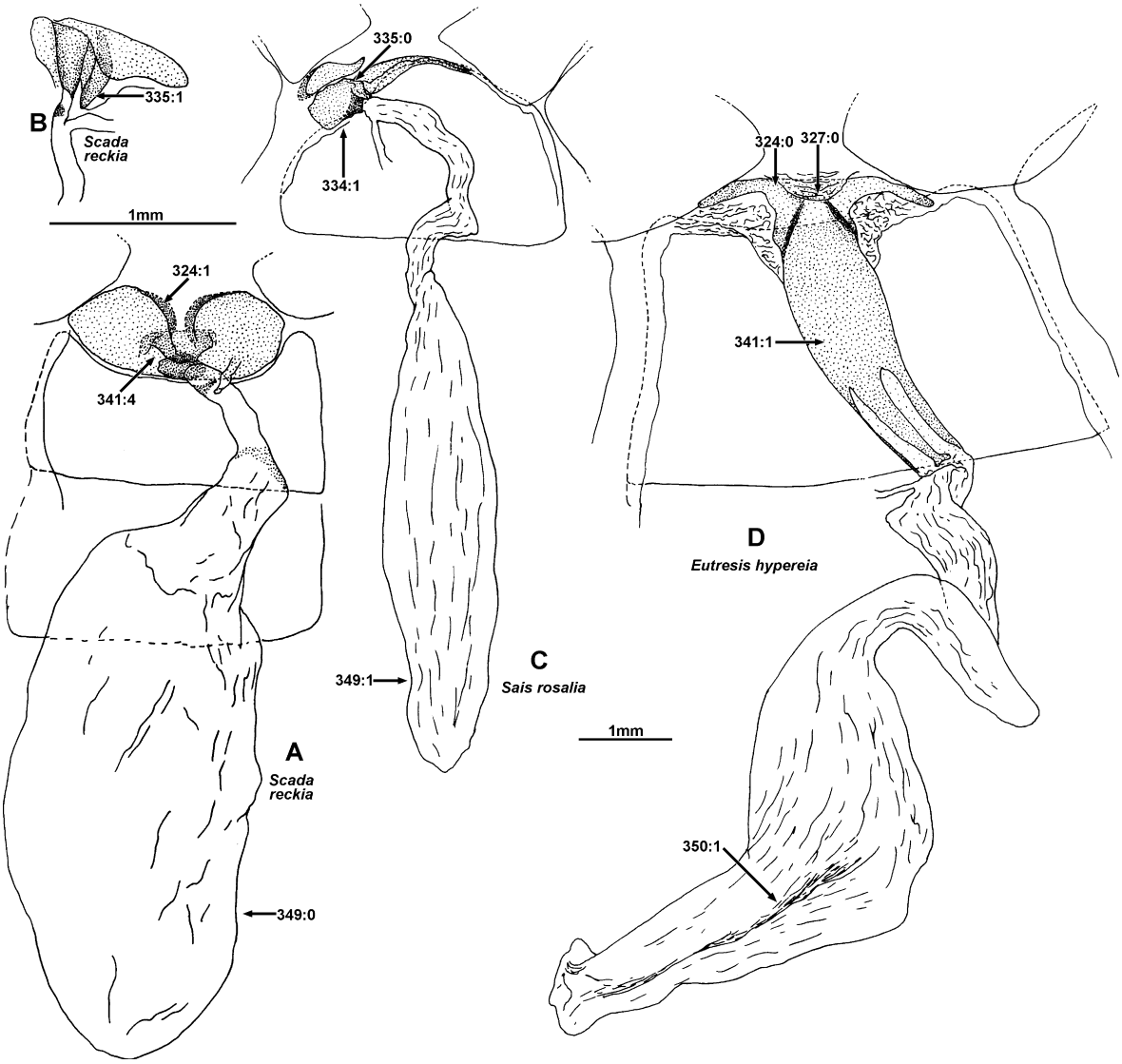

Fig. 30. Female genitalia, dorsal view. (A) *Scada reckia theaphia*; (B) *Scada reckia theaphia*, antrum and entrance ductus bursae, lateral view; (C) *Sais r. rosalia*; (D) *Eutresis h. hypereia.*

334. *Ostium bursae position on last sternite*: (0) central (Fig. 28L); (1) right-central (Fig. 30C); (2) left-central (Fig. 31D); (3) on right corner (Fig. 28K).

335. *Dorsal edge of antrum plate*: (0) flat (Fig. 30C); (1) recurved anteriorly (Fig. 30B). The antrum is usually tubular or broadens posteriorly to form a flat plate. In *Scada* the dorsal edge of this flat plate is recurved anteriorly.

336. *Flat, posteriorly protruding sclerotized plate between posterior edge seventh sternite and ostium bursae*: (0) absent (Fig. 27E); (1) present (Fig. 27H). State 1 occurs here only in four *Pseudoscada* species. In most species the ostium bursae is at the posterior edge of the seventh sternite, whereas in state 1 there is a distinct, sclerotized plate between the posterior edge and the ostium bursae, possibly formed of the pleural tissue at the edge of this sternite.

337. *Antrum ventrally*: (0) unsupported (Fig. 31A); (1) supported by a sclerotized "lip" (Figs 29F and 31G). The sclerotized "lip" in state 1 may be the posterior edge of the last sternite or part of the antrum, but in *Placidina* (Fig. 31G) and *Pagyris* it is present and there is also a sclerotized patch immediately anterior that appears to represent the actual antrum (see also discussion under Char. 338).

338. *Antrum sclerotization*: (0) a completely sclerotized tube (Fig. 28L); (1) sclerotized except in a dorsal band (Fig. 31A); (2) sclerotized except for a more weakly sclerotized ventral band (Fig. 29H); (3) semi-sclerotized (Fig. 31B); (4) sclerotized dorsally, more so

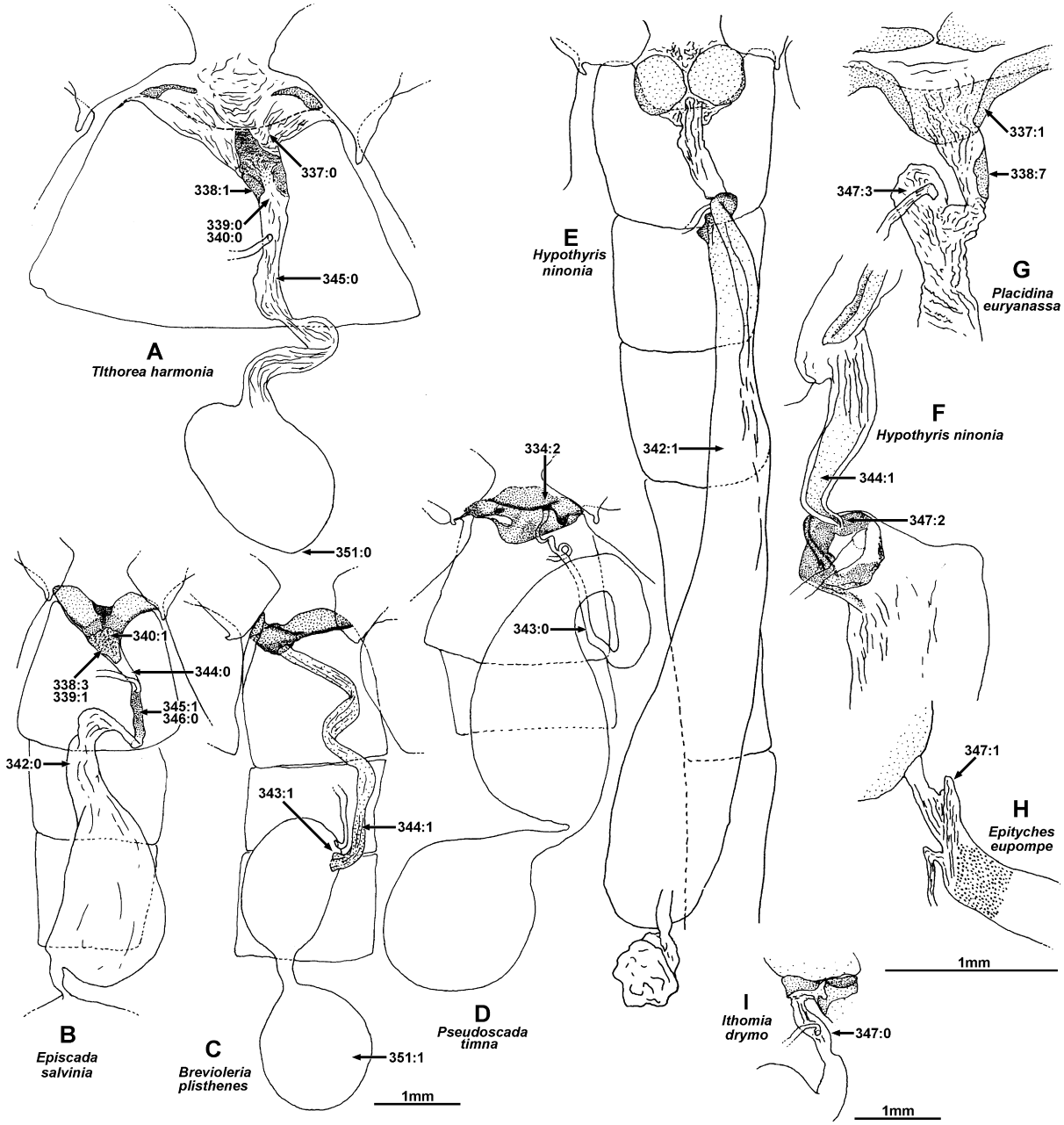

Fig. 31. Female genitalia. Dorsal view: (A) *Tithorea harmonia megara*; (B) *Episcada s. salvinia*; (C) *Brevioleria plisthenes*; (D) *Pseudoscada timna* ssp. n.; (E) *Hypothyris n. ninonia*. Antrum and base of ductus bursae: (F) *Hypothyris n. ninonia*, lateral view; (G) *Placidina euryanassa*, dorsal view; (H) *Epityches eupompe*, lateral view; (I) *Ithomia drymo*, lateral view.

in two parallel longitudinal bands (Fig. 28J); (5) sclerotized in a broad dorsal band only (Fig. 29A); (6) sclerotized in a dorsal plate only (Fig. 29B); (7) a ventral round sclerotized patch only (Fig. 31G); (8) a thin sclerotized ring (Fig. 29D); (9) unsclerotized (Fig. 28K). The antrum is usually a sclerotized ring or tube between the ductus bursae and ostium bursae. In primitive Ithomiinae, such as *Tithorea* (and other nymphalids, e.g., the limenitidine genus *Adelpha*), the antrum is a thickened half tube which is dorsally grooved. A similar form of antrum also occurs in *Methona* (Char. 341:3), which is entirely sclerotized, among other species, as well as *Pagyris* and *Placidina*, in which it is sclerotized in a small ventral patch only (state 7). In most other species the antrum is a more or less flattened tube, which is assumed to be homologous to the half tube in *Tithorea*, etc. Species coded state 8 have the ductus bursae almost completely unsclerotized, but a

more heavily sclerotized ring surrounding its mouth, usually extending on to the fused eighth sternite plates and inset into the posterior edge of the seventh sternite, is inferred to be the antrum.

339. *Antrum with a faint, internal sclerotized triangular patch*: (0) absent (Fig. 31A); (1) present (Fig. 31B). This character is coded equivocal if the antrum is heavily sclerotized.

340. *Antrum inner walls*: (0) smooth (Fig. 31A); (1) studded (Fig. 31B). State 1 is a synapomorphy for *Ceratinia* + *Episcada*.

341. *Shape of antrum*: (0) gradual funnel or tube similar in width to ductus bursae (Fig. 29B); (1) a large funnel (Fig. 30D); (2) a long, broad (3 × width ductus bursae), tube of almost even width (Fig. 29H); (3) a very long, narrow, dorsally grooved tube (Fig. 29C); (4) a tube broadening into a flat, perpendicular plate (Fig. 30A); (5) a very broad, shallow, "cup" curving at edges (Fig. 29A); (6) a semicylindrical plate (Fig. 29E). In *Methona* (state 3), the sclerotized tube connecting the corpus bursae to the eighth sternite plates is similar in morphology to the antrum in primitive species like *Tithorea* (see Discussion under Char. 338), and is therefore inferred to represent the antrum. State 5 is an autapomorphy for *Greta diaphanus*, state 6 is an autapomorphy for *Hypoleria lavinia*.

342. *Ductus bursae*: (0) medium or short [extending one to two tergites from ostium bursae] (Fig. 31B); (1) long [extending more than three tergites from the ostium bursae] (Fig. 31E); (2) absent (Fig. 29C). Reasons for considering the sclerotized tube connecting the corpus bursae to the eighth sternite in *Methona* to be the antrum, rather than the ductus bursae, are discussed under Char. 341.

343. *Ductus bursae portion anterior of ductus seminalis*: (0) present (Fig. 31D); (1) absent (ductus seminalis arises from corpus bursae) (Fig. 31C). State 1 is a synapomorphy for *Hypoleria adasa* + *Mcclungia* + *Brevioleria* + *Godyris mantura*. *Methona* is coded equivocal because the ductus bursae is inferred to be absent (see Char. 342).

344. *Ductus bursae just posterior of ductus seminalis with sclerotization fading posteriorly*: (0) absent (Fig. 31B); (1) present (Fig. 31C,F).

345. *Ductus bursae anterior of ductus seminalis with sclerotization fading anteriorly*: (0) absent (Fig. 31A); (1) present (Fig. 31B).

346. *If ductus bursae anterior of ductus seminalis has sclerotization fading anteriorly (Char. 345:1), then sclerotization is*: (0) evenly fading (Fig. 31B); (1) striated (Fig. 29D). State 1 is a synapomorphy for *Velamysta*.

347. *Ductus bursae with anterior and posterior sections*: (0) joined smoothly (Fig. 31I); (1) with anterior section projecting posteriorly beyond end of posterior section, ductus seminalis arising anterior of junction (Fig. 31H); (2) with posterior section joining on to a disc at end of much larger anterior section (Fig. 31F); (3) with anterior section projecting posteriorly beyond end of posterior section, ductus seminalis arising posterior of junction (Fig. 31G).

348. *Ductus bursae near junction with corpus bursae with a large, curved sclerotized pad*: (0) absent (Fig. 29H); (1) present (Fig. 29G).

349. *Corpus bursae anteriorly*: (0) rounded (Fig. 30A); (1) attentuated (Fig. 30C). This character is difficult to observe unless the corpus bursae is inflated, either immediately following dissection, or artificially using a syringe and water.

350. *Signa on corpus bursae*: (0) scattered; (1) in lines (Fig. 30D). The signa are numerous, tiny sclerotized spines on the inner surface of the corpus bursae, and they are usually dense and evenly scattered. In state 1 distinct lines of denser, larger or more strongly sclerotized signa are visible.

351. *Appendix bursae*: (0) absent (Fig. 31A); (1) present (Fig. 31C).

Wing pattern

352. *Male VHW with a white marking in cell Sc + R1-Rs anterior of discocellular veins*: (0) absent (Fig. 17AA); (1) present, confined to cell Sc + R1-Rs (Fig. 17AB); (2) present and extending into cell M1-Rs (Fig. 17AD).

353. If male with VHW white marking in cell Sc + R1-Rs anterior of discocellular veins (Char. 352: 1), then marking is: (0) single (Fig. 17AB); (1) double (Fig. 17AC). The double marking in *Olyras* and *Paititia* is regarded as homologous to the single marking in *Eutresis* because of similarity of position and because the scales forming these white markings are very similar in all three taxa, being notably translucent (more opaque in other taxa). *Veladyris* also has an additional white marking in cell Sc + R1-Rs, but because of the much more basal position of this marking it is regarded as independent of the white discal marking coded in Char. 352.

Larval hostplant (characters not included in cladistic analysis; coding in Table 3)

H1 & H2. *Larval hostplant*: (0) Apocynaceae; (1) Gesneriaceae; (2) *Brunfelsia* L. (Petunioideae); (3) *Cestrum* L. (Cestroideae, Cestreae); (4) *Nicandra* Adans. (Solanoideae, Nicandreae); (5) *Datura* L. clade (Solanoideae, Datureae); (6) *Solanum* clade (Solanoideae, Solaneae); (7) *Solandra* clade (Solanoideae, Solandreae); (8) *Capsicum* L. (Solanoideae, Capsiceae); (9) *Lycianthes* Dunal. (Solanoideae, Capsiceae); (A) *Withania* + *Iochroma* + *Physalis* clade (Solanoideae, Physaleae). See Table 3.

Following Olmstead et al. (1999), Solanaceae clades contain the following genera of ithomiine hostplants: (5) *Datura* L., *Brugmansia* Pers.; (6) *Solanum* L. (incl. *Cyphomandra* Mart., *Lycopersicon* Mill.); (7) *Dyssochroma* Miers, *Juanulloa* Ruiz & Pav., *Markea* A. Rich., *Merinthopodium* Donn. Sm., *Schultesianthus* Hunz., *Solandra* Sw., *Trianaea* Planch. & Lindeno; (A) *Athenaea* Sendt., *Aureliana* Sendt., *Cuatresia* Hunz., *Withania* Pauq., *Acnistus* Schott, *Dunalia* Kunth, *Iochroma* Benth., *Saracha* Ruiz & Pav., *Vassobia* Rusby, *Brachistus* Miers, *Physalis* L., *Witheringia* L'Her.

Appendix 2

Character matrix: ?" = indicates missing data, "–" = indicates a non-applicable state.

Appendix 3

Information sources for included species

Higher taxon	Species	Dissections examined[1]	Immature stage sources[2]
Tellervini (Tellervinae)	*Tellervo zoilus*	M: BMNH 7117; F: BMNH 7118, BMNH 7126	6
Tithoreini	*Elzunia pavonii*	M: BMNH 6624; F: BMNH 6625	1
Tithoreini	*Tithorea harmonia*	M: BMNH 6819, BMNH 6622, KWJH, BMNH 6820; F: BMNH 6623, KWJH, BMNH 6818	1
Tithoreini	*Tithorea tarricina*	M: BMNH 6812, BMNH 6814, BMNH 6816; F: BMNH 6813, BMNH 6815, BMNH 6817	1
Tithoreini	*Aeria eurimedia*	M: BMNH 6626, BMNH 7106; F: BMNH 7172, BMNH 7119	1
Tithoreini	*Aeria olena*	M: BMNH 7139; F: BMNH 7173, BMNH 7140	1
Methonini	*Methona megisto*	M: BMNH 7161; F: BMNH 7160	1
Methonini	*Methona themisto*	M: BMNH 6629; F: BMNH 6642	1
Melinaeini	*Athyrtis mechanitis*	M: BMNH 6634, BMNH 6638; F: BMNH 6647	1
Melinaeini	*Eutresis hypereia*	M: BMNH 6632, MGCL; F: BMNH 6645, MGCL, BMNH 7159	1
Melinaeini	*Melinaea ethra*	M: BMNH 7141; F: BMNH 7142	1
Melinaeini	*Melinaea ludovica*	M: BMNH 6631; F: BMNH 6644	1
Melinaeini	*Melinaea menophilus*	M: MGCL, BMNH 7143, BMNH 7149, KWJH; F: BMNH 7144	1,2
Melinaeini	*Olyras crathis*	M: BMNH 6633; F: BMNH 6646	1
Melinaeini	*Paititia neglecta*	M: BMNH 7133; F: BMNH 7132	1
Mechanitini	*Forbestra equicola*	M: BMNH 6637; F: BMNH 6650	3
Mechanitini	*Forbestra olivencia*	M: BMNH 7145; F: BMNH 7146	7
Mechanitini	*Mechanitis lysimnia*	M: BMNH 7150, KWJH; F: BMNH 7147, BMNH 7176, KWJH	1
Mechanitini	*Mechanitis polymnia*	M: BMNH 6639; F: BMNH 6651	1
Mechanitini	*Sais rosalia*	M: BMNH 6636; F: BMNH 6649	8
Mechanitini	*Scada karschina*	M: BMNH 7151; F: BMNH 7175, BMNH 7152	1
Mechanitini	*Scada reckia*	M: KWJH, KWJH, KWJH, KWJH, BMNH 6640; F: BMNH 7174, KWJH, BMNH 6652	1
Mechanitini	*Thyridia psidii*	M: BMNH 6635; F: BMNH 6648	1
New tribe	*Athesis clearista*	M: MGCL, BMNH 6627; F: BMNH 7112, MGCL	1
New tribe	*Patricia dercyllidas*	M: BMNH 7084, BMNH 7134, BMNH 7137, BMNH 7138, BMNH 6628; F: BMNH 6641	2, 18
Napeogenini	*Aremfoxia ferra*	M: BMNH 6653; F: BMNH 7131	–
Napeogenini	*Epityches eupompe*	M: BMNH 6654; F: BMNH 6664, MGCL	1
Napeogenini	*Hypothyris xanthostola*	M: BMNH 6655; F: BMNH 6665	1
Napeogenini	*Hypothyris cantobrica*	M: BMNH 6656; F: BMNH 6666	1
Napeogenini	*Hypothyris euclea*	M: KWJH, KWJH, KWJH, KWJH, BMNH 6662; F: BMNH 6673	1
Napeogenini	*Hypothyris moebiusi*	M: BMNH 6661; F: BMNH 6671	–
Napeogenini	*Hypothyris ninonia*	M: BMNH 6660; F: BMNH 6670	1
Napeogenini	*Hyalyris coeno*	M: BMNH 6657, KWJH; F: BMNH 6667, BMNH 6672	–
Napeogenini	*Hyalyris excelsa*	M: BMNH 6659; F: BMNH 6669	1
Napeogenini	*Hyalyris ocna*	M: BMNH 6658, KWJH; F: BMNH 6668	2
Napeogenini	*Napeogenes apulia*	M: BMNH 6349; F: KWJH 6676	2
Napeogenini	*Napeogenes inachia*	M: BMNH 6333; F: BMNH 6675, BMNH 6678	1, 14
Napeogenini	*Napeogenes rhezia*	M: BMNH 6332; F: BMNH 6674, BMNH 6677	–
Ithomiini	*Ithomia arduinna*	M: BMNH 7098; F: BMNH 7097	1
Ithomiini	*Ithomia drymo*	M: BMNH 6688, BMNH 7169; F: BMNH 6682, BMNH 6686	1
Ithomiini	*Ithomia terra*	M: BMNH 6687; F: BMNH 6681, BMNH 6685	2
Ithomiini	*Pagyris cymothoe*	M: BMNH 6690; F: BMNH 6680	1
Ithomiini	*Pagyris ulla*	M: BMNH 6689; F: BMNH 6679	–
Ithomiini	*Placidina euryanassa*	M: BMNH 6630; F: BMNH 6643	1, 15
Oleriini	*Hyposcada anchiala*	M: BMNH 6806, MGCL, KWJH, BMNH 7231; F: BMNH 7122, MGCL	4
Oleriini	*Hyposcada taliata*	M: BMNH 7107, KWJH OLERIA-39, BMNH 6810; F: KWJH OLERIA-50	–
Oleriini	*Hyposcada virginiana*	M: KWJH, BMNH 6805; F: MGCL	9
Oleriini	*Megoleria susiana*	M: BMNH 7227, BMNH 6683; F: BMNH 7228, BMNH 6684	5
Oleriini	*Oleria aegineta*	M: KWJH; F: KWJH OLERIA-46	–
Oleriini	*Oleria aegle*	M: BMNH 5941, BMNH 6807, MGCL; F: MGCL, MGCL	1
Oleriini	*Oleria aquata*	M: BMNH 6780, BMNH 7148; F: BMNH 6781	1
Oleriini	*Oleria astrea*	M: AME, BMNH 6246, BMNH 6760, BMNH 6761, BMNH 6763, ZMHU, BMNH 6263; F: MGCL, BMNH 6264	–

Appendix 3 *Continued.*

Higher taxon	Species	Dissections examined[1]	Immature stage sources[2]
Oleriini	*Oleria canilla*	M: BMNH 6270, MGCL; F: BMNH 6271, BMNH 7121	1
Oleriini	*Oleria olerioides*	M: KWJH OLERIA-15, BMNH 6808; F: KWJH OLERIA-47	–
Oleriini	*Oleria santineza*	M: BMNH 6402, AMNH, AMNH, BMNH 6399, BMNH 6429, BMNH 6430, ZMHU, MGCL, BMNH 6809, KWJH OLERIA-20, KWJH OLERIA-25; F: BMNH 6403, AMNH, BMNH 6434, BMNH 6435, KWJH, KWJH OLERIA-43	2
Oleriini	*Oleria zelica*	M: MGCL, BMNH 6691; F: MGCL	10
Dircennini	*Callithomia alexirrhoe*	M: BMNH 6328, BMNH 7085; F: BMNH 6692	–
Dircennini	*Callithomia lenea*	M: BMNH 6327; F: BMNH 6693	1
Dircennini	*Ceratinia neso*	M: BMNH 6776; F: BMNH 6700	1
Dircennini	*Ceratinia tutia*	M: BMNH 6777, KWJH; F: BMNH 6698, BMNH 7177	1
Dircennini	*Dircenna dero*	M: BMNH 6772, KWJH; F: BMNH 6695	1
Dircennini	*Dircenna jemina*	M: BMNH 6771; F: BMNH 6694	–
Dircennini	*Dircenna paradoxa*	M: BMNH 6326, BMNH 7182, BMNH 7185; F: BMNH 7191, BMNH 6696, BMNH 7183, BMNH 7184	2
Dircennini	*Episcada apuleia*	M: BMNH 6287; F: 6705	2
Dircennini	*Episcada clausina*	M: BMNH 6283, KWJH, BMNH 7156, BMNH 6284; F: BMNH 7153	1
Dircennini	*Episcada doto*	M: BMNH 6275; F: BMNH 6701	–
Dircennini	*Episcada hemixanthe*	M: BMNH 6292; F: BMNH 7178, BMNH 6706	–
Dircennini	*Episcada hymenaea*	M: BMNH 6278, BMNH 6778, SMF; F: BMNH 6703	1
Dircennini	*Episcada philoclea*	M: BMNH 6289, BMNH 7088; F: BMNH 6707	1
Dircennini	*Episcada salvinia*	M: BMNH 6280, BMNH 6279; F: BMNH 6704	1
Dircennini	*Episcada canaria*	M: BMNH 6276; F: BMNH 6702	1, 15
Dircennini	*Haenschia sidonia*	M: ZSBS; F: BMNH 7108	–
Dircennini	*Hyalenna pascua*	M: BMNH 7055; F: MUSM	1
Dircennini	*Hyalenna perasippa*	M: BMNH 6775, BMNH 7086; F: BMNH 7186, MUSM	–
Dircennini	*Pteronymia aletta*	M: BMNH 6305; F: BMNH 6708	1
Dircennini	*Pteronymia alida*	M: BMNH 6321, KWJH, KWJH, ZMHU, BMNH 6785, BMNH 6784; F: BMNH 6712	2
Dircennini	*Pteronymia artena*	M: KWJH, BMNH 6782; F: BMNH 6716, BMNH 7179	2
Dircennini	*Pteronymia carlia*	M: BMNH 6298; F: BMNH 7155	1
Dircennini	*Pteronymia euritea*	M: BMNH 6299; F: BMNH 7162	1
Dircennini	*Pteronymia hara*	M: BMNH 6320, USNM, BMNH 7087, KWJH, BMNH 6389, SMNS, KWJH; F: USNM, BMNH 6715	–
Dircennini	*Pteronymia inania*	M: KWJH; F: BMNH 6713	2
Dircennini	*Pteronymia latilla*	M: BMNH 6302; F: BMNH 6709	1
Dircennini	*Pteronymia lonera*	M: USNM; F: USNM 6714	1, 17
Dircennini	*Pteronymia zerlina*	M: KWJH, KWJH, BMNH 6316; F: BMNH 6711	2
Godyridini	*Brevioleria arzalia*	M: BMNH 6787, BMNH 6792; F: BMNH 7180, BMNH 6723	1
Godyridini	*Brevioleria plisthenes*	M: BMNH 7163, UFP; F: UFP	1
Godyridini	*Godyris dircenna*	M: BMNH 6746; F: BMNH 6735	1
Godyridini	*Godyris duillia*	M: BMNH 7090, BMNH 6377; F: BMNH 6717	2
Godyridini	*Godyris nero*	M: BMNH 6369, BMNH 6384; F: BMNH 6734	–
Godyridini	*Godyris zavaleta*	M: KWJH, BMNH 6786; F: KWJH, BMNH 6719	1
Godyridini	*Godyris mantura*	M: BMNH 6379, BMNH 7223; F: BMNH 6718, BMNH 7224	–
Godyridini	*Greta diaphanus*	M: BMNH 6375; F: BMNH 6725	11
Godyridini	*Greta morgane*	M: BMNH 6371; F: BMNH 6726	12, 19
Godyridini	*Heterosais edessa*	M: BMNH 7157; F: BMNH 7181, BMNH 7158	1
Godyridini	*Heterosais nephele*	M: BMNH 6804; F: BMNH 6732	–
Godyridini	*Hypoleria lavinia*	M: BMNH 6394; F: BMNH 6721	1, 13
Godyridini	*Mcclungia cymo*	M: BMNH 7091, BMNH 7165, BMNH 7166, BMNH 6788, BMNH 7164, BMNH 7167, BMNH 7168; F: BMNH 6724	1
Godyridini	*Hypoleria adasa*	M: BMNH 6790, BMNH 7171; F: BMNH 6722	1
Godyridini	*Pseudoscada erruca*	M: BMNH 6386, BMNH 6802; F: BMNH 6729, BMNH 6733	1
Godyridini	*Pseudoscada florula*	M: BMNH 6803, BMNH 6395; F: BMNH 6731	1
Godyridini	*Pseudoscada timna*	M: BMNH 6798, BMNH 6791, BMNH 6799, BMNH 6800, BMNH 6795, BMNH 6796, BMNH 6801, BMNH 6797; F: BMNH 6730	1
Godyridini	*Greta andromica*	M: BMNH 6352, BMNH 6368; F: BMNH 6728	2
Godyridini	*Greta ortygia*	M: BMNH 6374, BMNH 6354; F: BMNH 7050, BMNH 7051	2

Appendix 3 *Continued.*

Higher taxon	Species	Dissections examined[1]	Immature stage sources[2]
Godyridini	*Greta theudelinda*	M: BMNH 6467, BMNH 6469, BMNH 6351; F: BMNH 6727	2
Godyridini	*Veladyris pardalis*	M: BMNH 7170, BMNH 6789; F: BMNH 6720	–
Godyridini	*Velamysta phengites*	M: BMNH 6773, BMNH 7089; F: BMNH 7192	2

[1]M = male; F = female; AMNH = American Museum of Natural History, New York; BMNH = Natural History Museum, London; KWJH = K. Willmott & J. Hall Collection, Gainesville; MGCL = McGuire Center for Lepidoptera and Biodiversity, Gainesville; MUSM = Museo de Historia Natural, Universidad Nacional Mayor de San Marcos, Lima; SMF = Senckenberg Museum, Frankfurt am Main; SMNS = Staatliches Museum für Naturkunde, Stuttgarto; UFP = Universidade Federal do Paraná, Curitiba; ZMHU = Zoologisches Museum, Humboldt Universität, Berlin; ZSBS = Zoologische Sammlung des Bayerischen Staates, Munich. [2]Sources: 1 = Brown and Freitas (1994; unpub.); 2 = Willmott (unpub.); 3 = Brévignon (2003); 4 = G. Beccaloni (pers. comm.); 5 = H. Greeney (pers. comm.); 6 = A. G. Orr in Ackery (1987); 7 = R. Hill (pers. comm.); 8 = Freitas and Brown (2002); 9 = Haber (1978); 10 = Young (1974); 11 = Sourakov and Emmel (1995); 12 = Janzen and Hallwachs (2005); 13 = Young (1978); 14 = Freitas and Brown (2005); 15 = Freitas (1993); 16 = Brown and D'Almeida (1970); 17 = W. Haber (pers. comm.); 18 = M.D. Heredia (pers. comm.); 19 = Hall (1996).